I
L'influence sur la résistance et les déformations des phénomènes non-linéaires suivants
Der Einfluss auf die Traglast und die Verformung der folgenden nichtlinearen Vorgänge
The Influence on Strength and Deformations of the following Nonlinear Phenomena

I a
Plasticité et viscosité
Plastizität und Viskosität
Plasticity and Viscosity

Leere Seite

Blank page

Page vide

The Significance of Shake Down Loading

La signification du "Shake Down" des charges

Die Bedeutung des "Shake Down" der Belastungen

JACQUES HEYMAN
Professor of Engineering
University of Cambridge
England, GB

The incremental collapse of frames, calculated according to accepted ideas of simple plastic theory, has been illuminated recently by a new formulation [1, 2]. Suppose that a unit load acting at section j of a frame produces an elastic bending moment μ_{ij} at section i of the frame; μ_{ij} is computed in the usual way on the assumption that the frame is initially stress free. Then the actual load W_j acting at j will give rise to an elastic bending moment of value

$$\mathcal{M}_i = \mu_{ij} W_j \quad . \tag{1}$$

If the value of the load W_j is not fixed, but can take on any value within the range

$$W_j^{min} \leqslant W_j \leqslant W_j^{max} \quad , \tag{2}$$

then the value of the elastic moment $\mathcal{M}_i$ will also fluctuate. To determine its largest value, $\mathcal{M}_i^{max}$ say, the value of W_j will be taken to be as large or as small as possible according as the unit moment μ_{ij} is positive or negative, denoted by $+\mu_{ij}^+$ and $-\mu_{ij}^-$, where μ_{ij}^+ and μ_{ij}^- are themselves positive numbers. Thus

$$\mathcal{M}_i^{max} = \sum_j (\mu_{ij}^+ W_j^{max} - \mu_{ij}^- W_j^{min}) \quad , \tag{3}$$

and, similarly,

$$\mathcal{M}_i^{min} = \sum_j (-\mu_{ij}^- W_j^{max} + \mu_{ij}^+ W_j^{min}) \quad . \tag{4}$$

Now the basic equation for determining the full plastic moments $(M_p^s)_i$ of a frame so that is just on the point of incremental collapse by the formation of a mechanism with hinge rotations ϕ_i is

$$\sum (M_p^s)_i |\phi_i| = \sum (\mathcal{M}_i^{max} \phi_i^+ - \mathcal{M}_i^{min} \phi_i^-) \quad . \tag{5}$$

The numbers ϕ_i^+ and ϕ_i^- are themselves positive, and the same sign convention for the hinge rotations $+\phi_i^+$ and $-\phi_i^-$ has been used as that for the unit moments μ_{ij}. Each term in the sum on the left-hand side of equation (5) is essentially positive, since it represents work dissipated at a rotating plastic hinge. Thus, introducing equations (3) and (4) into (5),

$$\sum_i (M_p^s)_i |\phi_i| = \sum_i \{\sum_j (\mu_{ij}^+ W_j^{max} - \mu_{ij}^- W_j^{min})\}\phi_i^+ - \sum_i \{\sum_j (-\mu_{ij}^- W_j^{max} + \mu_{ij}^+ W_j^{min})\}\phi_i^- \quad . \quad (6)$$

It is convenient to introduce a corresponding <u>static</u> design $(M_p^o)_i$, calculated for the same mechanism ϕ_i, but with the loads W_j all having their <u>fixed</u> maximum values W_j^{max}. This static design is thus given by

$$\sum_i (M_p^o)_i |\phi_i| = \sum_i \{\sum_j (\mu_{ij}^+ W_j^{max} - \mu_{ij}^- W_j^{max})\}\phi_i^+ - \sum_i \{\sum_j (-\mu_{ij}^- W_j^{max} + \mu_{ij}^+ W_j^{max})\}\phi_i^- \quad , \quad (7)$$

and it will be seen that this is almost identical with equation (6); the only difference is that in (7) all bending moments are due to W_j^{max}. Subtracting the two equations,

$$\sum_i \{(M_p^s)_i - (M_p^o)_i\}|\phi_i| = \sum_i \left[\phi_i^+ \{\sum_j \mu_{ij}^- (W_j^{max} - W_j^{min})\} + \phi_i^- \{\sum_j \mu_{ij}^+ (W_j^{max} - W_j^{min})\}\right]. \quad (8)$$

Three important conclusions may be drawn immediately from a study of equation (8).

First, the whole of the right-hand side of equation (8) is positive or zero. The range of loading $(W_j^{max} - W_j^{min})$ is essentially positive or zero, while the products $\phi^+ \mu^-$ and $\phi^- \mu^+$ are positive by definition. Thus the equation indicates that the values of full plastic moment M_p^s required to prevent incremental collapse in a given mechanism ϕ will exceed (or at best equal) the corresponding values M_p^o for static collapse. In other words, a frame subjected to fluctuating loads will always require more material than a frame subjected to steady peak values of those loads.

Secondly, only the <u>range</u> of loading $(W_j^{max} - W_j^{min})$ occurs in equation (8), and not the absolute values of the loads. Now the equation is a measure of the difference between the incremental collapse design M_p^s and the static collapse design M_p^o; thus this <u>difference</u> in design cannot be affected by any dead load (or any other load of fixed magnitude). That is, the dead loads will affect the actual value of M_p^o, but are not concerned in any increase to M_p^s to guard against incremental collapse.

Thirdly, it is only products $\phi^+ \mu^-$ and $\phi^- \mu^+$ which appear in equation (8). The difference between M_p^s and M_p^o arises only from loads which produce unit

negative elastic moments at sections where there are <u>positive</u> hinge rotations, or which produce unit <u>positive</u> elastic moments at sections where there are <u>negative</u> hinge rotations.

As a numerical example, the uniform fixed-ended beam of fig.1 carries loads W_1 and W_2, where the values of the loads can vary randomly and independently within the ranges


Fig.1

(a)
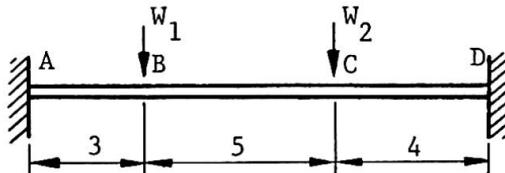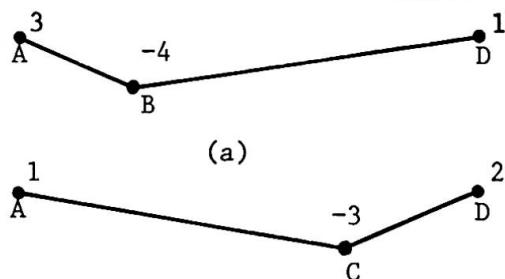
(b)   Fig.2

$$0 \leqslant W_1 \leqslant 352 \quad , \\ 0 \leqslant W_2 \leqslant 270 \quad . \tag{9}$$

If the loads W_1 and W_2 have their <u>fixed</u> maximum values, then the conventional methods of plastic design lead to the static value of full plastic moment:

$$M_p^o = 536 \quad . \tag{10}$$

Static collapse occurs by mechanism (b) of fig.2.

If, on the other hand, the loads are allowed to vary between the limits (9), then a shakedown analysis must be made. Conventional elastic theory leads to the following table of bending moments:

Table 1

Section	Moment due to		$\mathcal{M}$	$\mathcal{M}^{max}$	$\mathcal{M}^{min}$
	$W_1 = 352$	$W_2 = 270$			
A	594	240	834	834	0
B	-297	30	-267	30	-297
C	-22	-320	-342	0	-342
D	198	480	678	678	0

The column labelled $\mathcal{M}$ in table 1 represents the <u>static</u> elastic solution when both loads act together with their full values, and it may be noted that the design given by equation (10) can be recovered from the fundamental equation

$$\sum (M_p^o)_i |\phi_i| = \sum \mathcal{M}_i \phi_i \quad , \tag{11}$$

(where, indeed, the elastic moments $\mathcal{M}_i$ can be replaced by <u>any</u> distribution of

moments in equilibrium with the given external loading). Using the values $\mathcal{M}_i$
from table 1, equation (11) applied to mechanism (a) of fig.2 gives

$$8M_p^o = (834)(3) + (-267)(-4) + (678)(1) \quad ,$$

or $\quad M_p^o = 531 \quad ;$ \hfill (12)

a similar calculation for mechanism (b) gives the more critical $M_p^o = 536$ of
equation (10).

The last two columns of table 1 give values of $\mathcal{M}^{max}$ and $\mathcal{M}^{min}$ as the loads
vary between their limits (9). Using equation (5) with mechanism (a),

$$8M_p^s = (834)(3) + (-297)(-4) + (678)(1) \quad ,$$

or $\quad M_p^s = 546 \quad ;$ \hfill (13)

similarly, for mechanism (b),

$$6M_p^s = (834)(1) + (-342)(-3) + (678)(2)$$

or $\quad M_p^s = 536 \quad .$ \hfill (14)

Clearly equation (13), mechanism (a), is more critical; the design full plastic
moment must be increased from the value 536 of equation (10) for the static case
to the value 546 of equation (13) in order to prevent incremental collapse.

Now the formulation of equation (8) shows how this increase arises. Since
only products $\phi^+\mu^-$ or $\phi^+\mu^-$ can enter into the calculations, the first step is
to examine the signs of the elastic bending moments and of the corresponding
hinge rotations. The two mechanisms of fig.2 have positive (hogging) hinge
rotations at the ends A and D of the beam, and negative (sagging) rotations at
the internal points B and C. From table 1 it is seen that the signs of the
elastic bending moments due to the load W_1 are precisely the same as those of
the hinge rotations at the four critical sections; the conclusion is that the
load W_1 cannot contribute at all to any increase in the value of M_p,
(from M_p^o to M_p^s).

Similarly, the signs of the bending moments due to W_2 are the same as the
signs of the hinge rotations for mechanism (b); thus mechanism (b) must give
the same design value for M_p whether the loads are static or fluctuating, and
this is confirmed by the identity of equations (10) and (14).

The only opposition in sign of bending moment and of hinge rotation occurs

for section B with mechanism (a) and the load W_2; in this simple example, it is this single contribution which increases the value of M_p from the 531 of equation (12) to the 546 of equation (13).

This discussion indicates that equation (8) can be simplified for the purpose of calculation of shakedown limits. The right-hand side may be written

$$\sum_i \{\phi_i^+(\sum_j \mu_{ij}^- \bar{W}_j) + \phi_i^-(\sum_j \mu_{ij}^+ \bar{W}_j)\} \equiv \sum_i (\phi_i^+ \bar{\mathcal{M}}_i^- + \phi_i^- \bar{\mathcal{M}}_i^+) \equiv \sum_i |\phi_i \bar{\mathcal{M}}_i^*| \quad , \qquad (15)$$

where $\bar{W}_j$ represents the range of loading $(W_j^{max} - W_j^{min})$, leading to a change of elastic bending moment $\bar{\mathcal{M}}_i$, denoted plus or minus according as the change is an increase or a decrease from the datum. As before, only the products of a positive change of moment $\bar{\mathcal{M}}_i^+$ with a negative hinge rotation ϕ_i^-, and vice versa, are taken, and this is indicated by the final short notation $|\phi_i \bar{\mathcal{M}}_i^*|$ of (15). Thus, finally, if the static collapse equation is written

$$\text{Static:} \quad \sum (M_p^o)_i |\phi_i| = \sum (M_F)_i \phi_i \quad , \qquad (16)$$

where $(M_F)_i$ represents any convenient set of bending moments in equilibrium with the maximum values of the loads, then the incremental collapse equation for the same mechanism but with fluctuating values of the loads may be written

$$\text{Incremental:} \quad \sum (M_p^s)_i |\phi_i| = \sum (M_F)_i \phi_i + \sum |\bar{\mathcal{M}}_i^* \phi_i| \quad . \qquad (17)$$

The numerical example of fig.1 may be reworked by means of a rearrangement of table 1:

Table 2

Section	Maximum positive and negative change in bending moment		(a)		(b)	
	$\bar{\mathcal{M}}^+$	$\bar{\mathcal{M}}^-$	ϕ	$\mathcal{M}_\phi^*$	ϕ	$\mathcal{M}_\phi^*$
A	834	0	3	0	1	0
B	30	-297	-4	120		
C	0	-342			-3	0
D	678	0	1	0	2	0
Static collapse:			$8M_p^o = 4248$		$6M_p^o = 3216$	
Incremental collapse:			$8M_p^s = 4368$		$6M_p^s = 3216$	

As a second example, the collapse of the fixed-base portal frame will be investigated, both under static and under fluctuating loads. Figure 3 shows the frame, of uniform section, acted upon by loads V and H; the values of V and H are supposed to vary randomly and independently within the ranges

$$0 \leqslant V \leqslant V_o \quad , \qquad \qquad \left. \begin{array}{c} \\ \\ \end{array} \right\} \quad (18)$$
$$0 \leqslant H \leqslant H_o \quad .$$

Also shown in fig.3 are sketch elastic solutions for H = 1 and V = 1, together with the three possible modes of collapse.
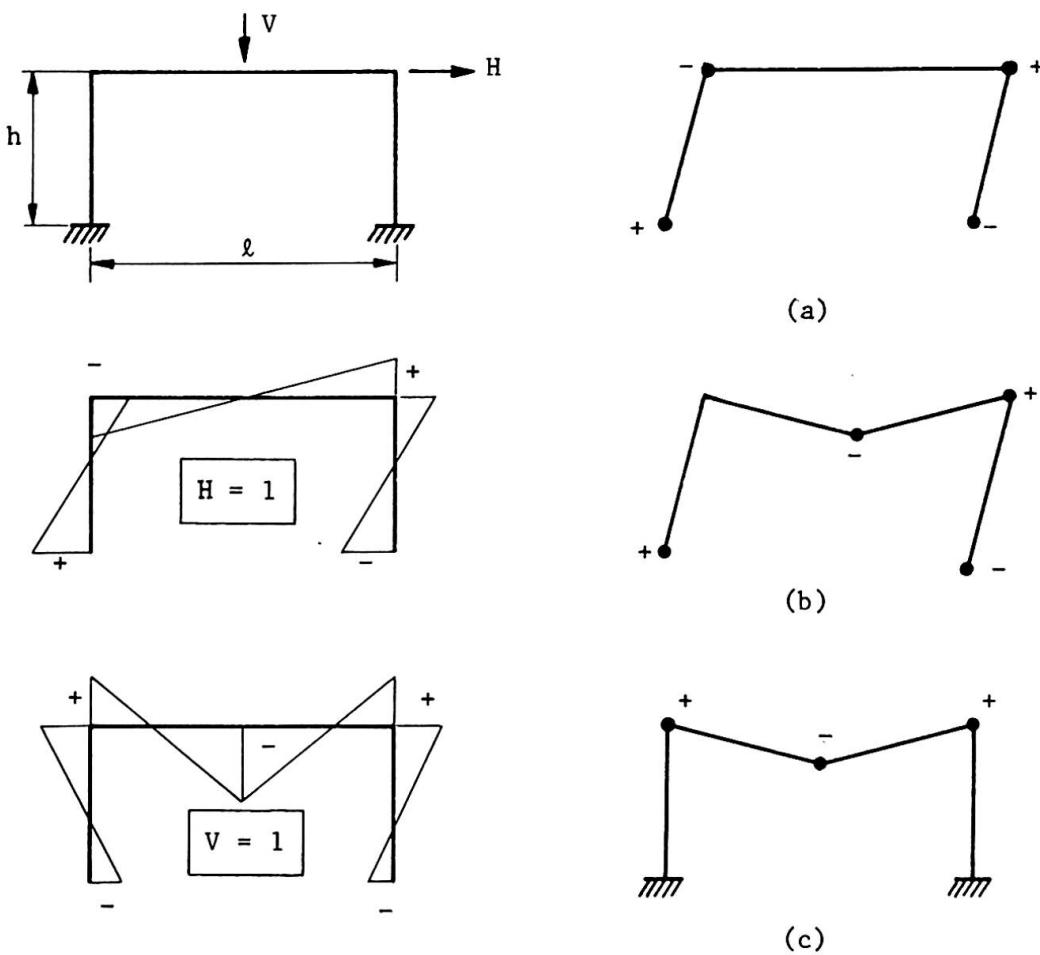
Fig.3

Comparing the elastic solution for H = 1 with mode (a), it will be seen that the signs of the bending moments at the hinge positions are the same in all cases as the signs of the hinge rotations. The conclusion is that there will be no "$M^*\phi$" terms arising from the side load H for mode (a), and that therefore the terms in H will be identical for the static collapse and the incremental collapse equation. On the other hand, the elastic solution for

$V = 1$ indicates an opposition in sign for the hinges in the left-hand column for mode (a), so that there <u>will</u> be an "$\mathcal{M}^{*}\phi$" contribution from the load V.

The final solution requires, of course, expressions for the elastic bending moments in the frame; using these known values, it will be found that collapse by mode (a) leads to the following equations

$$\text{Mode (a)}\begin{cases}\text{Static:} & H_o h & = 4M_p^o\ , \\[2ex] \text{Incremental:} & H_o h + \dfrac{V_o \ell}{8}\left(\dfrac{3\ell}{2\ell+h}\right) & = 4M_p^s\ ;\end{cases} \tag{19}$$

Similarly, examination of the unit bending moment distributions in fig.3 shows at once that the side load H will make no extra contribution to mode (b) of incremental collapse, and the vertical load V will make no extra contribution to the incremental collapse equation for mode (c). The final equations are

$$\text{Mode (b)}\begin{cases}\text{Static:} \quad\cdot & H_o h + \dfrac{V_o \ell}{2} & = 6M_p^o\ , \\[2ex] \text{Incremental:} & H_o h + \dfrac{V_o \ell}{8}\left(\dfrac{9\ell+4h}{2\ell+h}\right) & = 6M_p^s\ ;\end{cases} \tag{20}$$

$$\text{Mode (c)}\begin{cases}\text{Static:} & \dfrac{V_o \ell}{2} & = 4M_p^o\ , \\[2ex] \text{Incremental:} & \dfrac{H_o h}{2}\left(\dfrac{3h}{\ell+6h}\right)+ \dfrac{V_o \ell}{2} & = 4M_p^s\ .\end{cases} \tag{21}$$

Equations (19), (20) and (21) are plotted schematically in the interaction diagram of fig.4 (this diagram is drawn for $\ell = 2h$, but the general features of the diagram will be preserved for other ratios of ℓ/h). It will be noted
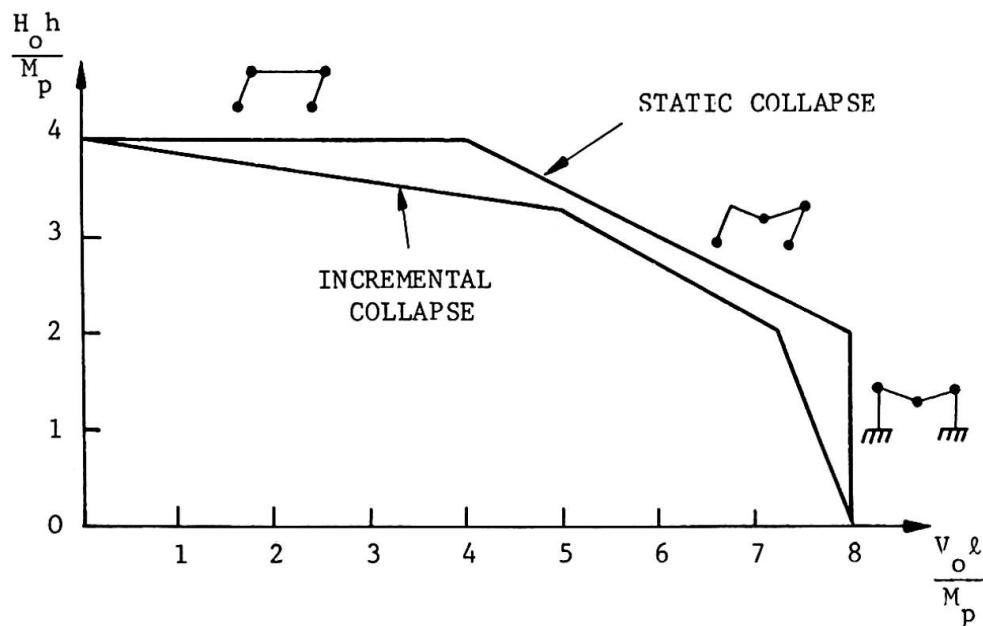

Fig.4

that the "yield surface" for incremental collapse lies entirely within (as it must) the corresponding yield surface for static collapse.

References

1. M. H. Ogle. Shakedown of steel frames. Ph.D. Thesis (Cambridge University), 1964.

2. J. Heyman. Plastic design of frames: Vol.2, Applications. Cambridge, 1971.

Summary

A new formulation of the basic equation of incremental collapse shows immediately which loads acting on a frame are of significance in shakedown design, and which loads are not. A simple numerical example illustrates the procedure, and an interaction diagram is given for the collapse of the fixed-base portal frame.

Ductility and Limit States

Ductilité et états limites

Duktilität und Grenzzustände

M. MARINČEK
Professor at the University of Ljubljana
Jougoslavia

INTRODUCTION   The limit states of the load carrying members and structu-
res clearly can be treated with the help of the typical load-displacement
diagram, obtained experimentally, or with the elasto-plastic theory, which
enables the prediction of the real deformational behaviour. With this the-
ory any shape of the stress-strain diagram of the material and the influ-
ence of the residual stresses can be taken into account. So the instability
loads and/or the suitable defined inelastic deflection limit load can be
established. Various secondary and local effects like lateral instability,
local instability, ductile, brittle, and fatigue fracture have to be refe-
red to the primary global elasto-plastic behaviour. The reliability of dif-
ferent approximate design methods may be estimated by correlating them to
the elasto-plastic behaviour. The dimensionless treatement (which repre-
sents also the model law for experimental work) and the appropriate clas-
sification make possible the wider use of the results of the elasto-plastic
theory.

In this article the inplanar treatement for the single loading of sim-
ple linear structures with time independent inelastic material behaviour is
presented.

DUCTILITY FUNCTIONS OF THE CROSS-SECTION   The nonlinear relationship be-
tween the internal force and corresponding specific deformation of the axe
of the bar can be expressed in the general case by

$$\varphi_x = \frac{M_x}{EI_x} K_{\varphi x} \qquad \varphi_y = \frac{M_y}{EI_y} K_{\varphi y} \qquad \varepsilon = \frac{N}{EA} K_\varepsilon$$

$$\gamma_x = \frac{\varkappa_x Q_x}{EA} K_{\gamma x} \qquad \gamma_y = \frac{\varkappa_y Q_y}{EA} K_{\gamma y} \qquad \theta = \frac{T}{EJ} K_\theta$$

(1)

where the ductility function of the cross-section K can depend on all in-
ternal forces, $K_i = f (M_x, M_y, Q_x, Q_y, N, T)$. Dimensionless, for the case of
uniaxial bending with the normal force, there is

$$K_\varphi = f (\bar{M} , \bar{N}) \tag{2}$$

with $\bar{M} = M : M^o$ and $\bar{N} = N : N^o$, where M^o and N^o are typical internal for-
ces (refered to the proportional limit, yield strength limit, or compres-
sion strength of material). Using the Bernoulli hypothesis for the chosen
strains over the cross-section, M and N are obtained with the corresponding
integration for a given stress-strain diagram of material.

For the stress-strain diagram after Ramberg-Osgood $\bar{\varepsilon} = \bar{\sigma}(1 + \bar{\sigma}^n)$, with
$\bar{\varepsilon} = \varepsilon : \varepsilon^o$, $\bar{\sigma} = \sigma : \sigma^o$, where $\varepsilon^o = \sigma^o : E$ and the yield strength σ^o, defined in
Fig.1, the curves in Fig.2 with different parameters n represent four typi-
cal dimensionless stress-strain behaviour. For n = 10 and the rectangular

cross-section the ductility functions K_φ are given in Fig.3, full lines for strain reversal with constant $\bar{N}$, and the dashed ones for nonlinear elastic material.

There is a simple relationship between the ductility functions of the individual parts of the cross-section and those of the whole composite one,

$$K_\varphi = \frac{\sum\limits_n EI}{\sum\limits_n \dfrac{EI}{K_\varphi}} \tag{3}$$

In this way calculated ductility functions for bending and compression of a concrete filled tube are presented in Fig.4, for an ideal elastic-ideal plastic stress-strain diagram of steel and according to CEB for concrete. The typical internal forces are here

$$M^o = \frac{\pi}{32}\left[\sigma_s^o(D^3-d^3) + \sigma_c^o d^3\right] \qquad N^o = \frac{\pi}{4}\left[\sigma_s^o(D^2-d^2) + \sigma_c^o d^2\right]$$

DUCTILITY FUNCTIONS OF THE LOAD CARRYING MEMBERS   The typical elasto - plastic load-displacement diagram can be performed for example with

$$\delta = \int_0^s \frac{M M_v}{EI} K_\varphi ds \tag{4}$$

One can replace the influence of K_φ with

$$\frac{EI}{K_\varphi} = EI_{eff} = E_{eff}I = (EI)_{eff} \,,$$

but the ductility factor K_φ has a clearer meaning, especially for composite cross-section.

Similar to the definition of K_φ , the ductility of the load carrying member, or structure K_δ , is the ratio between the elasto-plastic displacement and the corresponding elastic one,

$$K_\delta = \delta : \delta^e . \tag{5}$$

Consequently, the relationship between the dimensionless load $\bar{P} = P : P^o$ and dimensionless displacement $\bar{\delta} = \delta : \delta^o$, where P^o represents for example the limit state according to the theory of elasticity, and δ^o the corresponding elastic displacement, is

$$\bar{\delta} = \bar{P} . K_\delta . \tag{6}$$

SOME EXAMPLES   For the simple beam with constant properties along the axe there is the deflection under concentrated load, acting in any point,

$$K_\delta = \frac{3}{\bar{P}^3}\int_0^{\bar{P}} \bar{M}^2 K_\varphi d\bar{M} \,, \tag{7}$$

for the uniformly distributed load on a beam

$$K_\delta = \frac{6}{5\bar{P}^2}\int_0^{\bar{P}}\left(\frac{1}{\sqrt{1-\frac{\bar{M}}{\bar{P}}}}-1\right)\bar{M}K_\varphi d\bar{M}, \qquad (8)$$

and on a cantilever

$$K_\delta = \frac{2}{\bar{P}^2}\int_0^{\bar{P}}\bar{M}K_\varphi d\bar{M}, \qquad (9)$$

with $\bar{P} = \bar{M}_{max}$. Fig.5 shows the results for the rectangular cross-section and three different stress-strain diagrams with strain hardening.

For the examples in Fig.6 the dimensionless deflection limit load $\bar{P}_{1,1}$, defined with 10% irreversible deflection and the plastic hinge load, both related to the elastic limit loads, are presented in the table I. Thus there is the possibility for higher allowable stresses in elastic design, dependent on the cross-section and loading (in this case for the material with n = ∞, without residual stresses).

Table I

	●	■	D/t=20	D/t=∞	IPB$_v$100	IPB$_v$340	IPB$_l$300	
⊥⊥⊥⊥⊥⊥	1,43	1,31	1,23	1,17	1,21	1,14	1,08	$\bar{P}_{1,1}$
↓	1,54	1,39	1,29	1,22	1,23	1,16	1,10	$\bar{P}_{1,1}$
	1,70	1,50	1,34	1,27	1,24	1,16	1,10	$\bar{P}^\bullet$

The symmetric continuous beam, loaded as in Fig.7, has the ductility function

$$K_\delta = \frac{6(3+2\lambda)}{(3+10\lambda)(\bar{M}_1+\bar{M}_2)}\left(\int_{\bar{M}_2}^{\bar{M}_1}\bar{M}K_\varphi d\bar{M} + 4\lambda\frac{\bar{M}_1+\bar{M}_2}{\bar{M}_1^2}\int_0^{\bar{M}_1}\bar{M}^2 K_\varphi d\bar{M}\right), \qquad (10)$$

with

$$\int_0^{\bar{M}_2}\frac{\bar{M}K_\varphi d\bar{M}}{\sqrt{1-\frac{\bar{M}}{\bar{M}_2}}} = \int_0^{\bar{M}_1}\frac{\bar{M}K_\varphi d\bar{M}}{\sqrt{1+\frac{\bar{M}}{\bar{M}_2}}} + \frac{4\lambda}{\bar{M}_1^2}\sqrt{(\bar{M}_1+\bar{M}_2)\bar{M}_2}\int_0^{\bar{M}_1}\bar{M}^2 K_\varphi d\bar{M}$$

as the deformational condition. There is strong dependence on λ, the ratio of spans.

Fig.8 shows for $\lambda = 1$ the influence of different stress-strain para-meters n , compared with the plastic hinge theory, and Fig.9 the influence of the cross-section properties for $\lambda = 0$.

In Fig.10 the load carrying capacities are given for a beam-column, made of the material with n = 10, as the function of the slenderness λ. The dashed lines represent the influence of strain reversal at $\bar{N}$ = const and growing $\bar{Q}$.

In Fig.11 the elasto-plastic load deflection diagram $\bar{Q} - \bar{\delta}$ for $\bar{N}$ = 0,1 for different parameter n of material can be compared with those of the second order elastic theory and the second order plastic hinge theory. Si-milarly in Fig.13 for $\bar{N}$ = 0,25 and in Fig.14 for $\bar{N}$ = 0,525 are $\bar{Q} - \bar{\delta}$ curves for weak axial bending of DIE20, material with n = ∞, dashed curves for the presence of residual stresses and nonhomogeneity, dimensionless given in Fig.12. For higher $\bar{\lambda}$ and higher $\bar{N}$ the difference between elastic limit load, plastic hinge limit load, and elasto-plastic instability limit load, with and without residual stresses, are substantional.

For the case when Q = const, in Fig.15 and 16, the relationship $\bar{N} - \bar{\delta}$ is presented for the material with n = ∞ and the rectangular cross-section.

In Fig.15 for $\bar{Q} = 0,5$ there exists the elastic limit curve and the plastic hinge curve, whereas in Fig.16 the value $\bar{Q} = 1$ alone represents already the elastic limit state, but for all that there is a large additional normal force carrying capacity, particularly for lower slendernesses.

The dimensionless buckling curves for column with the composite cross-section can be represented in the same diagram as for columns with the single material. So in Fig.17 the lower curve is the tangent modulus curve for the plain concrete, CEB stress-strain diagram, and the upper curve is the Euler curve for the ideal elastic - ideal plastic diagram of steel. Three curves in between belong to columns with concrete filled tubes and encased I-profile (numbers describe the steel cross-section, steel yield strength, and concrete compression strength). The slenderness of concrete filled steel tube is

$$\bar{\lambda} = \frac{4L}{\pi D} \sqrt{\frac{1 + c\frac{G_c^o}{G_s^o}}{1 + c\frac{E_c}{E_s}}} \qquad \text{with} \qquad c = \frac{1}{\frac{D^4}{d^4} - 1} \tag{11}$$

Of course, the real columns have geometrical and structural imperfections. Therefore, the corresponding instability limit loads with the help of the beam-column elasto-plastic theory have to be determined. Fig.18 gives the $\bar{Q} - \bar{\delta}$ curves with the instability limit states for different slender beam-columns with concrete filled tube cross-section, having ductility functions in Fig.4.

FINAL REMARKS   The consequent dimensionless treatement would have larger effects in using the results of the elasto-plastic theory for better understanding of the ductile behaviour of structures and with this more rational use of material.

The deterministic treatement of structures with the elasto-plastic theory supports and supplies the probabilistic treatement because a significant variation is possible only with representative parameters for separated influences. On the contrary, the pure empirical statistical analysis of the complex phenomena appearing in the ductile bahaviour of structures is rather questionable, if not impossible.

The extension of the elasto-plastic theory on the problems, taking into account more complicated loading and structural geometry, the Bauschinger effect, the influence of the temperature (also fire), and strain velocity, calls even more attention to the international collaboration in finding the appropriate classification of the shapes for stress-strain diagrams of the material, cross-sections, structural and geometrical imperfections.

SUMMARY   Presented results of the elasto-plastic theory, compared with the corresponding elastic theory and plastic hinge theory, show on the one side, that the possibility exists for better exploatation of material also for statical determined structures when inelastic deflection limit state has to be decisive, and on the other side, that one should be carefull with the unlimited use of the plastic hinge theory for stability limit states.
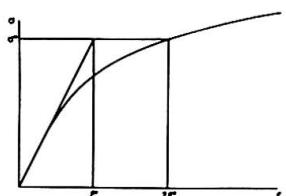
Fig. 1
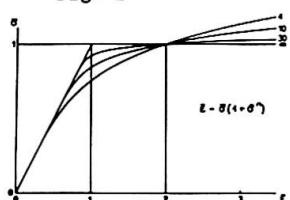
Fig. 2
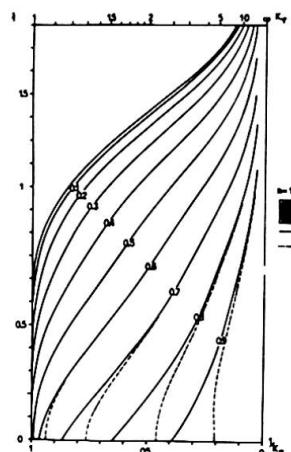
Fig. 3
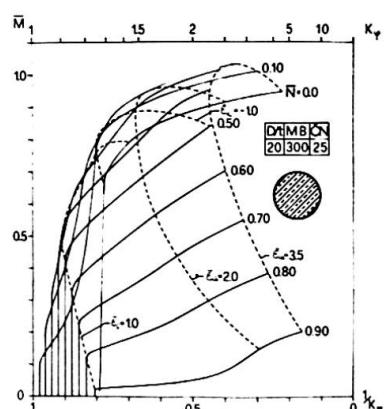
Fig. 4
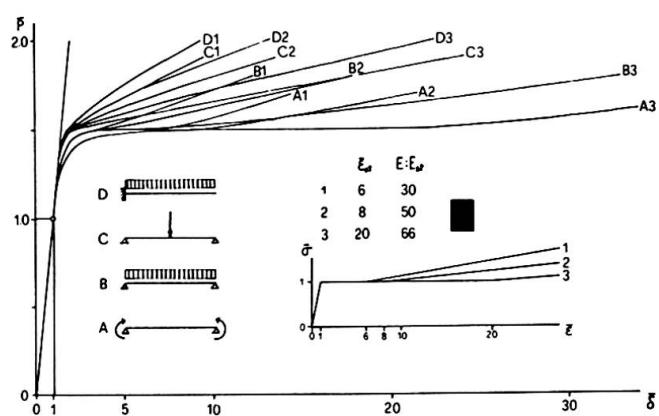
Fig. 5
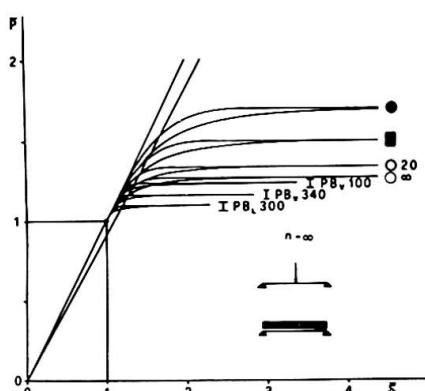
Fig. 6
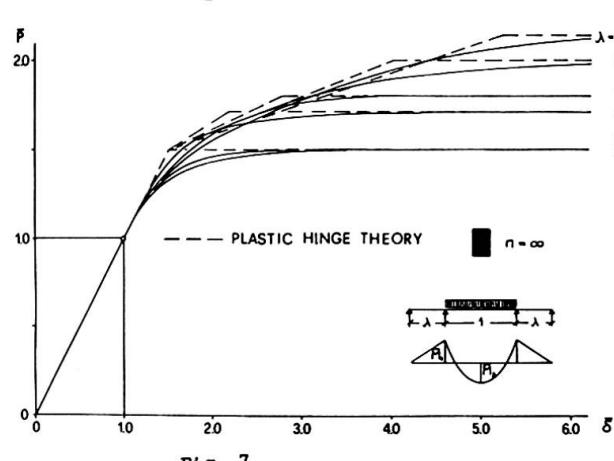
Fig. 7
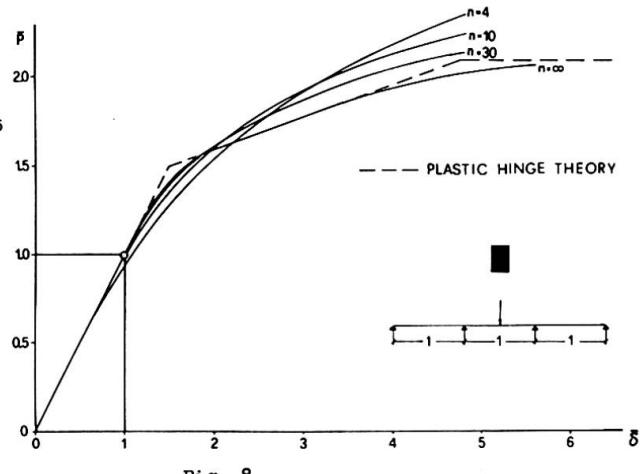
Fig. 8
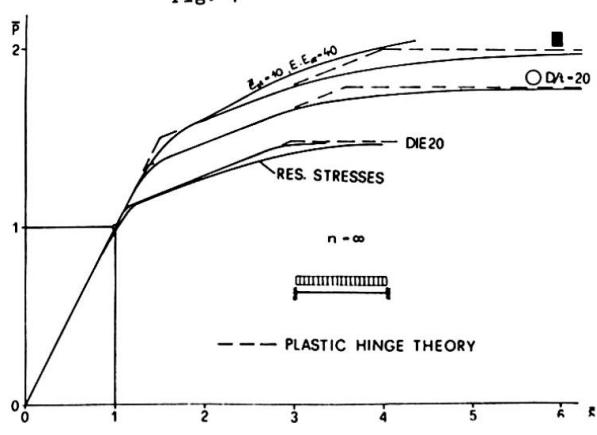
Fig. 9
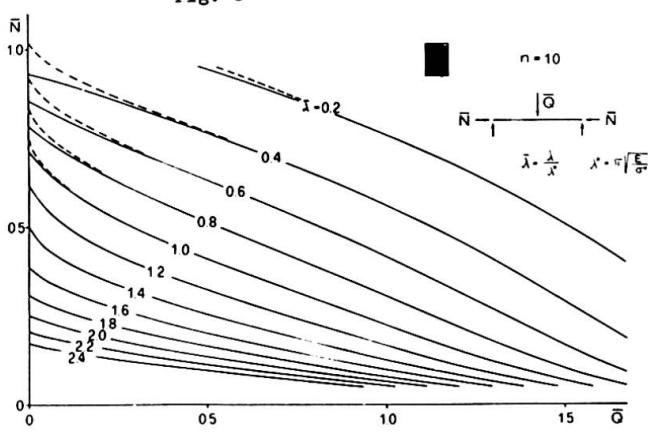
Fig. 10
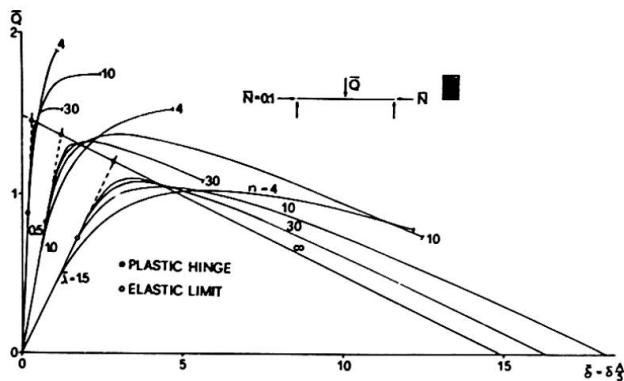
Fig. 11
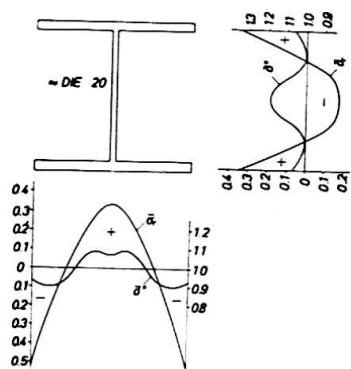
Fig. 12
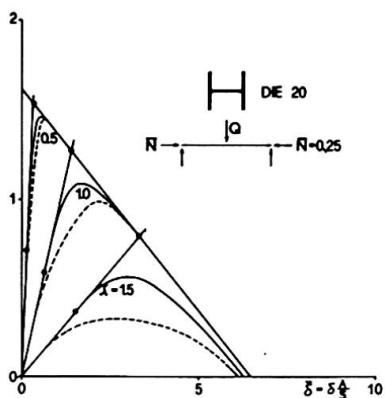
Fig. 13
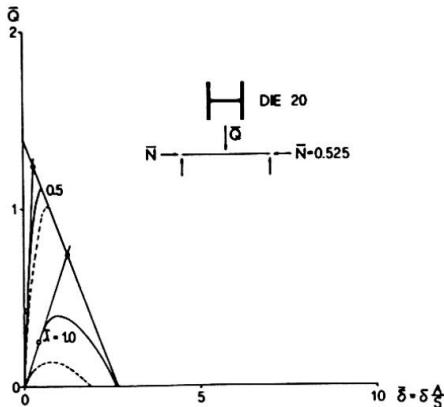
Fig. 14
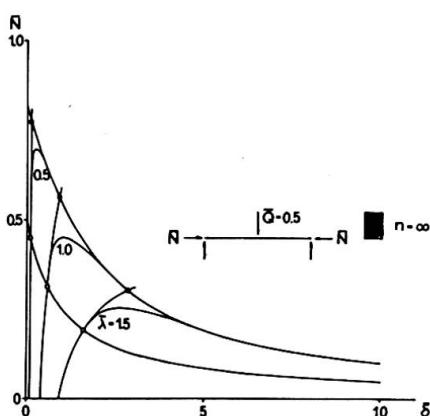
Fig. 15
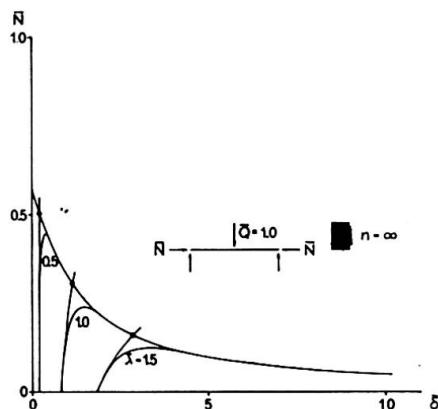
Fig. 16
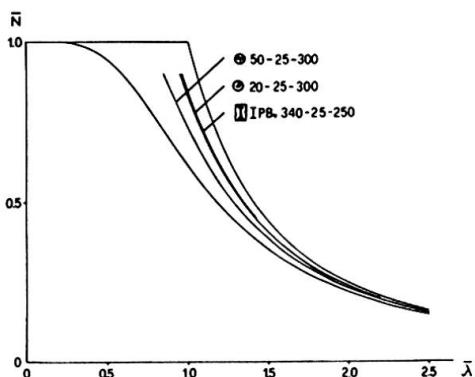
Fig. 17
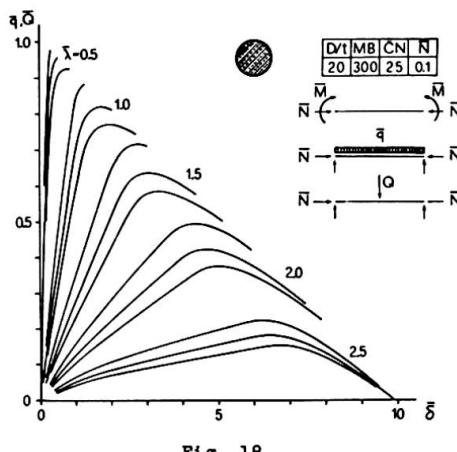
Fig. 18

Theorems for a Simplified Second Order Limit Analysis of Elastic-Plastic Frames

Méthode réduite de seconde ordre pour la détermination de la charge limite des portiques élasto-plastiques

Hilfssätze für eine vereinfachte Traglastberechnung zweiter Ordnung elastisch-plastischer Rahmentragwerke

OTTO HALÁSZ
Prof.
Technical University
Budapest, Hungary

Introduction

The use of simple (or "first order") limit analysis – assuming rigid-plastic material – is restricted to a limited class of frames as the computed failure load P_{FI} ("first order failure load") may give unsafe estimate in presence of axial forces.

Several attempts were made to include the effect of change in geometrie and thus to establish a "second order" limit analysis (resulting in a "second order failure load P_F), ranging from the most simple Rankine-formula to different computer methods [1], [2], [3], [4], [5].

Introducing simplifications this paper is to offer some theorems, which can be used as techniques for preliminary limit design of a class of simple frames, requiring generally an additional check by a more exact method. Because of lack of space the prove of theorems couldn't be reproduced and only reference can be given either to works treating the problem more generally [6] or to the authors previous reports [7], [8].

Attention is paid to the fact, that while the first order failure load depends basically on the value of full-plastic moment M_p of the cross sections only, the second order failure load is influenced by the flexural rigidity "EI" of the constituting members as well. Thus a preliminary design procedure has to include criteria for the required value of both flexural rigidity and full-plastic moment in case of a prescribed failure load P_F.

Assumptions

The model of a frame in the elastic-plastic range is taken as composed of perfectly elastic, initially straight members (of number s) and plastic hinges supposed to develop at certain cross sections only; their greatest possible number be m. The full-plastic moment of the cross sections is assumed to be constant independently of the axial force N acting in the corresponding member. Concentrated loads are allowed to act at joints only, increasing proportionally to a single load factor P (Fig.1.).

We restrict us to cases where in the equations expressing requirements of equilibrium and continuity the shortening of members due both to flexural deformation and direct axial compression can be neglected (excluding thus triangulated frames).

This way the analysis of a perfectly elastic frame can be carried out by solving two simultaneous matrix equations [1] of the form

$$P \cdot \underline{q} = \underline{\underline{S}} \cdot \underline{\delta} \tag{1}$$

$$\underline{N} = P \cdot \underline{q}_1 + \underline{\underline{S}}_1 \cdot \underline{\delta} \tag{2}$$

where vector $\underline{q}$ and $\underline{q}_1$ depends on the distribution of external loads only (quantities α in Fig.1.); $\underline{\underline{S}}$ is the stiffness matrix (its elements being functions of the axial forces in the members), and vector $\underline{\delta}$ represents the "free" displacements of the joints. Second equation expresses, that vector $\underline{N}$ representing the axial forces in the members depends on external loads and displacements of joints as well.
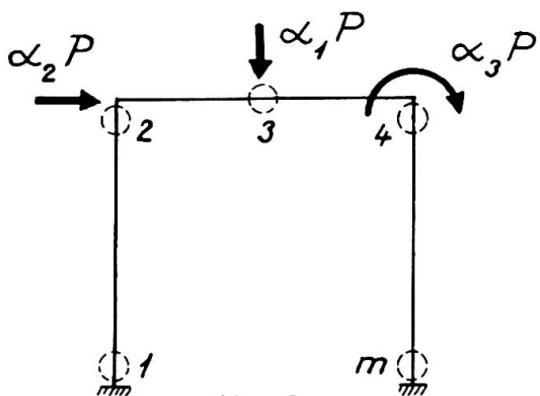
Fig.1.

Basic simplification will be introduced by omitting equation (2) and replacing it by

$$\underline{N} = P \cdot \underline{\beta} \tag{3}$$

i.e. assuming axial forces to increase proportionally to the load factor. $\underline{\beta}$ can be taken from the solution of a first order elastic analysis or rather of a rigid-plastic limit analysis. This assumption allows the use of superposition as well and thus bending moments M in an elastic-plastic frame can be expressed $M = M_e + M(\mathcal{X})$; the first term being bending moment of the perfectly elastic frame, the second term the moment originated be hinge-rotations $\mathcal{X}$ in the plastic hinges. Dividing the plastic hinges into "active" ($M = M_p$) and "inactive" ($|M| < |M_p|$) groups (of number i and $m-i$ respectively), the vector $\underline{M}$ representing the bending moments at the cross sections of the active plastic hinges can be written as

$$\underline{M} = \underline{M}_e + \underline{\underline{B}} \, \underline{\mathcal{X}} + \underline{\underline{A}} \, \underline{\mathcal{X}} = \underline{M}_p \tag{4}$$

where i-vector $\underline{M}_e$ represents the moments of an elastic frame, i-vector $\mathcal{X}$ the rotations in active, $m-i$ vector $\mathcal{X}_r$ the rotations

in the inactive plastic hinges; the elements b_{pq} and a_{pq} of
$i \times m-$ and $i \times i$ matrix $\underline{\underline{B}}$ and $\underline{\underline{A}}$ give the moment at cross-section
p of an elastic frame in presence of axial forces $\underline{N} = P.\underline{\beta}$ origi-
nated by an angular discontinuity $\mathcal{X}_q = 1$ in the cross section q.
Positiv direction of M and $\mathcal{X}$ is given in Fig.2. Sign-convention
is used to have $\underline{\mathcal{X}} \geq 0$ and $\underline{M} \geq 0$ in equation (4).
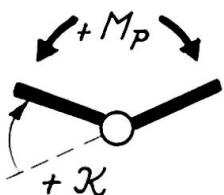
We shall refer to as "active loading
process" if at increasing load no
local unloading in plastic hinges
takes place. In this case no in -
active plastic hinges exist and

$$\underline{M} = \underline{M}_e + \underline{\underline{A}} \underline{\mathcal{X}} = \underline{M}_p \qquad (5)$$

Fig.2.

Stability considerations

Simplification introduced by equation (3) allows to formu-
late the condition of stability of the state of equilibrium
defined by equation (4) as follows:

$$\sum_b \left(\int_0^\ell EIy''^2 \, dx - P\int_0^\ell \beta_s \, y'^2 \, dx \right) = 0 \qquad (6)$$

for any function y describing geometrically possible transverse
displacements of the points of the members having angular dis-
continuities $\mathcal{X} \geq 0$ at the cross sections of active plastic hinges
only. To facilitate stability investigation, the state of equi-
librium defined by equation (4) (having i plastic hinges) should
be accompanied by an elastic subsystem "i" (Fig.3.), loaded by
axial forces $\underline{N} = P. \underline{\beta}$ only and
containing real hinges of
number i at the location of
plastic hinges. The lowest
critical load-factor causing
buckling of this subsystem is
denoted by $P_{cr,i}$ and is re-
ferred to as "deteriorated
critical load" in the litera-
ture [1]. The buckling-mode
of this subsystem at $P = P_{cr,i}$
be described by eigenfunction
$\tilde{y}_i$ (containing angular dis-
continuities $\tilde{\mathcal{X}}_i$ at the real
hinges).
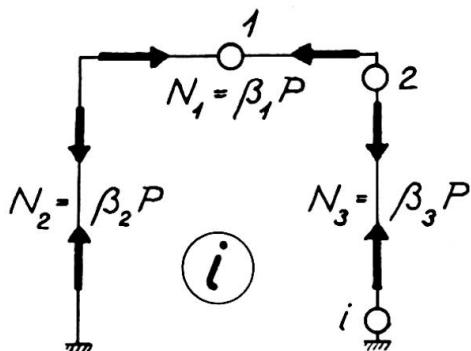
Fig.3.

Using above notations following statements can be done:

Theorem (I)

Supposed that at load factor P the elastic-plastic frame
contains i active plastic hinges:

If $P < P_{cr,i}$ the state of equilibrium is stable,

If $P_{cr,i} < P < P_{cr,i-1}$ ($P_{cr,i-1}$ being the lowest critical
load of an elastic subsystem containing i-1 hinges only)
two cases has to be dealt with:
If $\widetilde{\underline{X}}_i \geq 0$ the state of equilibrium is unstable,
If $\widetilde{\underline{X}}_i$ has negative component the state of equilibrium
                   is stable.

Quadratic programming approach

Starting from the state defined by equations (4) and chang-
ing load factor to P + dP, the incremental forces and deforma-
tions can be described:

$$d\underline{M} = d(\underline{M}_e + \underline{\underline{B}}\,\underline{X}_r) + d\underline{\underline{A}}\,\underline{X} + \underline{\underline{A}}\,d\underline{X} . \qquad (7.a)$$

Additionally the nature of plastic hinges requires:

$$d\underline{M} \leq 0; \qquad d\underline{X} \geq 0 \quad \text{and} \quad d\underline{X} . d\underline{M} = 0, \qquad (7.b)$$

as either incremental rotation or decrease of full-plastic moment
in the same hinge must be zero.

As pointed out elsewhere in the literature [9],[10] problems
of this kind can be solved by a quadratic programming approach,
as (7.a) and (7.b) can be written in form of

$$\underline{u} = \underline{a} - \underline{\underline{A}}\,\underline{x} \qquad (8.a)$$

$$u \geq 0; \qquad \underline{x} \geq 0 \quad \text{and} \quad \underline{x} . \underline{u} = 0 \qquad (8.b)$$

By introducing the scalar function

$$z(\underline{x}) = \underline{a}\,\underline{x} - \frac{1}{2}\,\underline{x}\,\underline{\underline{A}}\,\underline{x}$$

the solution of problem (8) can be defined as a non-negative
vector $\underline{x} = \underline{x}_1 \geq 0$, in case of which the value of function $z=z(x_1)$
doesn't exceed the values $z(\underline{x}_1 + d\underline{x})$ in its vicinity, provided
$\underline{x}_1 + d\underline{x} \geq 0$. By virtue of known mathematical theorems [11] a
solution always exist if $\underline{x}\,\underline{\underline{A}}\,\underline{x} < 0$ for $\underline{x} \geq 0$, $\underline{x} \neq 0$. As condi-
tion $\underline{x}\,\underline{\underline{A}}\,\underline{x} = d\underline{X}\,\underline{\underline{A}}\,d\underline{X} < 0$ for $d\underline{X} \geq 0$ is fullfilled in a stable
state of equilibrium, following statement can be done:

Theorem (II)

Starting from a stable state of equilibrium at load factor
P, equilibrium will exist at P + dP as well. Thus failure
load (peak load) can be reached only in an unstable state
of equilibrium.

If dealing with active loading process only and supposing
that plastic hinges can develop in cross sections of number i only
with given direction of rotation (chosen to be positiv), the mo-
ments and hinge-rotations at a load factor can be determined by
transforming equation (5):

$$\underline{M}_p - \underline{M} = \underline{M}_p - \underline{M}_e - \underline{\underline{A}}\,\underline{X} \qquad (9.a)$$

and considering additionally that according to the nature of
plastic hinges:

$$\underline{M}_p - \underline{M} \geq 0; \quad \underline{X} \geq 0 \quad \text{and} \quad (\underline{M}_p - \underline{M}) . \underline{X} = 0. \quad (9.b)$$

Problem (9) can be regarded as integrated form of (8), made equivalent by assuming that local unloading in plastic hinges is excluded. Problem (9) can be rewritten in form of (8) again and investigating the properties of $i \times i$ matrix $\underline{\underline{A}}$ (its components being function of P), we can state:

Theorem (III)

    If $P < P_{cr,i}$ there exists one and only one solution.

Theorem (IV)

    If $P_{cr,i} < P < P_{cr,i-1}$, the existence and number of solutions depend on the sign of the components of i-vector

$$\underline{\mathcal{X}}_o = \underline{\underline{A}}^{-1} (\underline{M}_p - \underline{M}_e)$$

    If all components of $\underline{\mathcal{X}}_o$ are positive ($\underline{\mathcal{X}}_o > 0$), two different solutions exist, one describing a stable, the other an unstable state of equilibrium.

    If all components of $\underline{\mathcal{X}}_o$ are non-negative, but at least one of them equals zero ($\mathcal{X}_{oj} = 0$), a single solution exists, describing an unstable state of equilibrium.

    If not all components of $\underline{\mathcal{X}}_o$ are non-negative, no solution exists.
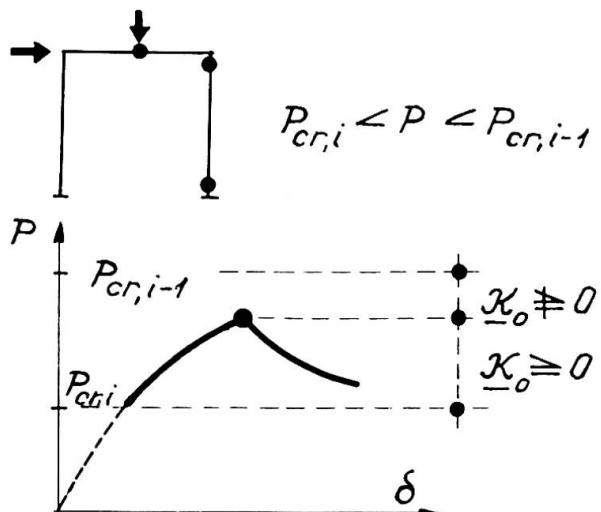

Fig.4.
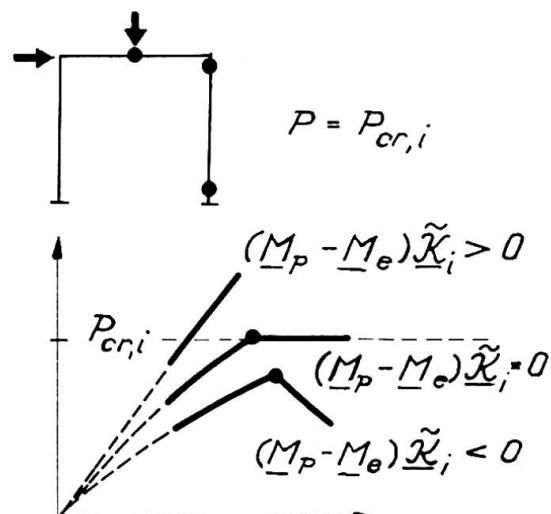
Fig.5.

Theorem (V)

    As special case let be $P = P_{cr,i}$. The existence and number of solutions depends on the sign of the scalar product $(\underline{M}_p - \underline{M}_e) \underline{\tilde{\mathcal{X}}}_i$.

    If $(\underline{M}_p - \underline{M}_e) \underline{\tilde{\mathcal{X}}}_i > 0$ one solution exists, describing a stable state of equilibrium.

If $(\underline{\mathbf{M}}_p - \underline{\mathbf{M}}_e)\,\underset{\sim}{\mathcal{X}}_i < 0$ no solution exists.

If $(\underline{\mathbf{M}}_p - \underline{\mathbf{M}}_e)\,\underset{\sim}{\mathcal{X}}_i = 0$ an infinite number of solution exists, describing indifferent states of equilibrium.

Theorem (IV) and (V) can be illustrated by Fig.4. and Fig.5.

Application I. Limit design of "stiff frames"

In a limit design problem the value of P_F be given and the flexural rigidity EI of the members and full plastic moment M_p of cross sections are to be determined. The design problem can be solved on various ways as both EI and M_p contribute to the value of the failure load. So additional restrictions can be given.

We require additionally, that failure should take place if the number of plastic hinges has reached the number n of plastic hinges contained in a yield-mechanism (rigid-plastic collapse-mechanism), thus $i = n$. Frames designed this way will referred to as "stiff frames". Supposing active loading process, theorems (I) – (IV) can be applied.

The subsystem n corresponding to a yield-mechanism is unstable in presence of any forces and thus $P_{cr,n} = 0$ can be taken and the corresponding buckling-mode (eigenfunction) $\tilde{y}_n$ coincides with the displacements of a rigid-plastic yield-mechanism, having angular discontinuities $\underset{\sim}{\mathcal{X}}_n$ most easily to determine. According to theorem (I) the chosen yield-mechanism prescribes not only the location, but possible rotational direction of plastic hinges as well, as $\underset{\sim}{\mathcal{X}}_n \geq 0$ has to be taken. The additional requirement given above states, that

$$0 < P_F < P_{cr,n-1}$$

$P_{cr,n-1}$ being the deteriorated critical load of a subsystem produced by removing any of the hinges in the yield-mechanism. As $P_{cr,n-1}$ can be written symbolically

$$P_{cr,n-1} = \frac{c_{n-1}\ EI}{L^2}$$

c_{n-1} being a constant, EI and L representing flexural-rigidity and geometrical data, the criterion for flexural rigidity can be given in the form

$$EI > \frac{L^2}{c_{n-1}}\,P_F \qquad (10)$$

The required values of full plastic moments $\underline{M}_p$ should be determined according to theorem (IV)

$$\underline{\mathcal{X}}_0 = \underline{\underline{A}}^{-1}(\underline{M}_p - \underline{M}_e) \geq 0 \quad \text{for } P \leq P_F \qquad (11)$$

This later requirement can be illustrated practically by Fig.6., as according to virtual-work considerations $\underline{\mathcal{X}}_0$ represents hinge-rotations of the frame under the action of external loads and full-plastic moments at the hinges of number n (axial forces supposed to be $\underline{N} = P.\beta$). Thus this method is equivalent to that referred to as "last hinge method" in the literature [1].
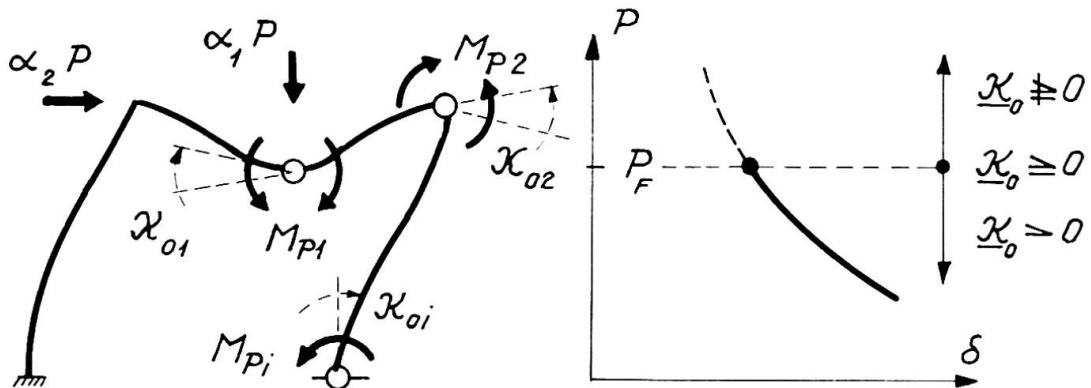
Fig.6.

If $m > n$, more than one yield mechanism should be considered. To make appropriate choice, following theorem can be used.

Theorem (VI)

Supposing active loading process, at

$$P = P_F < P_{cr,n-1}$$

the moments will not exceed the value of full plastic moment at any of the cross sections m, if unequality (11) is fullfilled for all groups of hinges of number n corresponding to a possible yield-mechanism.

This theorem can be formulated as a minimum principle for failure loads P_F computed with respect the different possible yield-mechanisms (Fig.7.) or as a maximum principle for a multiplier, if the ratio of full-plastic moments is previously prescribed.
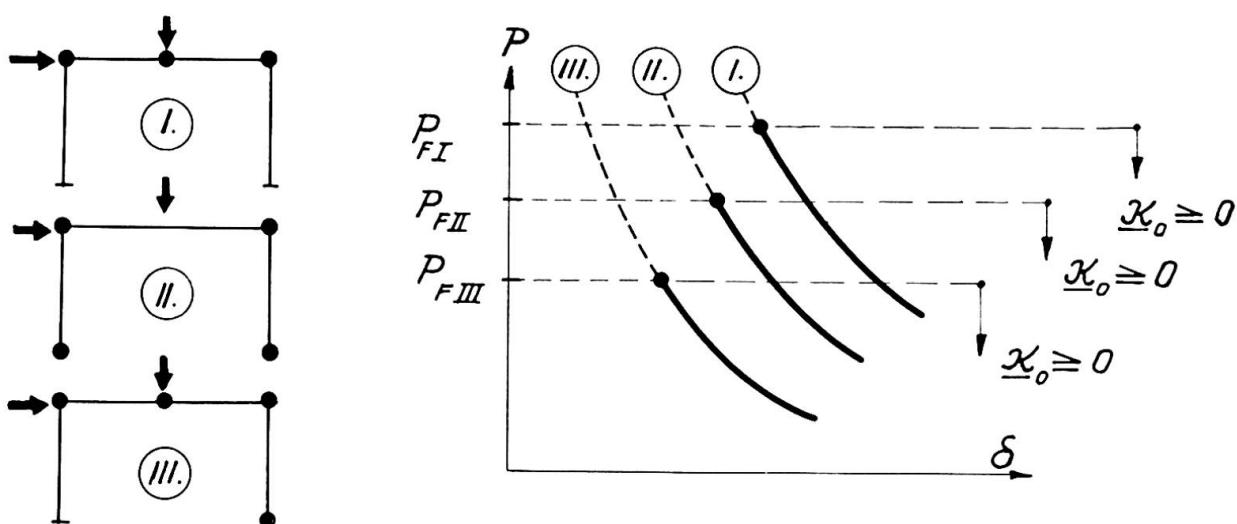
Fig. 7.

Application II. Limit design of "flexible frames"

If requirement (10) results in an unrealistic flexural rigidity, it has to be allowed to reach failure load in presence of a lower number of plastic hinges, than that transforming the structure into a yield-mechanism ($i < n$). Frames designed this way will referred to as "flexible frames". A possible way of limit design easy to carry out results from an additional restriction in form of

$$P_F = P_{cr,i} = \frac{c_i EI}{L^2} \quad , $$
$$EI = \frac{L^2}{c_i} P_F \tag{12}$$

which can be regarded as criterion for the flexural rigidity required.

Using theorem (V) the values of full-plastic moments in cross section i can be determined as – supposing active loading process – equilibrium can exist at $P = P_{cr,i}$ only if:

$$(\underline{\underline{M}}_p - \underline{\underline{M}}_e) \, \underset{\widetilde{}}{\underline{\mathcal{X}}}_i \geq 0$$

This condition can brought to a more convenient form by using virtual work consideration, resulting in

$$P_F \sum_{\circlearrowleft} \alpha_j \, \tilde{u}_j \; \leq \; \underline{\underline{M}}_p \, \underset{\widetilde{}}{\underline{\mathcal{X}}}_i \tag{13}$$

where $\tilde{u}_j$ and $\underset{\widetilde{}}{\underline{\mathcal{X}}}_i$ represent the displacements and hinge-rotations due to the buckling-mode (eigenfunction $\tilde{y}_i$) of the plastic subsystem "i" at $P = P_F = P_{cr,i}$ (Fig.8.). This inequality resembles the virtual-work inequality used in a single-plastic limit analysis, but displacements and rotations of a rigid-plastic yield mechanism should be replaced by those belonging to the buckling-mode described by eigenfunction $\tilde{y}_i$.
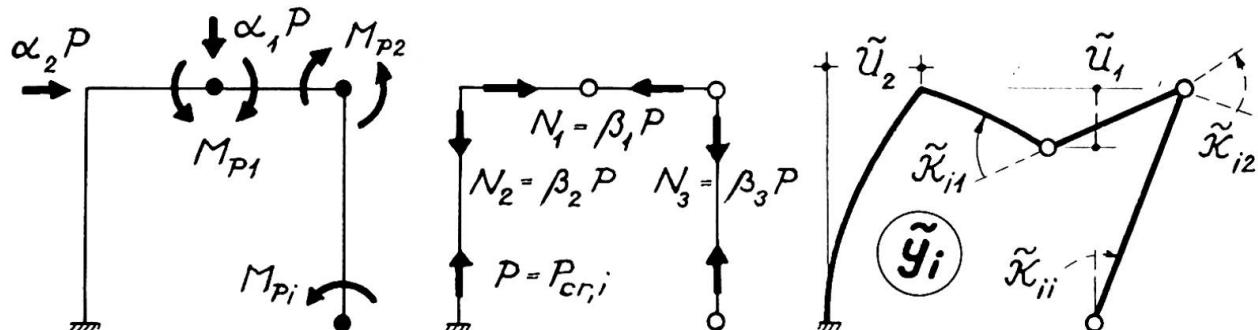
Fig.8.

Using this method an additional check must be carried out with respect to the moments at cross sections being not represented as possible locations of plastic hinges in the subsystem.

Application III. Bifurcation of equilibrium

Attention is to be paid to the fact, that the assumption of active loading process disregards the possibility of bifurcation of equilibrium which can take place in stable state of equilibrium as well [6], due to the "two-faced" nature of plastic hinges.

As illustrativ example a symmetric and symmetrically loaded frame should be regarded with only two possible locations 1. and 2. for plastic hinges, assuming that at a load factor

$$P_{cr,2} < P < P_{cr,1}$$

($P_{cr,1}$ and $P_{cr,2}$ denoting the deteriorated critical load of a subsystem containing one and two real hinges respectively) both plastic hinges are active (Fig.9.).
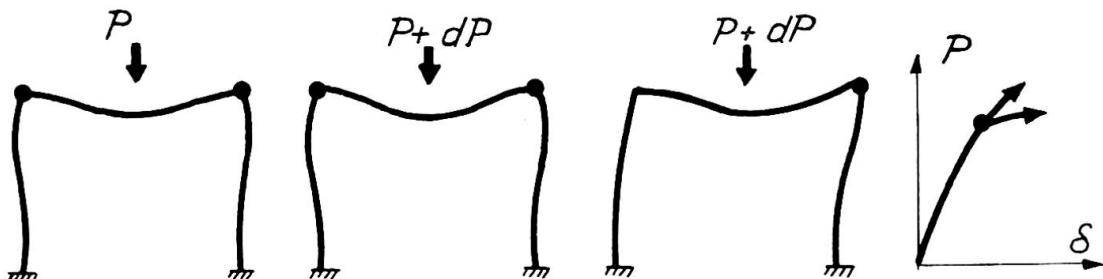
Fig.9.

The possible direction of rotation in plastic hinges is given and taken to be positive. As the buckling-mode at $P = P_{cr,2}$ of the subsystem containing two real hinges is antimetric, according to theorem (II) $\tilde{\mathcal{X}}_2 \not> 0$ and the equilibrium is stable.

Analysing incremental deformations by equation

at P $\qquad \underline{M} = \underline{M}_e + \underline{\underline{A}} \, \mathcal{X} \,,$

at $P + \triangle P$: $\quad d\underline{M} = d\underline{M}_e + d\underline{\underline{A}} \, \mathcal{X} + \underline{\underline{A}} \, d\mathcal{X}$

$$d\underline{M} \le 0, \quad d\mathcal{X} \ge 0, \quad d\underline{M} \cdot d\mathcal{X} = 0$$

Supposing now, that at $P + \triangle P$ a symmetric state of equilibrium with two active hinges exists,

$$d\underline{M} = 0 \quad \text{and}$$

$$d\mathcal{X} = \underline{\underline{A}}^{-1} (d\underline{M}_e + d\underline{\underline{A}} \, \mathcal{X}) > 0,$$

according to theorem (IV) a second solution exists. Thus at P, although having stable state of equilibrium two different loading paths are possible: a symmetric one and another including side-sway as well.

Appendix

As illustration, the prove of theorem (IV) is given as follows:

(a) If $P_{cr,i} < P < P_{cr,i-1}$ and $\tilde{\underset{\sim}{\mathcal{X}}}_i$ angular discontinuities of eigenfunction $\tilde{y}_i$ are all positive

$$\underset{\sim}{\mathcal{X}} = \underset{=}{A}^{-1}\, \underset{\sim}{M} \geq 0, \quad \text{when} \quad \underset{\sim}{M} \geq 0 \qquad (14)$$

This can be proved by describing the displacements of the structure originated by moments $\underset{\sim}{M}$ acting at the hinges by function y and rotations $\underset{\sim}{\mathcal{X}}$ and investigating the expression

$$\sum_{\delta} \left[EI \int_0^\ell \left(y'' + c_j \tilde{y}_i''\right) dx - P\beta_\delta \int_0^\ell \left(y' + c_j \tilde{y}_i'\right)^2 dx \right] > 0 \qquad (15)$$

$$c_j = - \frac{\mathcal{X}_j}{\tilde{\mathcal{X}}_{ij}} \qquad (16)$$

as $y + c_j\, y_i$ are geometrically possible displacements of subsystem "i-1" being stable at $P < P_{cr,i-1}$. Transforming and regarding the virtual work equations

$$\underset{\sim}{M}\,\underset{\sim}{\mathcal{X}} = -\sum\left(EI \int_0^\ell y''^2 dx - P\beta_\delta \int_0^\ell y'^2 dx\right),$$

$$\underset{\sim}{M}\,\tilde{\underset{\sim}{\mathcal{X}}}_i = -\sum_{\delta}\left(EI \int_0^\ell y''\tilde{y}_i'' dx - P\beta_\delta \int_0^\ell y'\tilde{y}_i' dx\right),$$

we receive:
$$-\underset{\sim}{M}\,\underset{\sim}{\mathcal{X}} - 2\,\frac{\mathcal{X}_j}{\tilde{\mathcal{X}}_{ij}}\,\underset{\sim}{M}\,\tilde{\underset{\sim}{\mathcal{X}}}_i > 0 \qquad (17)$$

Multiplying by $\mathcal{X}_{ij}\, M_j > 0$ and adding up similar expressions for $j = 1,2 \ldots i$:

$$(\underset{\sim}{M}\,\underset{\sim}{\mathcal{X}})\,(\underset{\sim}{M}\,\tilde{\underset{\sim}{\mathcal{X}}}_i) > 0 \qquad (18)$$

which together with equation (17) proves statement (14).

The solution of problem (9) can be written in the form

$$\underset{\sim}{\mathcal{X}} = \underset{=}{A}^{-1}(\underset{\sim}{M}_p - \underset{\sim}{M}_e) - \underset{=}{A}^{-1}(\underset{\sim}{M}_p - \underset{\sim}{M}) \geq 0, \qquad (19.a)$$

$$\underset{\sim}{M}_p - \underset{\sim}{M} \geq 0 \quad \text{and} \quad (\underset{\sim}{M}_p - \underset{\sim}{M})\,\underset{\sim}{\mathcal{X}} = 0. \qquad (19.b)$$

As the second term in (19.a) according to (14) is non-negative, $\underset{\sim}{\mathcal{X}} \geq 0$ is impossible if

$$\underset{=}{A}^{-1}\,(\underset{\sim}{M}_p - \underset{\sim}{M}_e) \not\geq 0,$$

and no solution exists.

If

$$\underset{\sim}{\mathcal{X}}_o = \underset{=}{A}^{-1}\,(\underset{\sim}{M}_p - \underset{\sim}{M}_e) > 0, \qquad (20)$$

one solution is given by (20). A second solution can be found as well. With reference to those stated earlier in connection with problem (8), a local minimum of the function

$$z(\underline{x}) = (\underline{M}_p - \underline{M}_e)\underline{x} - \frac{1}{2} \underline{x} \; \underline{\underline{A}} \; \underline{x} \qquad (21)$$

in the subspace $\underline{x} \geq 0$ will define a solution. Chosing one component of $\underline{x}$ to be $\overline{x}_j = 0$, and omitting all elements of $\underline{M}_p$, $\underline{M}_e$ and $\underline{\underline{A}}$ with indices j, we have an $i - 1 -$ dimensional expression

$$\widetilde{z}(\widetilde{\underline{x}}) = (\widetilde{\underline{M}}_p - \widetilde{\underline{M}}_e) \; \widetilde{\underline{x}} - \frac{1}{2} \widetilde{\underline{x}} \; \widetilde{\underline{\underline{A}}} \; \widetilde{\underline{x}} \qquad (22)$$

which has always a minimum (denoted by $\dot{z}_{j,min}$) for $\widetilde{\underline{x}} \geq 0$ as because of $P < P_{cr,i-1}$ $\widetilde{\underline{\underline{A}}}$ is negative definite. The value $z_{j,min}$ is therefore a minimum on the boundary-plane of subspace $\underline{x} \geq 0$ defined by $x_j = 0$. A series of such minimums can obtained by chosing $j = 1,2...i$. This among them having the lowest value be denoted by $\widetilde{z}_{min}$ (at a location given by $\widetilde{\underline{x}}_0$).

Considering equations (20), (21) and (22) the values of function $\widetilde{z}$ on the boundary of subspace $\underline{x} \geq 0$ can be expressed as

$$\widetilde{z} = \frac{1}{2} \underline{x}_0 \; \underline{\underline{A}} \; \underline{x}_0 - \frac{1}{2} \underline{r} \; \underline{\underline{A}} \; \underline{r} \qquad (23)$$

where $\underline{r}$ denotes the vector between point $\underline{x} = \underline{x}_0$ and the point on the boundary. As because of $P_{cr,i} < P$ $\underline{\underline{A}}$ is indefinite, the boundary contains points, where

$$\widetilde{z} < \underline{x}_0 \; \underline{\underline{A}} \; \underline{x}_0$$

and so

$$\widetilde{z}_{min} < \frac{1}{2} \underline{x}_0 \; \underline{\underline{A}} \; \underline{x}_0 \; ; \qquad \underline{r}_0 \; \underline{\underline{A}} \; \underline{r}_0 > 0, \qquad (24)$$

where vector $\underline{r}_0$ connects points given by $\underline{x}_0$ and $\widetilde{\underline{x}}_0$. Equation (23) and (24) prove, that z_{min} is a minimum on the boundary and a local minimum in the subspace $\underline{x} \geq 0$, thus defining a second solution of problem (19), representing a stable state of equilibrium, being z_{min} on the boundary of the subspace $\underline{x} \geq 0$. A third solution is impossible, as supposing its existence $\widetilde{\underline{x}}_0'$ and using notations of problem (8)

$$\underline{u} = \underline{a} - \underline{\underline{A}} \; \widetilde{\underline{x}}_0 \; , \qquad \widetilde{\underline{x}}_0 \geq 0, \qquad \underline{u} \geq 0, \qquad \underline{u} \cdot \widetilde{\underline{x}}_0 = 0$$

$$\underline{u}' = \underline{a} - \underline{\underline{A}} \; \widetilde{\underline{x}}_0' \; , \qquad \widetilde{\underline{x}}_0' \geq 0, \qquad \underline{u}' \geq 0, \qquad \underline{u}' \cdot \widetilde{\underline{x}}_0' = 0$$

would require

$$(\widetilde{\underline{x}}_0 - \widetilde{\underline{x}}_0') \; \underline{\underline{A}} \; (\widetilde{\underline{x}}_0 - \widetilde{\underline{x}}_0') > 0,$$

which is impossible according theorem (I), as the vector $\widetilde{\underline{x}}_0 - \widetilde{\underline{x}}_0'$ connecting two points on the boundary of subspace $\underline{x} \geq 0$ can't be composed of non-negative components only.

Literature

1 M.R.HORNE: The stability of elastic-plastic structures, in:
        Prog.in Sol.Mech., Vol. II. North-Holland Publ.
        Amsterdam, 1961.

2 R.K.LIVESLEY, The application of computers to problems in-
        volving plasticity. Proc.Symp.Use of Electronic
        Computers in Struct.Engng. Univ. of Southampton,1959.

3 M.R.HORNE, W.MERCHANT, The stability of frames. Pergamon
        Press 1965.

4 U.VOGEL, Die Traglastberechnung stählerner Rahmentragwerke
        nach der Plastizitätstheorie II. Ordnung.
        Stahlbauverlag Köln, 1965.

5 L.S.BEEDLE, Ductility as a basis for steel design, in:
        Engineering Plasticity, Cambridge, 1968.

6 R.HILL, A general theory of uniqueness and stability in
        elastic-plastic solids. Journal of the Mechanics and
        Physics of Solids, 1958, Vol.6.

7 O.HALÁSZ, Design of elastic-plastic frames under primary
        bending moments, Periodica Polytechnica, Vol.13.,
        No.3-4. Budapest 1969.

8 O.HALÁSZ, Limit design of steel structures. Report of Dept.
        for Steel Structures, Technical University Budapest
        1969. (Manuscript)

9 G.MAIER, A quadratic programming approach for certain classes
        of non linear structural problems.
        Meccanica, No.2. Vol.III. 1968. Milano.

10 G.MAIER, Quadratic programming and theory of elastic-per-
        fectly plastic structures.
        Meccanica, No.4., Vol.III. 1968. Milano.

11 H.P.KÜNZI, W.KRELLE, Nichtlineare Programmierung,
        Springer Verl. Berlin, 1962.

Summary

The second order limit analysis — including the effect of
change in geometrie — of certain class of frames can be simpli-
fied by assuming (i) axial forces to increase proportionally to
a load factor (ii) disregarding local unloading in plastic
hinges and (iii) taking full-plastic moments to be independent
of axial forces. Using these assumptions paper offers some
theorems to be used in preliminary limit design of frames.

The Influence of Plasticity and Viscosity on the Strength and Deformation of Structures

L'influence de la plasticité et de la viscosité sur la résistance et la déformation des constructions

Der Einfluss der Plastizität und der Viskosität auf die Traglast und die Verformung von Tragwerken

A.M. FREUDENTHAL
Professor
George Washington University
Washington, D.C., USA

1. Material Behavior

1.1 Elasticity

Of the various mechanical properties that determine the usefulness of a structural material, its elastic modulus is undoubtedly the single most important one since it alone determines wether the material is rigid enough to satisfy the limitations on deformability that are imposed on any structure by its function and that usually delimit its "serviceability." Although the elastic modulus is also directly proportional to the cohesive strength of the material[1] since, theoretically at least, both can be related to the action of interatomic or intermolecular forces, it has long been recognized that materials that attain a significant portion of their theoretical cohesive strength while strained elastically are not usable as structural materials, because the unavoidable inhomogeneities in their microstructure are bound to cause premature "brittle" fractures that are not only the more explosive the higher the level of elastic strain energy stored in the volume element and suddenly released at fracture, but also the less predictable or reproducible. Therefore, a useful structural material, expected to deform elastically within the limit of serviceability of the structure, must be prevented from explosively failing elastically beyond this limit by energy disipation mechanisms in its microstructure that prevent the build-up of potentially destructive elastic strain energy as soon as the forces acting on the structure exceed its serviceability limit. The avoidance of brittle failure by providing structural materials the deformational response of which to forces beyond the limit of serviceability deviates from elasticity not only sufficiently but also sufficiently fast to achieve this aim under all loading and environmental conditions which structures must, with an adequate level of confidence, be expected to withstand, is one of the foremost tasks of the material .producing industry.

1.2 Plasticity and Viscosity of Structural Materials.

Plasticity and viscosity are the phenomenological expressions of the two basic strain energy disipation processes in the metallic microstructure: the weakly strain-rate and temperature sensitive transgranular (plastic) slip and the strongly strain-rate and temperature sensitive inter-granular (quasi-viscous)flow. While in all metals both mechanisms are simultaneously present as soon as the limit of technologically elastic deformation is exceeded (the true physical elastic limit is lower and depends essentially on the limit of accuracy with which deviation from linear elastic behavior can be observed), one or the other will predominate as the loading and environmental conditions change, with low temperatures or high strain-rates suppressing the viscous response, while high temperatures and low strain-rates amplify it. The post-elastic response of structural metals at room and low temperatures is therefore reasonably well represented by plastic flow with constant or strain-dependent (hardening) yield-limit, while the operational stress level in the structural members is governed by the elastic response, although it is well-known that the full utilization of the elasticity of the members depends on sufficient constrained plastic deformation in the overstrained connections being available to prevent localized elastic (brittle) failures through overstrain.

In the non-metallic microstructures of ceramics and concrete almost linear quasi-viscous flow characterizes the binder already at very low stresses[2], so that a real "elastic limit" does not exist, while a highly nonlinear viscosity which is almost indistinguishable from "plasticity" is the expression, at stress-levels closer to the unconfined com-pressive (shear) strength, of processes of progressive destruction of the microstructure. Thus, structural concrete is a linear visco-elastic material at any stress above zero, so that the limit of serviceability of concrete structures, particularly at relatively high sustained compressive operational stresses, cannot be identified with the complete absence, but only with a specified limiting amount of irreversible deformation, a limitation that is made possible by the asymptotic increase of the apparent coefficient of viscosity of the con-crete in the course of the hardening process that transforms the initial visco-elastic into the fully hardened elastic compound. Experiments[3] have shown that the range of linear visco-elasticity does not extend beyond a stress level of 25 to 30 percent of the compressive strength, which is the usual range of operational stresses. Beyond this stress-intensity the viscous response of the material becomes increasingly non-linear until, at about 80 percent of the compressive strength it is, on first loading,

indistinguishable from plastic response since the associated
destruction proceeds at constant stress. Thus, the linear
visco-elastic response of the concrete governs the range of
serviceability of the structure. As the viscous component
becomes increasingly non-linear in stress at stress levels
beyond this range, stress relaxation processes governing
prestress levels become increasingly rapid, with the result that
the higher the prestress, the more difficult to sustain it.
In heavily overreinforced beam sections the effect of the
highly non-linear viscous redistribution of stresses as well
as of moments produces the deceptive appearance of "plasticity"
of the concrete. However, this plasticity cannot, as in
metals, be depended upon to produce a reliable "overloading
capacity" that could be sustained under repeated loading or
that could lead to a "shakedown" condition under load
repetition, since the increasing local destruction of the
microstructure that is reflected in the increasing non-linearity
of the apparent viscosity of the concrete leads to rapid
large-scale destruction of the overstrained compressive zone
after a relatively small number of load-cycles. Only in
underreinforced beams does the plastic yielding of the metal
reinforcement at low concrete stresses produce conditions
resembling "plastic hinges",[4] however, at the usually
unacceptable price of large, concentrated cracks in the
concrete. The extension of rigid-plastic limit analysis to
redundant reinforced concrete is therefore not without
serious problems.[5]

2. Design Criteria

    The influence of plasticity and of viscosity on the
strength and deformation of structures and thus on their
analysis and design can hardly be adequately assessed or
even discussed without carefully considering the implications
of the dual design requirements of serviceability and failure
resistance as well as of the relations to these requirements,
of plasticity or near plasticity on the one hand (highly
non-linear viscosity) and of plasticity and quasi-linear
viscosity on the other. Unfortunately the Introductory
Report misses these critical implications almost completely
and presents, instead, a simplistic rigid-plastic limit
analysis of one-parametrically loaded steel structures as
well as a simplified version of linear-viscoelastic analysis
applicable to reinforced concrete structures, presumably as
representative illustrations of the "state of the art" in the
field of research and engineering practice encompassed by
Theme Ia. And this in spite of the fact that every single one
of the eight preceding International Congresses of IABSE has
devoted part of its attention to some aspect of this theme, and that

in the Proceedings of these eight Congresses as well as in
the Memoir volumes published by the Association many of the
pioneering papers on the various aspects of the influence of
plasticity and viscosity on strength and deformation of
structures have been published.

2.1   Plastic Limit Design

However, the reader of this Introductory Report which is
intended, presumably, to prepare the ground for the discussion
of this theme at the Ninth Congress would never suspect this
preoccupation over many years on the part of IABSE. Nor is
he made aware of the general perspective that has emerged
from this preoccupation and that reflects a balance between
the applied mechanics, the materials engineering, and the
structural design view-points relating to this theme, which
would seem to preclude juxtapositions like that between the
pre-1940 "pessimistic" elastic theory and the post-1940
"optimistic" plastic theory[6], as if anybody concerned with the
ultimate carrying capacity of structures, from Galileo and
Mariotte to the research workers in the nineteen forties,
had ever seriously considered the elastic theory as a
procedure for the determination of a "failure load" or
carrying capacity, or as if the purpose of the plastic theory
were to replace the elastic theory that "refers to a
physically unrealistic limit state" by a method "that is in
agreement with experimental results" and makes it possible to
"refer the safety of statically determinate and indeterminate
structures to the uniform base of a real limiting state
(failure mechanism)" (p. 9).

This exaggerated assessment of the relevance of the
theory of rigid-plastic limit design is obviously compatible
neither with the dual aspect of design for serviceability and
failure nor with those experimental results that contradict
even for structures of low redundancy the assumption of this
theory that the full plastic carrying capacity associated with
the fully developed failure mechanism can actually be
attained in spite of the fact that the large plastic hinge
rotations required for its development are frequently preceded
by local instability phenomenon that cause premature failure
below the full plastic moment. In a basic paper Stüssi[7] has
in fact demonstrated by an extremely simple experiment that the
real carrying capacity of a redundant structural beam of mild
steel lies somewhere above the limiting elastic but below the
fully plastic carrying capacity. The failure of redundant
metal structures to attain their full plastic carrying capacity
has also been demonstrated in many other experiments[8], and the
rules that have to be followed to ensure this carrying capacity[9]
can be successfully applied only to a very narrow range of
structural types.

    The orthodox adherents of plastic limit design also chose
to discount the practical relevance of the results of experiments
on structures loaded by movable or reversed loads or by repeated
loads or loads of variable intensity and/or configuration which
have conclusively shown[10] that the limiting loads reached in
plastic shake-down processes are much closer to the elastic than
to the plastic limit loads, so that the range of applicability
of the simple plastic limit load analysis is, in fact, severely
restricted and becomes doubtful even in the case of multiple
floor frame structures of heights at which the wind stresses in
the principal members attain intensities comparable to the
load-stresses. The small differences between the results of
shake-down analysis and of elastic analysis makes it, in fact,
appear that under the many conditions under which shake-down
analysis would be necessary, elastic analysis with limiting
conditions derived from low-cycle fatigue tests is fully adequate.

2.2 Elastic-Plastic Analysis.

    In their assessment of the rigid-plastic limit analysis for
metal structures as "more realistic than the elastic analysis"
(p. 9) the authors of the Introductory Report[6] subscribe to the
thesis that rigid-plastic analysis, being superior to the
elastic analysis, makes the latter superfluous and can therefore
completely replace it, independently of the nature of the
phenomena arising in the transition from the assessed rigid
(in reality elastic) into the fully plastic state. Most of
the relevant references of the Introductory Report subscribe
to this point of view, from which it follows that theoretical
and experimental investigations of this transition have been
and are, from an engineering point of view, unnecessary; their
results are, therefore, best relegated to oblivion being
irrelevant: they either support the assumptions of plastic
limit-analysis, in which case they are "self-evident", or
they contradict it, in which case they are unwelcome. The
list of references of the Introductory Report reflects this
point of view clearly, though perhaps not deliberately: after
the usual courtesy to Kazinczy (1914) and Kist (1917)[11], the
next reference to plastic analysis dates from 1951. The
period of the really pioneering experimental and analytical
engineering research relative to plasticity and structural
design between 1920 and 1940, in the course of which the basis of
the plastic limit analysis has been carefully established, and
many of the important results of which can be found in the
IASBE Congress Proceedings has, therefore, been deleted from
memory. As far as the reader of the Introductory Report is
concerned, the basic research on the subject of Theme Ia by
J. Fritsche[12], E. Melan[13], H. and F. Bleich[14], Chwalla[15], Stussi[7],
and others[16] might have never been done, nor might this theme
have ever attracted the attention of a previous IABSE Congress.

This curious distortion of perspective, reinforced by the statement that "until 1940 the only method taught and applied was elastic theory" reflects the suprisingly widely held belief that plastic limit design somehow originated in England at about 1950. This belief may have arisen because at the Fourth IABSE Congress (1952) the English group not only completely dominated the proceedings on Theme I3 (Plastic Design), but also consistently omitted to refer to any work done before 1950, except for an oblique reference to Meier-Leibnitz as "having first introduced the concept of the plastic hinge," although in his classic survey of the experimental work in structural plasticity[8], Meier-Leibnitz rather than "introduce" the concept of the plastic hinge has scrutinized the experimental evidence and, on this basis, carefully discussed and specified the conditions limiting the application of this concept in design.

2.3 Decision Rules.

The Introductory Report puts considerable emphasis on the fact that problems of plastic limit analysis can be formulated as problems in linear programming, so that computerized plastic analysis and automatic minimum weight design on this basis can be expected to replace most of the effort of the designer. It should be remembered, however, that apart from the physical limitations of the validity of such analysis, the question of when or whether a minimum weight or minimum material cost criterion provides a valid decision rule for structural design, or whether such a rule leads to a unique answer has never been even formulated. In the absence of a clear answer it appears that a minimum weight or minimum material cost criterion may not produce a minimum cost design, in view of the fact that in structures the cost of labour (fabrication, erection) is inversely rather than directly proportional to the weight of the material.

2.4 Linear Visco-elastic Analysis of Concrete.

The Introductory Report recommends the theory of linear visco-elasticity as a basis for the analysis of reinforced concrete structures, referring to creep experiments that were limited to low compressive stress levels for support of this recommendation. While the application of linear-visco-elastic analysis within the range of applied operational stresses can thus be justified, the difficulty arises of selecting visco-elastic models relevant for loads of long duration on the one hand, and loads of relatively short duration and dynamic loads on the other. Attempts to cover the whole time-range with a single model are futile since differential models would involve differential quotients of too high order to permit complete specification of initial conditions for the solution of problems, while the experimental determination of a memory function for a Boltzman integral representation presents

practically unsurmountable difficulties.[18] Obviously, the
Kelvin model, suggested in the Introductory Report, is identical
with the elastic medium for loads of long duration and completely
useless for dynamic loads because of the unlimited increase
of its damping with frequency. It has been shown that Burgers
model[19] with parameters derived from tests of long duration
containing a nonlinear "dashpot" that may become linear for
low stresses is the simplest representation of the long-term
mechanical response of concrete, to be used for analysis of
dead load stresses and deformations, as well as of other long-
term phenomena such as shrinkage and temperature stresses as
well as of the effect of creep and relaxation on prestress-
level and deformation of prestressed structures. For
operational stresses of short duration and dynamic effects the
Standard Solid[20] with short-time parameters seems adequate.

It appears that students nowadays do not spend enough
time on exploring the literature in the field of their
intended research before starting their own work, as otherwise
the student referred to in the Introductory Report (p. 12)
could have found that problems of increase, with time, of
"second order" moments (moments in the deformed structure) due
to creep, particularly in flat, long span arches where this
increase tends to lead to instability[21] ("creep-buckling"),
as well as of unexpectedly large relaxation of prestress due to
the non-linearity of the creep[3] have been analytically
treated quite some time ago. This knowledge might have induced
him to expand his research beyond the limits of previous
research efforts, considering, for instance, that it has been
shown that even within the stress-range within which the use of
linear visco-elastic theory is applicable, the fact of the
increase with time of the coefficients of viscosity of the model
due to time-hardening of the concrete, which requires the
replacement of these parameters by time functions, severely
curtails the usefulness of the correspondence principles,
since it leads to differential equations with variable coefficients
that have no correspondence in elastic theory and can usually
not be solved in closed form. These difficulties, which arise
from the discrepancy between the assumptions of linear visco-
elastic theory and the behavior of a real material like concrete,
must be carefully considered in the application of this theory
as a method of structural anaylsis.

2.5 Non-linear and Failure Analysis of Reinforced Concrete.

Problems of non-linear analysis of reinforced concrete,
as distinct from failure analysis, are of limited practical
significance and arise only when compressive stresses in
the concrete attain between one third and two thirds of the
unconfined compressive strength while the reinforcement remains
elastic. Such conditions, which are rarely considered in design,

cause, where they occur, moderate redistribution of elastic
stresses and moments and can be repeatedly applied without
producing deterioration of the micro-structure followed by
destruction of the concrete or abnormal cracking in the
tension zone.

Failure of reinforced concrete sections subject to
transient,sustained or repeated bending moments is initiated
either when the compressive stress attains not less than 80 to
85 percent of the compressive strength under single load
application, or when the stress in the reinforcement attains
the yield limit or the fatigue strength associated with the
number of load cycles, or both. While a substantial "plastic"
redistribution of stresses and of bending moments may
accompany the gradual crushing of the concrete or the plastic
yielding of the reinforcement, the state attained is one of
incipient or progressive destruction; it is not comparable,
in its implications, to the "plastic resistance" of metals
which is accompanied by a capacity for substantial, irreversible,
but non-destructive deformation. This is the reason that the
early analysis of similar conditions in reinforced plates was
not introduced as plastic design, but as failure or rupture
design and the traces of destruction as "rupture lines",
in accordance with the realistic assessment of this condition,
which is missing in the more recent attempts to apply plastic
limit analysis to reinforced concrete. The objections to these
attempts have been clearly summarized by G. Winter at the
Miami Symposium[22] and repeated in the Introductory Report,with
implied dissatisfaction at the "reluctance of the engineers
to exploit the inelastic phenomena in beams". This
reluctance is, however, well founded, and can hardly be
compensated by the "advantages" of mathematical optimization
of the design in terms of "economic functions" of similarly
dubious engineering relevance as in the case of plastic design
of metal structures for minimum weight or minimum material cost.

The fact that design for failure[2,3]utilizing lines of
rupture, can be successfully applied to the prediction of the
carrying capacity of plates does not imply that this procedure
represents a kinematic limit design as understood in the theory
of plasticity. Such plates are usually under-reinforced and
fail simultaneously within the span and along the (fixed or
continuous) supports by yielding of the reinforcement, with
heavy fissurization of the concrete; problems of moment-
redistribution and capacity of hinge,rotation do not arise.

Extension of this method to shells is difficult and
uncertain, particularly because of the effect of creep due to
the sustained compressive forces. The recommendation of the
Introductory Report to obtain the necessary information for
creep failure analysis of reinforced concrete shells from

model tests using "a material that represents as closely as
possible the real material" is, in fact, a call for full-scale
testing since the rules of similitude preclude meaningful
structural model tests with reduced geometric dimensions but
unchanged material rigidity and creep response.

3. Design Procedures.

It appears from the Introductory Report that there is a
divergence in the approach to "limit-design" between those
concerned with steel structures and those concerned with
reinforced concrete structures. While the former seem to
consider limit-design for plastic collapse as the unique
design procedure, to be applied to the exclusion of any other
and in particular of elastic design, thus completely dis-
regarding the dual aspect of design for operation (serviceability)
and design against failure (reliability), the latter, becoming
increasingly conscious of the fact that between the stages of
the first appearance of fine cracks in the concrete and final
structural failure (usually by collapse due to a mixture of total
and partial destruction of the resistance of a relatively
small number of critical section) there are many intermediate
stages, seem to have developed the belief that engineering
design should, ideally, consist in matching of the structural
resistance at several intermediate stages with their "corresponding
loads" and associated probabilities of occurence[24]. This latter
point of view as much over states the complexity of the design-
problem as the former under states it. In the Preliminary
Publication of the Eighth IASBE Congress an attempt was made
to present the principal aspects of the probabilistic approach
to safety[25], which provides the only rational way to a balanced
design procedure, and to discuss the effect of the deformational
response of the structural material on this procedure[26]. In the
light of this discussion it can be concluded that the consid-
eration of "intermediate" stages between the limits of
serviceability and of failure, which would have to include
consideration of their respective statistical dispersions, com-
plicates the procedure unnecessarily, since only in the cases
of very costly structures subject to purely stochastic
destructive loads, such as sea-walls, break-waters and off-
shore platforms as well as, perhaps, tall buildings subject to
earthquakes does it become necessary to consider conditions of
partial damage, so that the cost of repair of structural
damage associated with such pre-failure (intermediate) conditions
which, in decision theory, are known as conditions of "success-
loss", may strongly affect the design decisions[27]. This is,
however, not the case in the design of the majority of engineering
structures for operational loads for which, therefore, the
recommendation of CEB to design for the two criteria of
serviceability and of failure seems fully adequate. It would be
desirable to use the same approach also in the design of metal
structures.

References

1. Kelly A., Strong Solids, Oxford University Press (1966),
   1-35.
2. Bingham E.C. and Reiner M., The rheological properties
   of cement and cement-mortar-stone, Physics vol. 4
   (1933) 88-96
3. Freudenthal A.M. and F. Roll, Creep and Creep Recovery
   of Concrete under High Compressive Stress, J. Am.
   Concrete Inst. vol. 29 (1958) 1111-1142. (also RILEM
   Symposium, Munich 1958 Bull. No. 3, 1959
4. Melan J., Das plastische Verhalten des Betons, Beton &
   Eisen, vol. 31 (1932) 548
   Kazinczy G. v., Das plastische Verhalten von Eisenbeton,
   Beton & Eisen, vol. 32 (1933), 74-80
5. Freudenthal A.M., Plastizitaetstheoretische Methoden
   bei der Untersuchung statisch unbestimmter Tragwerke
   aus Eisenbeton, Memoirs IABSE vol. 2 (1933-34) 180-192.
6. Massonnet Ch. and Save M., L'influence de la plasticite
   et de la viscosite sur la resistance et la deformation
   des constructions. Introductory Report Ninth Congress
   IABSE (1972), 18.
7. Stüssi F. and Kollbrunner, Beitrag zum Traglastverfahren,
   Bautechnik, vol. 13 (1935) 264
   Stüssi F., Zur Auswertung von Versuchen uber d. Traglast-
   verfahren, Final Report, Second Congress IABSE (1936)
   74-76.
8. Meier-Leibnitz H., Test Results, their Interpretation and
   Application. Preliminary Publication, Second Congress
   IABSE, Berlin (1936) 103-136.
9. Reference 29 of Introductory Report, Ninth Congress IASBE
   by Massonnet and Save [6].
10. Grüning M., Die Tragfähigkeit unbestimmter Tragwerke aus
    Stahl bei beliebig häufig wiederholter Belastung,
    J. Springer, Berlin 1926
    Fritsche J., Die Tragfähigkeit von Balken aus Baustahl bei
    beliebig oft wiederholter Belastung, Bauingenieur,
    vol. 12 (1931) 827.
    Bleich F., Calculation of Statically Indeterminate Systems
    Based on the Theory of Plasticity. Preliminary Publication
    Second Congress IABSE, Berlin (1936) 137-150.
    Bleich H., Uber die Bemessung statisch unbestimmter Trag-
    werke etc., Bauingenieur, vol. 13 (1932) 261
    Kloeppel K., Ausnutzbarkeit der Plastizität bei dauer-
    beanspruchten Durchlaufträgern, Final Report, Second
    Congress IABSE, Berlin (1936), 77-81
11. The contributions of Kazinczy and Kist are not limited to
    their first basic papers, usually referred to, but
    comprise a series of additional publications in La
    Technique des Travaux, 1930, Construction et Travaux
    Publics, 1933 (N.C. Kist) and in the Reports of the

Internat. Congress f. Steel Construction, Liege 1930
and the Second Congress IABSE, Berlin 1936 (g.v. Kazinczy).

12. Fritsche J., Die Tragfähigkeit von Balken aus Stahl mit
    Berücksichtigung des plastischen Verformungsvermögens,
    Bauingenieur, vol. 11 (1930) 851, 873, 888.
    Arbeitsgesetze bei elastisch-plastischer Balkenbiegung,
    Zeitschrift f. angew. Math. u. Mech., vol. 11 (1931)
    Näherungsverfahren zur Berechnung der Tragfahigkeit etc.,
    Stahlbau, vol. 8 (1935) 137.
    Grundsatzliches zur Plastizitatstheorie, Stahlbau vol. 9
    (1936), 65
    Fundamental Principles of the Theory of Plasticity,
    Preliminary Publication, Second Congress IABSE Berlin
    (1936) 15-41.
13. Melan E., Theory of Statically Indeterminate Structures,
    ibid. 103-136
14. Bleich F., La ductilité de l'acier. Son application etc.
    L'Ossature Métallique vol. 3 (1934), 93.
    La théorie et la recherche experimentale en construction
    métallique, ibid. 627
15. Chwalla E., Drei Beiträge zur Frage des Tragvermögens
    statisch unbestimmter Tragwerke, Memoirs IABSE, vol. 2
    (1933-34), 96-125.
    Der Einfluss der Querschnittsform auf das Tragvermögen
    aussermittig gedruckter Baustahlstaebe, Stahlbau, vol. 8
    (1935) No. 25, 26.
16. Girkmann K., Uber die Auswirkung der Selbsthilfe des Bau-
    stahls in rahmenartigen Stabtragwerken, Stahlbau, vol 5.
    (1932) 121
    Joukoff A.S., Principes d'application de la plasticité
    an calcul des constructions métalliques hyperstatiques,
    L'Ossature Métallique, vol. 3 (1934), 379
    Coppée R., Consideration sur le calcul et la securite des
    pieces fléchies. Mémoirs IABSE vol. 3 (1935) 19-46
    Lévi R., Sécurite des Constructions, Preliminary Publication,
    Second Congress IABSE, Berlin (1936) 83-102.
17. Various authors, Theme I 3, Preliminary Publication,
    Fourth Congress IABSE, Cambridge (1952) 75-122, 147-164,
    Final Report (1953) 109-123.
18. Freudenthal A.M., and Geiringer H., The Mathematical Theories
    of the Inelastic Continuum, Handbuch d. Physik, vol. 6
    Springer Berlin (1958) 275.
19. Reiner M., Rheology, ibid. 472
20. Ref. 18, 269-271
21. Freudenthal A.M., Théorie des Grandes Voutes en Béton et
    Béton Armé, Mémoirs IABSE vol. 4 (1936) 249-264
22. Ref. 6, p. 15-16
23. Johansen K.W., Bruchmomente kreuzweise bewehrter Platten,
    Memoirs IABSE vol. 1 (1932)
24. Ref. 6, p. 13

25. Freudenthal A.M., Critical Appraisal of Safety Criteria
    and Their Basic Concepts. Preliminary Publication,
    Eighth Congress IABSE, New York (1968) 13-24.
26. Freudenthal A.M., Combination of the Theories of Elasticity,
    Plasticity and Viscosity in Studying the Safety of
    Structures, Preliminary Publication, Eighth Congress
    IABSE, New York (1968) 45-55
27. Freudenthal A.M. and Gaither W.S., Probabilistic Approach
    to Economic Design of Maritime Structures, Proc. 22nd
    Internat. Navigation Congress, Paris (1969) Section II-5.

S. KALISZKY
Sc.D., Professor of Civil Engineering
Technical University
Budapest, Hungary

Large Plastic and Viscous Deformations of Dynamically Loaded Structures

Les grandes déformations plastiques et visqueuses des structures sous charge dynamique

Grosse plastische und viskose Verformungen dynamisch belasteter Konstruktionen

1. INTRODUCTION

The general report points out very clearly that under statical conditions the plastic and viscous deformations and the effects of geometry changes influence significantly the ultimate behavior of structures. The purpose of this report is to illustrate, that these phenomena play even more important role in structures which are subjected to impulsive or pressure (blast-type) loading and undertake large deformations. At this special kind of loading the maximum deflections and the load carrying capacity depend on the energy which can be absorbed by the structure. In case of elasto-plastic material the plastic energy dissipation capacity is usually dominant and allowing moderately large plastic deformations the changes in geometry also influence its magnitude in a considerably manner. In addition, some materials (e.g. mild steel) are sensitive to strain-rate, therefore, considering rapid loading the viscous properties can have also an important effect.

The exact analysis of this kind of problems even at very simple structures results in fairly complicated calculations, which cannot be used widely in the practice (see e.g. [6,7]). In order to overcome these difficulties among others a simple approximate method has been elaborated for the estimation of the permanent deflections [4,5,8]. This method will form the basis of our forthcoming investigation.

2. THE CONCEPT OF THE APPROXIMATE METHOD

The state of a rigid-plastic structure with density ρ is characterized by the displacement, velocity and acceleration fields u_i, $\dot{u}_i$ and $\ddot{u}_i$.

At <u>pressure loading</u> the external pressure can be described in the form $T_i = p(t) T_i^0$. Here T_i^0 is the function of coordinates x_i and defines the distribution of loading, while the load parameter $p(t)$ gives its magnitude in any instant of time. In our investigations

$$\text{if} \quad 0 < t < t_0 \qquad p(t) \equiv p_0$$
$$\text{if} \quad t > t_0 \qquad p(t) \equiv 0.$$

The initial conditions of motion are: at $t=0$, $u_i = \dot{u}_i = 0$.

At <u>impulsive loading</u> $p(t) \equiv 0$, but an initial velocity field V_i is prescribed: at $t=0$, $u_i = 0$, $\dot{u}_i = V_i$.

During the dynamic response the displacements of the structure change not only their magnitude but their distribution, as well (travelling hinges etc.). Consequently, they can be expressed in the general form $u_i(x_i, t)$. The aim of our approximate method is to replace the actual displacements by a <u>stacionary</u> kinematically admissible displacement field u_i which can be expressed in a product form $u_i^* = W_0(t) u_i^C(x_i)$. Using this mode approximation the determination of the maximum permanent displacements is reduced to the solution of a one-degree-of-freedom system [8]. The differential equation of motion of this equivalent system is

$$W_0 = K\left[p(t) - r(t)\right] \tag{1}$$

where
$$K = \frac{\int_A T_i^o u_i^C \, dA}{\int_V \rho \, u_i^C u_i^C \, dV} \tag{2}$$

and $r(t)$ is the resistance displayed by the structure under quasi-static conditions. This function can also be approximated in a produict-form

$$r(t) = p_c \, r_1(W_0) r_2(\dot{W}_0) \tag{3}$$

where p_c is the simple collapse load factor and r_1 and r_2 express the influence of changes in geometry and strain-rate sensitivity, respectively. They all are related with the predicted displacement field u_i^C .

In most structures r_1 and r_2 can be expressed in the simple form:

$$r_1 = 1 + z_1 w_0^n , \qquad r_2 = 1 + z_2 \dot{w}_0^m . \tag{4}$$

Here z_1, z_2, n and m are constants, $w_0 = W_0/H$ and H is a characteristic dimension (thickness) of the structure. Then, equation (1) can be transformed as bellow.

a/ <u>Pressure loading</u>:

$$\frac{d^2 w_0}{d\tau^2} + \frac{\lambda_0^2}{\eta^2}\left[1 + z_1 w_0^n\right]\left[1 + z_2\left(\frac{dw_0}{d\tau}\right)^m\right] = \delta \frac{\lambda_0^2}{\eta} \tag{5}$$

Where $\tau = t/t_0$, $\lambda_0 = KI^2/Hp_c$, $I = p_0 t_0$, $\eta = p_0/p_c$

and   if $0 < \tau < 1$, $\delta = 1$,

        if $\tau > 1$ $\delta = 0$.

b/ <u>Impulsive loading</u>:

$$\frac{d^2 w_o}{dt^2} + \frac{v_o^2}{\lambda_o}\left[1 + z_1 w_o^n\right]\left[1 + z_3\left(\frac{1}{v_o}\frac{dw_o}{dt}\right)^m\right] = 0 \qquad (6)$$

Here $z_3 = v_o^m z_2$ and $v_o = V_o/H$. The latter denotes the parameter of the initial velocity field and can be determined from the impulse I, wich represents the dynamic pressure.

The purpose of our investigation is to determine the maximum value of W_o when the structure is in rest: i.e. at $t=t_f$, $\dot{W}_o=0$, and $W_o=W_o^{max}$. Then, the maximum permanent displacements can be estimated:

$$u_i^{max} \approx W_o^{max}\, u_i^c$$

Using the present approximate method the investigation of different problems is relatively simple. The quasi-static solutions are available in the literature or can be gained by the suitable assumption of the functions (4). The non-linear second order differential equations (5) and (6), respectively, are to be solved numerically.

3. APPLICATIONS

In order to illustrate the application of the method and the influence of geometry changes and viscous effects on the dynamic response of structures some results of our investigations will be presented.

3.1 CIRCULAR PLATE

The simply supported circular rigid-viscoplastic plate with outer radius $r=R$ and fully plastic moment M_o is subjected to a uniformely distributed dynamic pressure represented by an <u>impulse</u> per unit area(I).The transverse deflections and the initial velocities are assumed

$$w = w_o(t)\left(1 - \frac{r}{R}\right)$$
$$v = v_o\left(1 - \frac{r}{R}\right)$$

Here $v_o=V_o/H$ and from dynamical considerations $V_o= 2\,I/\mu$, $\mu=\rho H$. The simple collapse load factor is $p_c=6M_o/R^2$ and according to equation (2) $K=2/\mu$.

The effect of membrane forces at large deflections will be taken into account by choosing $z_1=1/3$ and $n=2$ in equation (6) [1]. The influence of strainrate sensitivity in steel plates can be also significant. In case of linear viscosity the parameters of equation (6) are $z_3'=0,8(HV_o/\gamma R^2)$, $m'=1$. Here the viscous constant γ can be determined from experiments [3]. In case of non-linear viscosity $z_3'' = 1,13\left(HV_o/2DR^2\right)^{1/m''}$, where for steel $m''=1/5$ and $D=4o,4$ sec^{-1} [6].

Some results of our investigations are plotted in Fig.1.
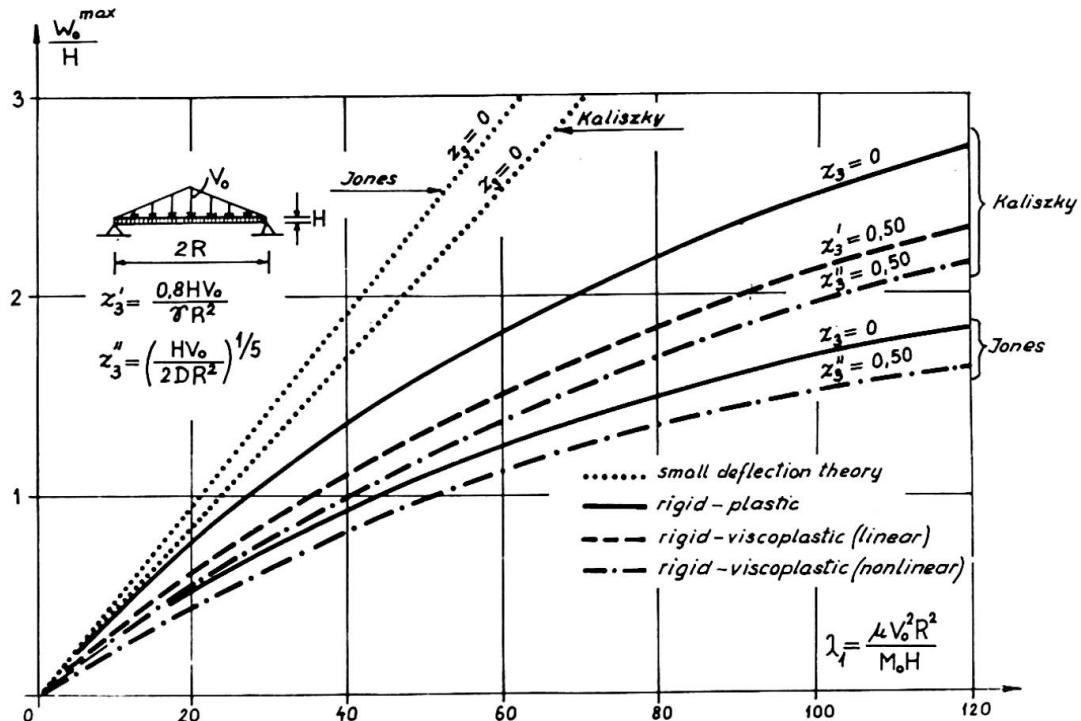
Fig.1. Circular plate under impulsive loading.

Here, for the sake of comparison, N.Jones' more accurate solution and the results of the simple bending theory are also illustrated [6,7] . Fig.2. represents the maximum permanent deflections in case when the structure is subjected to a pressure loading and the viscous effects are not taken into consideration.

3.2 SHALLOW SPHERICAL SHELL

Consider a rigid-plastic shallow spherical membrane shell whith a hinged edge and subjected to an internal dynamic pressure uniformly distributed over the plane (Fig.3.). According to the membrane solution the simple collapse load factor is $p_c = 2N_0/R$, $N_0 = \sigma_0 H$ and assuming the transverse deflections in the form

$$w = w_0(t)\left[1 - \left(\frac{r}{L}\right)^2\right]$$

the constant defined by equation (2) is $K = 3/2\mu$. As the quasi-static solution of problem shows [9] taking into consideration the influence of changes in geometry the parameters in equation (5) can be chosen as $n=1$,

$$z_1 = \frac{2}{(R/H)(L/R)^2} \quad \text{and omitting the viscous effects} \quad z_2 = 0.$$
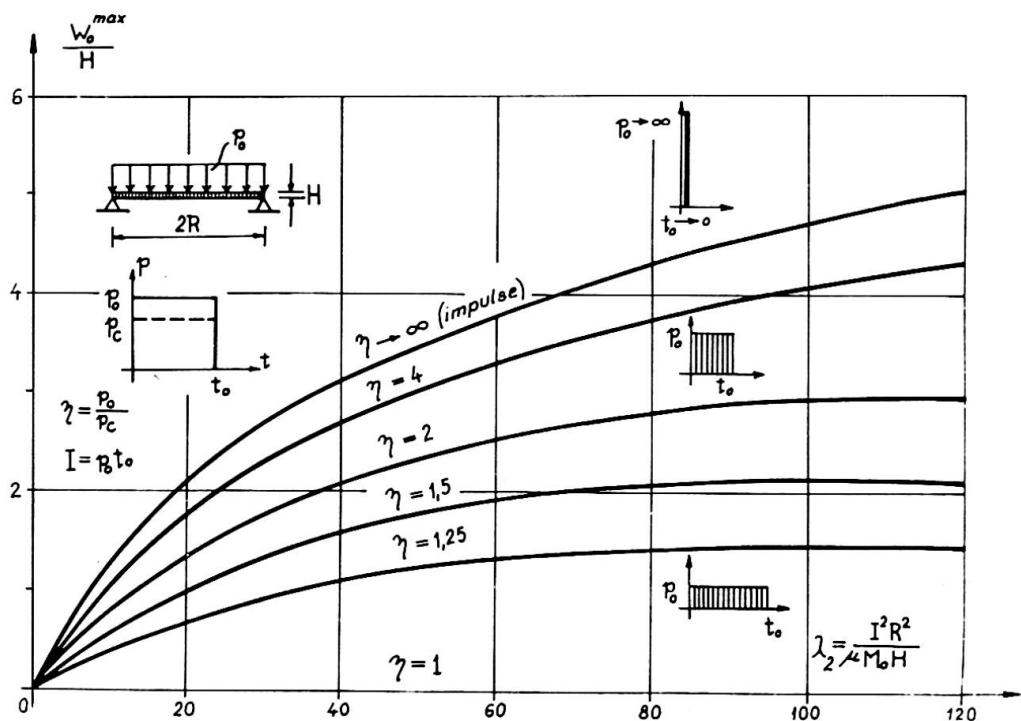
Fig.2. Circular plate under pressure loading.
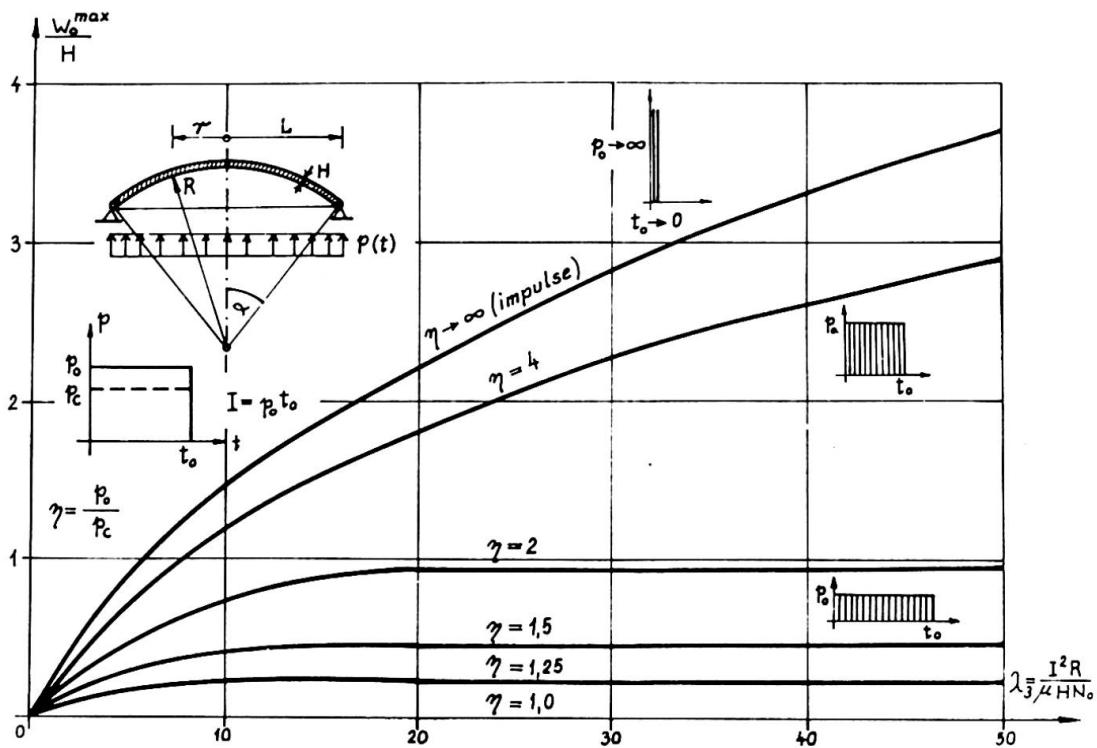
Fig.3. Spherical shell under pressure loading.

To illustrate the results the maximum permanent deflections in the function of $\eta = p_0/p_c$ and $\lambda_3 = I^2 R/\mu H N_0$ for the parameters $R/H=25$ and $L/R=\sin\alpha = 0,20$ are given in Fig.3.

3.3 PORTAL FRAME

Consider an encastred rigid-plastic portal frame with constant fully plastic moment M_0 subjected to constant vertical loads V and to uniformely distributed horizontal dynamic pressure $p(t)$ (Fig.4.). Assuming plastic hinges at the top and the bottom of the columns the simple collapse load factor and the constant defined by equation (2) can be obtained $p_c=8M_0/L^2$ and $K=3/5\mu_0$. Here μ_0 is the mass per unit length.

In our former examples the changes in geometry were increasing the resistance of the structure. At the present problem, however, during the horizontal displacements the increasing moments caused by the vertical loads are decreasing the resistance of the frame. Taking into account this effect the parameters of equation (5) can be determined from simple statical considerations: $z_1=-(V/p_c L)(H/L), n=1$ and omitting the viscous effects $z_2=0$.

Using the parameters $H/L=1/10$ and $V/P_c L=5$ the maximum horizontal displacements in the function of $\lambda_4 = I^2 L^2/\mu_0 H M_0$ are illustrated in Fig.4. Here H denotes the constant heigth of the cross-sections.
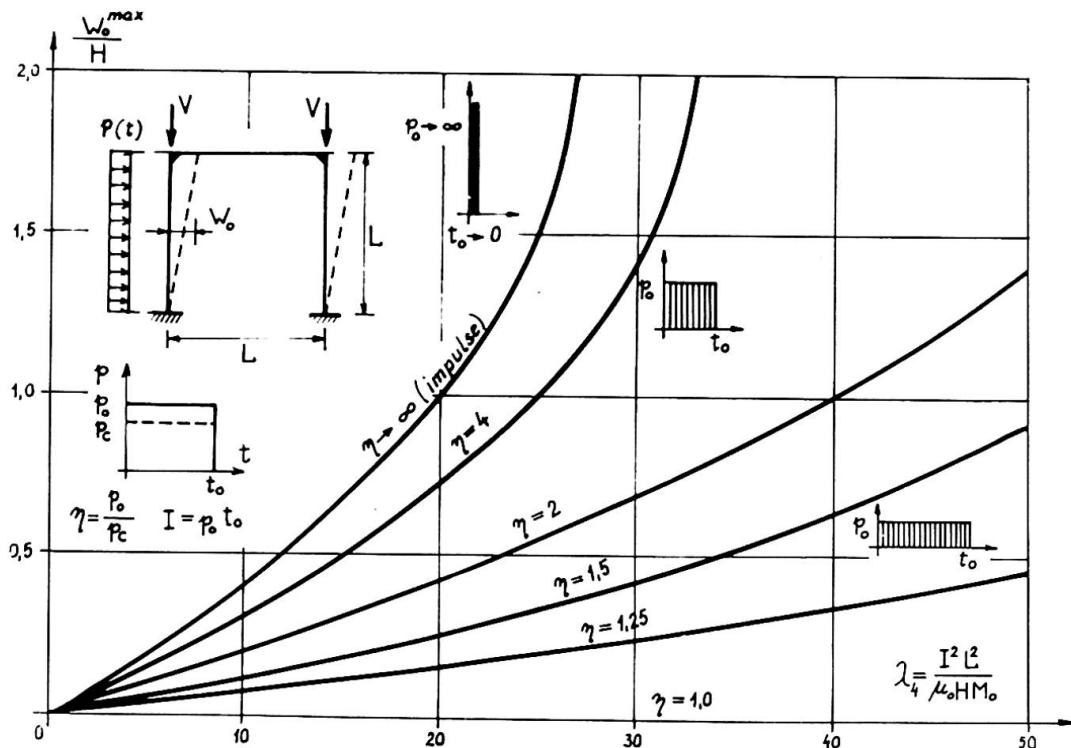

Fig.4. Portal frame under pressure loading.

4. CONCLUSIONS

According to our investigations the changes in geometry can influence the maximum permanent deflection of structures significantly. In particular this effect is very important when as a consequence of compressive forces the resistance of the structure is of derceasing character. Then, the neglection of the second order effects is at the safety's cost. The strain-rate sensitivity even in steel structures does not have a great importance.

Whenever the load-deflection and deflection-rate relation of the corresponding static problem is known or can be described approximately, the method presented can be used for the rapid calculation of the maximum permanent deflections of any kind of structures subjected to pressure or impulsive loading. The idea of the method can be extended for the investigation of other piecewise linear or non-linear phenomena as e.g. strain-hardening and elasto--plastic deformations.

REFERENCES

1   T.Wierzbicki, Bounds on large dynamic deformations of Structures, Journal of Engineering Mechanics Division, ASCE, Vol.96,No.EM3, Proc.Paper 7344, June, 1970. /257-276/

2   B.J.Martin and P.S.Symonds, Mode approximations for impulsively--loaded rigid-plastic structures.J.Engng.Mech.Div.ASCE 92.EM5. 43. /1966/.

3   T.Wierzbicki, A Method of approximate solution of boundary value problems for rigid-viscoplastic structures. Acta Mechanica Vol. III/1, 1967.

4   S.Kaliszky, Approximate solutions for impulsively-loaded inelastic structures and continua. Int.J.Non-Linear Mechanics,Vol. 5, /143-158/ /1970/.

5   S.Kaliszky, Approximate solutions for impulsively-loaded rigid--plastic structures and continua.Bull.Acad.Polonaise, Vol.XVII. No.5. /1969/.

6   N.Jones, Finite deflections of a rigid-viscoplastic strain-hardening annular plate loaded impusively.Journal of Applied Mechanics Vol.35, No.2, /349-356/ 1968.

7   N.Jones, A theoratical study of the dynamic plastic behavior of beams and plates with finite-deflections.Int.J.Solids Structures.Vol.7. 1971. /1007-1029/.

8   S.Kaliszky, Large deformations of rigid-viscoplastic structures under impulsive and pressure loading. Journ.of Structural Mechanics /in press/.

9   M.Duszek, Plastic analysis of shallow spherical shells at moderately large deflections. IUTAM Symposium,Copenhagen, 1967.

SUMMARY

An approximate method is presented for the prediction of the maximum permanent deflections of structures undertaking large plastic and visco-plastic deformations under impulsive or pressure loading. As illustrative examples a circular plate, a shallow spherical shell and a portal frame are investigated. According to the numerical results mainly the effect of changes in geometry can influence the response of dynamically loaded structures significantly.

Rheological Theory of Membranes Undergoing Large Deformations
(Physical, Geometrical and Engineering Aspects)

Théorie rhéologique des membranes soumises aux grandes déformations
(Ses aspects physiques, géometriques et techniques)

Rheologisch-theoretische Untersuchung von Membranen unter Berücksichtigung
grosser Deformationen
(Deren physikalische, geometrische und ingenieur-technische Aspekte)

Z. BYCHAWSKI   W. OLSZAK
Assoc. Prof. Dr.   Prof. Dr., Dr. h.c.
Poland

Introduction

In the last years, a rapid development of the theory of large deformations can be observed. It is due to the need of obtaining a more powerful tool in investigating the modern structural materials and their mechanical properties. However, the research work in this field is mostly concentrated on the elastic behaviour of rubberlike materials under certain specific conditions. A systematic development of this direction is given in the books of Green and Zerna [1] and Green and Adkins [2]. In the latter, we also find some indications which may lead to further generalizations of the theory as far as materials with rheological properties are concerned. It should be mentioned, however, that because of the generality of considerations, lack of physical aspects and applications they only point out clearly the difficulties encountered in formulating the problem.

In recent structural mechanics and the design of engineering structures, we are oftne faced with the necessity of considering nonlinearities of different kinds, even within the classical concepts of strain and stress states. However, all of them cumulate, if large displacements and, especially, large deformations of flat or spatial modern constructions have to be taken into account. Then the problem is that of a double nonlinearity: physical and geometrical. A typical example of such a problem in engineering are the deformation and stress states in a pneumatic structure. Except some particular cases, the theory of pneumatic structures must necessarily be based on that of nonlinear membranes. Furthermore, since the materials used, such as, for example, plastics and textiles, are very extensible, the constructions undergo large deformations.

Depending on the physical properties of the applied material and loading conditions, it is then necessary to take into account not only the instantaneous effects which occur at the instant of pressure application, but also time-dependent phenomena. These are of rheological nature and may considerably influence the resulting states of strain and stress.

Although the rheological aspects of the theory of nonlinear membranes are of great practical importance in different fields of applications, the available in formation to be found in literature is rather scarce. It is evident that one of the reasons of such a situation is the lack of an appropriate theoretical approach to interpreting experimental data for real materials in question. On the other hand, it seems to be clear that without such data concerned particularly with large deformations in multiaxial states of strain and stress, the rheological the ory of nonlinear membranes may less be determined in an explicit way as could be expected on the basis of its mathematical strictness.

Even if a physical nonlinear theory is founded on proper assumptions, the problem of solving the resulting nonlinear integral or differential equations for the considered concrete cases of practical significance still remains. It is evi dent that solutions can be found only by applying approximate methods. If these methods are appropriate and carefully chosen, we may, in some particular cases, even expect to obtain analytical results. It would then be possible to have a more general basis for discussions than in the case of a numerical solution.

The main difficulty in establishing a physical theory of large rheological deformations, besides that mentioned above, lies in a proper choice of the form of constitutive equations and physical variables which we want to expose as those of outstanding importance. In the theory of nonlinear membranes it is preferable to have stresses expressed through strains or strain rates. Therefore, all theo- ries which are founded on strain superposing rather than stress are not very suitable in application. This is due to the fact that usually the inversion of a constitutive equation, if at all possible, leads to complicated expressions for stresses, particularly in high nonlinear cases.

According to our opinion, the most convenient approach in founding a physical theory for our purposes, especially concerned with nonlinear membranes of rota- tional symmetry, is that based on energy considerations. Since a nonlinear rheo- logical process is mainly associated with dissipation of mechanical energy, it seems to be reasonable to introduce into investigation the form of dissipation power.

On the other hand, in order to obtain a more clear physical significance of constitutive relations, it is possible to make use of the known concepts of ther- modynamical potentials of deformation states. Independently of the fact that ther modynamical equalities find, in principle, application to stationary reversible processes, they can also be utilized under certain conditions by analogy in in- vestigating quasi-stationary irreversible ones. Thus, the stresses can be found as derivatives of the corresponding energy forms which are functions of the strain state invariants.

Expecially, use can be made of dissipative potentials (often introduced in analogy to elastic potentials) when solving plastic and creep problems by apply- ing variational theorems and methods.

It is the main aim of our paper to give a comprehensive dis-
cussion of the problem of setting up a physical theory of nonli-
near viscoelastic materials which can be adapted directly to mem-
branes exhibiting large deformations . Because of specific featu-
res of the problem in the case of rotational symmetry , which we
want to study exclusively , characterized by symmetry of strain
and stress states , it is possible to base our considerations on
purely homogeneous deformation . Therefore , we do not intend to
go deeper into generalities than necessary for our purposes . We
shall touch these questions only which , according to our opinion,
are fundamental and can lead us directly to effective results .
In realizing this aim we bear in mind the possible applications .
     In our further investigation we shall assume that materials
considered are isotropic , homogeneous and incompressible .

1.Geometrical aspects of the theory

     We consider geometry of deformation of a nonlinear membrane
the middle surface of which at time $t = t_{0}^{-}$ (neutral state) is de-
noted by S_{o} and represented by dotted lines in Fig.1 . S_{o} is ge-
nerated by the revolution
of a plane curve f through
a full angle about x_{3}-axis
in its plane . The curve f
has no multiple points and
is smooth . All kinds of
singularities are excluded
from our considerations .
     The membrane is of
very small thickness $2h_{o}$
which is constant in the
neutral state .
     S_{o} is given in a sys-
tem of cylindrical coordi-
nates x_{i} (i=1,2,3) .
     At $t=t_{o}$ the membrane
is loaded by a uniform
pressure p = p(t) and at
an arbitrary instant t ,in
consequence of deformation
process , we obtain a dif-
ferent rotational membrane
with initial axis of symme-
try . Its middle surface
is now S and thickness 2h .
The latter varies with sur-
face coordinates and time .
     We assume for S a sys-
tem of cylindrical coordi-

Fig.1

nates $\bar{x}_{i}$. Both the systems assumed satisfy the relations

$$x_{i} = x_{i}(\bar{x}_{j},t) \quad , \quad \bar{x}_{i} = \bar{x}_{i}(x_{j},t) \quad , \qquad (1.1)$$

where j = 1,2,3 for every i .
     On the other hand , we introduce a system of curvilinear co-
ordinates θ_{i} in which θ_{α} (α=1,2) coincide with lines of main
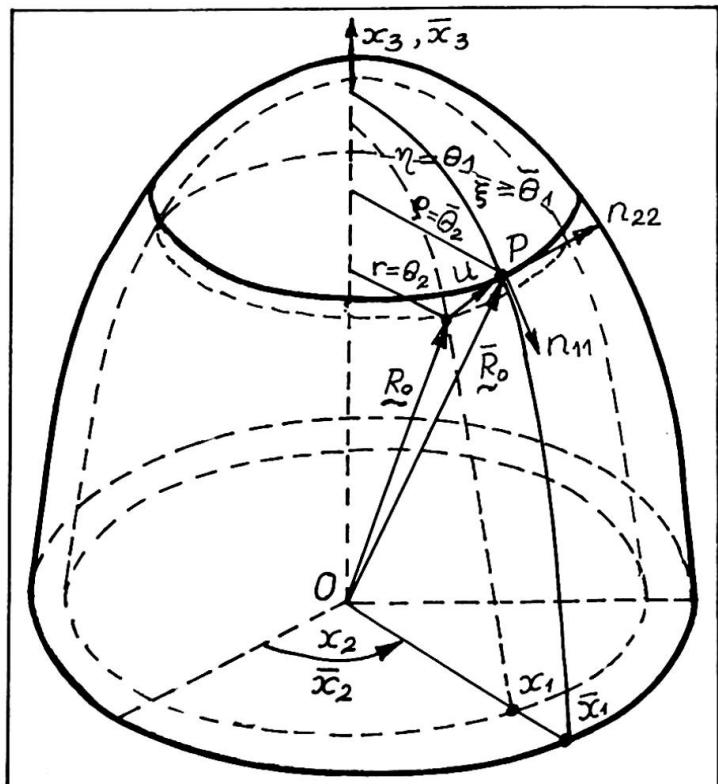
curvatures on S_o . θ_1 varies within the values $\pm h_o$ on the direction of outward normal to S_o and $\theta_3 = 0$ defines S_o. This system deforms in time together with membrane and the set of θ_i related to a fixed (at t_o) point P_o remains attached to it as it moves to a new position P at t . Thus , we may write

$$x_i = x_i(\theta_j) \quad , \quad \bar{x}_i = \bar{x}_i(\theta_j,t) \quad , \tag{1.2}$$

where $j = 1,2,3$ for every i .

Displacement vector of P_o to P is given as the difference of corresponding radius vectors of these positions from the origin O

$$\underset{\sim}{u}(\theta_i,t) = \bar{\underset{\sim}{R}}_o^*(\theta_i,t) - \underset{\sim}{R}_o^*(\theta_i) = \bar{\underset{\sim}{R}}_o(\theta_\alpha,t) - \underset{\sim}{R}_o(\theta_\alpha) + \theta_3[\bar{A}_3(\theta_\alpha,t) - \underset{\sim}{a}_3(\theta_\alpha)] \quad , \tag{1.3}$$

where the vectors $\underset{\sim}{R}_o$ and $\bar{\underset{\sim}{R}}_o$ are related to S_o and S , respectively , and $\underset{\sim}{a}_3$ and $\bar{A}_3$ are vectors normal to S_o and S . Thus , for a point on the middle surface we find from (1.3)

$$\underset{\sim}{u}_o(\theta_\alpha,t) = \underset{\sim}{R}_o(\theta_\alpha,t) - \underset{\sim}{R}_o(\theta_\alpha). \tag{1.4}$$

The line elements on S and S_o , corresponding to the vectors $\bar{R}_o$ and $\dot{R}_o$ are , respectively ,

$$ds^2 = A_{\alpha\beta} \, d\theta_\alpha d\theta_\beta \quad , \tag{1.5}$$

$$ds_o^2 = a_{\alpha\beta} \, d\theta_\alpha d\theta_\beta \quad , \tag{1.6}$$

where $A_{\alpha\beta}$ and $a_{\alpha\beta}$ are covariant base tensors of S and S_o , respectively .

According to the existing symmetry we define the principal extension ratios λ_i ($i=1,2,3$) in meridional , latitudinal and normal directions . These coincide with the principal directions of strain . Denoting by $\bar{\theta}_1$ and θ_1 the arc lengths measured along meridians from A to P and A_o to P_o , respectively , we have

$$\lambda_1 = d_{\theta_1}\bar{\theta}_1 \quad , \quad \lambda_2 = \bar{x}_1/x_1 \quad , \quad \lambda_3 = \lambda = (\lambda_1 \lambda_2)^{-1}, \tag{1.7}$$

where $d_{\theta_1} = d/d\theta_1$; the value of λ (from the condition of incompressibility) being dependent on both the remaining ratios .

On the basis of Eq. (1.7) we may write Eqs. (1.5) and (1.6) as follows

$$ds^2 = \lambda_1^2 (d\theta_1^1)^2 + \lambda_2^2 x_1^2 (d\theta^2)^2 \quad , \tag{1.8}$$

$$ds_o^2 = (d\theta^1)^2 + x_1^2 (d\theta^2)^2 \quad , \tag{1.9}$$

and thus define the surface strain tensor

$$\gamma_{\alpha\beta} = \tfrac{1}{2}(A_{\alpha\beta} - a_{\alpha\beta}) \quad , \tag{1.10}$$

given by the difference of Eqs. (1.8) and (1.9)

$$2\gamma_{\alpha\beta} d\theta_\alpha d\theta_\beta = ds^2 - ds_o^2 = (\lambda_1^2 - 1)(d\theta^1)^2 + x_1^2(\lambda_2^2 - 1)(d\theta^2)^2 \quad . \tag{1.11}$$

The relative extension of the line element ds is then found to be

$$\gamma = (ds-ds_0)/ds_0 \ , \quad (1+\gamma)^2 - 1 = 2\gamma_{\alpha\beta}d\theta_\alpha d\theta_\beta(ds_0)^{-2} \ . \tag{1.12}$$

Let us consider now the strain rate tensor which plays an important part in what follows . If the rheological process of deformation is such that at t_0 the line element ds_0 is given by Eq.(1.6) and at t by Eq.(1.5), then at $t+dt$ its length becomes equal to

$$ds + d(ds) = (1+\gamma) ds_0 + d(ds) \ , \tag{1.13}$$

the rate of extension being $d(ds)/dt$. Thus , the deformation rate is obtained as the ratio $[d(ds)/dt]/ds$

$$\omega = \dot\gamma(1+\gamma)^{-1}, \quad \dot\gamma = d\gamma/dt \ . \tag{1.14}$$

On the other hand , by differentiating Eq.(1.12) at fixed t we find

$$\dot\gamma(1+\gamma) = \dot\gamma_{\alpha\beta}d\theta_\alpha d\theta_\beta(ds)^{-2} \ , \tag{1.15}$$

and from Eq.(1.14) follows that

$$\omega = \dot\gamma_{\alpha\beta}d\theta_\alpha d\theta_\beta[(1+\gamma)ds]^{-2} \ , \tag{1.16}$$

the counterpart of Eq.(1.11) being

$$\dot\gamma_{\alpha\beta}d\theta_\alpha d\theta_\beta = \dot\lambda_1\lambda_1(d\theta^1)^2 + x_1^2 \ \dot\lambda_2\lambda_2(d\theta^2)^2 \ . \tag{1.17}$$

Since on the basis of Eq.(1.11) we have main strains at the middle surface

$$\gamma_{11} = \lambda_1^2 - 1 \ , \quad \gamma_{22} = (\lambda_2^2 - 1)x_1^2 \ , \tag{1.18}$$

main strain rates are

$$\dot\gamma_{11} = \dot\lambda_1\lambda_1 \ , \quad \dot\gamma_{22} = \dot\lambda_2\lambda_2 \ x_1^2 \ . \tag{1.19}$$

The nondimensional strain tensor components are obtained by means of transformation

$$e_{\alpha\beta} = \gamma_{\alpha\beta}(a_{\alpha\alpha} \ a_{\beta\beta})^{-\frac{1}{2}} \ , \tag{1.20}$$

which instead of Eq.(1.18) gives

$$e_{11} = e_1 = \lambda_1^2 - 1 \ , \quad e_{22} = e_2 = \lambda_2^2 - 1 \ . \tag{1.21}$$

Thus , the nondimensional strain rate tensor components are

$$\dot e_1 = \dot\lambda_1\lambda_1 \ , \quad \dot e_2 = \dot\lambda_2\lambda_2 \ . \tag{1.22}$$

The remaining components of the general strain tensor γ_{ij}

are found on the basis of general metric tensors for S and S_o ,denoted G_{ij} and g_{ij} , respectively .
For an arbitrary point of the membrane we may write , respectively ,

$$G_{\alpha\beta} = A_{\alpha\beta} - 2\theta_3 B_{\alpha\beta} \quad , \quad G_{\alpha 3} = 0 \quad , \quad G_{33} = \lambda^2 \quad , \qquad (1.23)$$

where
$$A_{11} = \lambda_1^2 \ , \ A_{22} = x_1^2 \lambda_2^2 \ , \ A_{\alpha\beta} = 0 \ (\alpha \neq \beta) \ , \ B_{11} = -k_{11} \ , \qquad (1.24)$$

$$B_{22} = -k_{22} \quad , \quad B_{\alpha\beta} = 0 \ (\alpha \neq \beta) \quad , $$

and
$$g_{\alpha\beta} = a_{\alpha\beta} - 2\theta_3 b_{\alpha\beta} \quad , \quad g_{\alpha 3} = 0 \quad , \quad g_{33} = 1 \quad , \qquad (1.25)$$

where
$$a_{11} = 1 \ , \ a_{22} = x_1^2 \ , \ a_{\alpha\beta} = 0 \ (\alpha \neq \beta) \ , \ b_{11} = -k_{11}^o \ , \qquad (1.26)$$

$$b_{22} = -k_{22}^o \quad , \quad b_{\alpha\beta} = 0 \ (\alpha \neq \beta) \quad . $$

Here $B_{\alpha\beta}$, $b_{\alpha\beta}$ are tensors associated with the second fundamental form of the surfaces S and S_o , respectively , and $k_{\alpha\beta}$ and $k_{\alpha\beta}^o$ are corresponding curvatures .
From Eq.(1.23) and Eq.(1.25) it follows that

$$\gamma_{\alpha 3} = 0 \quad , \quad \gamma_{33} = \tfrac{1}{2}(\lambda^2 - 1) = \tfrac{1}{2}\left[(\lambda_1 \lambda_2)^{-1} - 1\right] \quad , \qquad (1.27)$$

and its rate is

$$\dot{\gamma}_{33} = \dot{\lambda}\lambda = -\tfrac{1}{2}(\lambda_1 \lambda_2)^{-2}(\dot{\lambda}_1 \lambda_2 - \lambda_1 \dot{\lambda}_2) \quad . \qquad (1.28)$$

Furthermore , from Eq.(1.2o) we conclude that

$$e_{33} = e_3 = \tfrac{1}{2}(\lambda^2 - 1) \quad , \quad \dot{e}_3 = \dot{\lambda}\lambda \quad . \qquad (1.29)$$

We shall express now the components of strain tensor through the components of displacement vector given by Eq.(1.3)(for $\theta_3 = 0$), or Eq.(1.4). In order to do that, we represent displacement vector in the form

$$\underset{\sim}{u} = u_i \underset{\sim}{g}^i = u^i \underset{\sim}{g}_i \quad , \qquad (1.3o)$$

where $\underset{\sim}{g}_i$ and $\underset{\sim}{g}^i$ are covariant and contravariant vectors of the base , respectively ,

$$\underset{\sim}{g}_i \underset{\sim}{g}_j = g_{ij} \quad , \quad \underset{\sim}{g}^i \underset{\sim}{g}^j = g^{ij} \quad . \qquad (1.31)$$

Taking into account the relation between base vectors

$$\underset{\sim}{G}_i = \underset{\sim}{g}_i + \underset{\sim}{u}_{,i} \quad , \qquad (1.32)$$

and , hence ,

$$G_{ij} = g_{ij} + \underset{\sim}{g}_i \underset{\sim}{u}_{,j} + \underset{\sim}{g}_j \underset{\sim}{u}_{,i} + \underset{\sim}{u}_{,i} \underset{\sim}{u}_{,j} \quad , \qquad (1.33)$$

where

$$u_{,i} = u_k|_i g^k \quad , \quad u_k|_i = u_{k,i} - \Gamma_{ki}^l u_l \quad , \tag{1.34}$$

we find strain tensor γ_{ij} by introducing Eq. (1.34) into Eq. (1.33). Thus , we obtain

$$\gamma_{ij} = \frac{1}{2}\left(u_i|_j + u_j|_i + u^k|_i u_{k\ j}\right), \quad u^k|_i = u^k{}_{,i} + \Gamma_{li}^k u^l \quad , \tag{1.35}$$

where Christoffel's symbols Γ are calculated for S_o from the metric tensors g_{ij}, g^{ij} of S_o .

By performing the indicated in Eq.(1.35) operations on displacement components and having in mind Eq.(1.2o) we find physical components of strain state (for S_o , $\theta_3 = 0$)

$$e_1 = \partial_{\theta_1} u_1 + \frac{1}{2}\left(\partial_{\theta_1} u_1 + k_{11}^o u_3\right)^2 + \frac{1}{2}\left(\partial_{\theta_1} u_3 - k_{11}^o u_1\right)^2 \quad , \tag{1.36}$$

$$e_2 = k_{22}^o u_3 + \frac{1}{2}\left(k_{22}^o u_3\right)^2 \quad , \tag{1.37}$$

$$e_3 = -\frac{1}{2}\left(k_{11}^o u_1\right)^2 \quad . \tag{1.38}$$

These are geometrical formulas expressing strain state components through displacement components . As it is seen , the first equation depends on Eqs.(1.37) and (1.38). By solving the latter with respect to u_3 and u_1 , respectively , and introducing the results into the former , we thus obtain the condition of compatibility of strain state .

From Eqs.(1.37) and (1.38) we find , respectively ,

$$u_3 = -R_2^o\left(1 + \sqrt{1+2e_2}\right) \quad , \quad u_1 = R_1^o\sqrt{-2e_3} \quad , \quad e_3 < 0 \quad , \tag{1.39}$$

and the said condition gives

$$\partial_\eta\left(R_1^o\sqrt{2\bar{e}_3}\right) + \frac{1}{2}\left[\partial_\eta\left(R_1^o\sqrt{2\bar{e}_3}\right) - R_2^o R_1^{o-1}\left(1+\sqrt{1+2e_2}\right)\right]^2 + \frac{1}{2}\left\{\partial_\eta\left[R_2^o\left(1+\sqrt{2e_2+1}\right)\right] + \right.$$

$$\left. + \sqrt{2\bar{e}_3}\right\}^2 - e_1 = 0 \quad , \quad \bar{e}_3 = -e_3 \quad , \quad \eta = \theta_1 \quad . \tag{1.40}$$

Here , R_1^o, R_2^o denote main curvature radii

$$k_{11}^o = R_1^{o-1} \quad , \quad k_{22}^o = R_2^{o-1} \quad . \tag{1.41}$$

The curvatures of Eq.(1.41) satisfy the equation

$$d_\eta\left(r k_{22}^o\right) = k_{11}^o\, d_\eta r \quad , \quad r = x_1 \quad , \tag{1.42}$$

where

$$k_{11}^o = -d_\eta^2 r\left[1 - (d_\eta r)^2\right]^{-\frac{1}{2}} \quad . \tag{1.43}$$

Substituting Eq.(1.43) into Eq.(1.42)and taking into account the fact that k_{22}^{o} is finite for $r=0$ and $d_{\eta}r = 1$ for $r=0$, through integration we obtain

$$k_{22}^{o} = r^{-1}\left[1 - (d_{\eta}r)^2\right]^{\frac{1}{2}} \ . \tag{1.44}$$

Analogous formulae are valid for the curvatures k_{11} and k_{22} at arbitrary instant t of the deforming membrane . Thus[1], we have

$$k_{11} = - d_{\xi}^{2}\varrho \left[1 -(d_{\xi}\varrho)^2\right]^{-\frac{1}{2}} \ , \quad k_{22} = \varrho^{-1}\left[1 -(d_{\xi}\varrho)^2\right]^{\frac{1}{2}} \ , \tag{1.45}$$

where we put $\varrho = \overline{x}_1$ and $\xi = \overline{\theta}_1$. Thus , Eqs.(1.43)and (1.44) can be considered as initial conditions for Eqs.(1.45)describing continuous change of curvatures during deformation process

$$k_{11}(t) =\left[R_1(t)\right]^{-1} \ , \quad k_{22}(t) =\left[R_2(t)\right]^{-1} \ , \tag{1.46}$$

where R_1,R_2 are radii of main curvatures at instant t .
Finally , it should be mentioned that the corresponding components of strain rate state may be found by differentiating Eq.(1.35) or Eqs.(1.36)-(1.38) with respect to time .

2.Statical aspects of the theory

According to the membrane theory,we neglect all moments and shearing forces in our considerations of quasi static equilibrium of rheological process . In what follows we refer all results to the undeformed membrane .
The physical stress resultants per unit length are given by the relation

$$n_{\alpha\beta} = n^{\alpha\beta}\left(a_{\beta\beta} / a^{\alpha\alpha}\right)^{\frac{1}{2}} \ , \tag{2.1}$$

where $n^{\alpha\beta}$ satisfy the conditions of equilibrium

$$n^{\alpha\beta}|_{\alpha}= 0 \ , \quad n^{\alpha\beta}b_{\alpha\beta}+ p = 0 \ , \quad p = p_1 - p_2 \ . \tag{2.2}$$

Here, p is the resultant pressure in the direction of the outward normal to the middle surface and

$$n^{\alpha\beta}|_{\alpha} = n^{\alpha\beta}{}_{,\alpha} + \Gamma_{\alpha\gamma}^{\beta}n^{\alpha\gamma} + \Gamma_{\alpha\gamma}^{\alpha}n^{\gamma\beta} \ . \tag{2.3}$$

In our particular case we have only two stress resultant components n_{11} and n_{22} and two non-vanishing components of the Christoffel tensor , and Eq.(2.2) furnishes

$$n^{11}{}_{;1} + \Gamma_{21}^{2}n^{11}+ \Gamma_{22}^{1}n^{22} = 0 \ , \tag{2.4}$$

or

$$d_{\eta}(rn_{11}) = r^2 n_{22}d_{\eta}r \ , \tag{2.5}$$

if Eq.(2.1) is taken into account . On the other hand , the second of Eq.(2.2) gives

$$k_{11}^{o}n_{11} + r^2 k_{22}^{o}n_{22} = p \tag{2.6}$$

Three Remarks on Viscoelasticity and Inelasticity of Concrete

Trois remarques sur la viscoélasticité et inélasticité du béton

Drei Bemerkungen zur Viskoelastizität und Unelastizität des Betons

ZDENĚK P. BAŽANT
Associate Professor
Department of Civil Engineering
Northwestern University
Evanston, Illinois, USA

The intent of this discussion is to make three remarks calling attention to some recent developments in inelasticity of concrete extending the exposition of this subject in the Introductory Report to Theme Ia.

(1) In the Introductory Report it is stated that the theory of linear viscoelastic bodies with age-dependent properties can be applied to concrete structures. It would be, however, more accurate to say that no better theory is available at present. The theory of viscoelasticity can accurately describe the behavior of concrete under low stress only when its specific water content and temperature are constant, which is a rare condition in actual structures. Otherwise concrete is not viscoelastic but exhibits a more general behavior in which the strains are functionals not only of the history of stress but also of the histories of specific water content and temperature. As a consequence, the stress problem is coupled with a diffusion problem. Taking this fact into account, the number of unknown material parameters is immensely increased so that their determination from the available creep and relaxation data alone would hardly be possible. It is therefore necessary to turn attention to the physical processes in the microstructure and try to determine the form of the stress-strain relations on this basis. The main source of shrinkage, delayed thermal dilatation and creep of concrete at working stress levels is presently believed to be some kind of diffusion processes in the microstructure of cement paste, involving hindered adsorbed water, interlayer hydrate water, calcium ions and capillary water [3]. This approach has recently received a good deal of attention and the latest advances can be found in references [1] and [2]. The constitutive equation which follows from the above mechanism appears to be amenable to structural analysis with the help of electronic computers [1].

(2) Even if the behavior of concrete is assumed to obey the linear theory of viscoelasticity of age-dependent bodies, the structural analysis is not easily accomplished. Among the simplified stress-strain relations used in practical problems, the relatively best ones are those of the type used by Arutyunyan, as quoted in the Introductory Report. These are able to reflect both the reversible and irreversible deformations and also the so-called aging. However, for simplicity of analysis, the time shape of the creep curve in these relations is being assumed as a simple exponential, which implies only a single retardation time. In reality, the shape of the creep curves observed is quite different, which can be seen in the logarithmic time scale; the creep curves continue to rise significantly over many decades of the time elapsed and have thus a very broad retardation spectrum, with many exponential components. Therefore it is important to carry out the structural analysis for the actual unit creep curves. This can be done only numerically, e.g. by the methods described in references [4] and [5].

If the structure is large (i.e. requires too many nodes), this approach runs into difficulties because the need of storing the complete history of the stress state in the structure and evaluating from it the hereditary integrals overtaxes the storage capacity of the computers presently available and requires too much machine time. These requirements can be circumvented by characterizing the entire stress history with a few suitably defined hidden state variables of the material, as has been proposed in reference [6].

(3) Alternatively, the stress-strain law can be also represented by a spring-dashpot model. The Introductory Report refers to this approach in conjunction with the applications of the finite element method by Zienkiewicz, Watson and King. For an accurate representation of the shape of creep curves, as discussed above, a relatively long chain of Kelvin elements or Maxwell elements is needed. In pursuing this approach, there are, however, two obstacles. First the method of determining the model parameters from creep data has not yet been clarified, for the case when aging is involved. The second obstacle arises in numerical application. Namely, the usual numerical algorithms (of Euler, Runge-Kutta or predictor-corrector type) become numerically unstable when the time step is increased beyond the value of the shortest retardation time. Because this time is for concrete quite short, analysis of the long-term response would require an impractically high number of small time steps (about 10^6), regardless of the fact that under steady conditions the solution must vary very slowly after long times elapsed. This obstacle may be overcome and an arbitrary increase of the time steps (without causing numerical instability) can be made feasible by introducing a certain special set of hidden material variables (see Eqs. 70 to 79 in Ref. [1]).

REFERENCES

1. Z.P. Bažant, "Thermodynamics of interacting continua with surfaces and creep analysis of concrete structures", Nuclear Engineering and Design, Vol. 20, No. 2

2. Z.P. Bažant, Thermodynamics of hindered adsorption with application to cement paste and concrete, Cement and Concrete Research, Vol 2, No. 1, 1972

3. Z.P. Bažant, Constitutive equation for concrete creep and shrinkage based on thermodynamics of multiphase systems, Materials and Structures (RILEM), Vol. 3, pp. 3-36, 1970

4. Z.P. Bažant, Prediction of concrete creep effects using age-adjusted effective modulus method, American Concrete Institute Journal (in press)

5. Z.P. Bažant, Numerical determination of stress history from strain history in concrete, Materials and Structures (in press)

6. Z.P. Bažant, Nummerically stable algorithm with increasing time steps for integral-type aging creep, First Intern. Conference on Structural Mechanics in Reactor Technology (BAM, Berlin, and Commission of European Communities, Ed. T.A. Jaeger), Vol. 3, Paper H2/3, West Berlin, Sept. 1971

SUMMARY

The discussion presented calls attention to some recent developments which include (1) the theory of creep of concrete based on diffusion processes in the microstructure, (2) the numerical integration methods based on superposition of unit creep curves and (3) those based on an equivalent rate-type formulation.

I b
Instabilité dans le domaine post-critique
Instabilität im überkritischen Bereich
Post-Critical Buckling

Leere Seite

Blank page

Page vide

Some Practical Considerations on the Postcritical Behaviour of Structures

Quelques remarques pratiques sur le comportement des structures dans le domaine post-critique

Praktische Bemerkungen über das Verhalten der Konstruktionen ·im überkritischen Bereich

LAJOS KOLLÁR
Dr. techn.
Budapest, Hungary

In the following the postcritical behaviour of structures would be dealt with from the viewpoint of their practical applications.

Basically, three different types of postbuckling behaviour can be distinguished. The load-bearing capacity of the structure can be - after exceeding the critical load P_{cr}^{lin} of the classical /linear/ theory - either increasing, or constant, or decreasing. Plotting the load P against some average value of the buckling deformation w, these three cases can be represented by the diagrams of Figs. 1a,b,c. Here, in addition to the perfect /centrally compressed/ case, some curves corresponding to initially imperfect structures have been represented too.

Structures with <u>increasing</u> postbuckling load-bearing capacity /Fig. 1a/ are insensitive to initial imperfections and/or creep because their diagrams have no peak which could be influenced by these two factors. On the other hand, structures with <u>decreasing</u> diagrams /Fig. 1c/ are extremely sensitive to initial imperfections and creep as well, for the peak value of their P/w/-curves depend markedly on the magnitude of both. /The influence of creep is similar to that of initial imperfections because creep increases buckling deformation, thus it augments the influence of the imperfection./ We can thus choose a much smaller safety factor for structures corresponding to Fig. 1a than to those of Fig. 1c.

Structures corresponding to Fig. 1c form a case of transition between the two other groups. Its importance comes mainly from the fact that it can be treated theoretically in a simple way, but it also describes, at least approximatively, the behaviour of some structures /e.g. buckling of bars/.
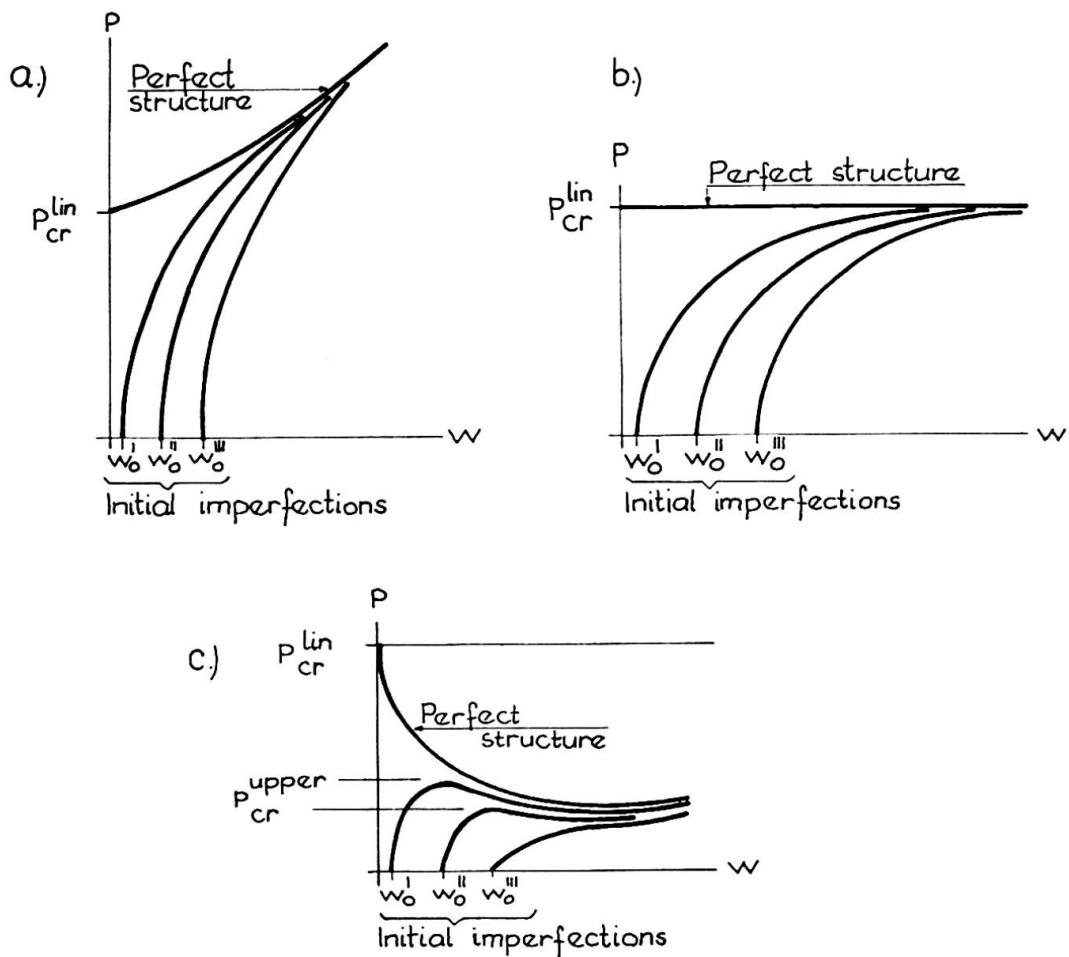
Fig. 1.

From all that has been said follows that when designing a structure, it is most important to know whether its postbuckling load-bearing capacity increases or decreases. For some structures we know this from theoretical investigations to be found in the literature. But if we have to design a structure the postbuckling analysis of which has not yet been made, some simple criteria to determine the kind of its postbuckling behaviour could be of great value. In the following some such criteria will be shown.

Theoretically it can be said [2], [3] that a structure has an increasing postbuckling load-bearing capacity if the following two conditions are fulfilled:

a/ The structure must have some parts which can bear more load, even without the other, more buckled /weaker/ parts, than the whole structure.

b/ The redistribution of stresses that is necessary for con-

dition a/ must be physically possible in the structure it-
self as well as at the supports.
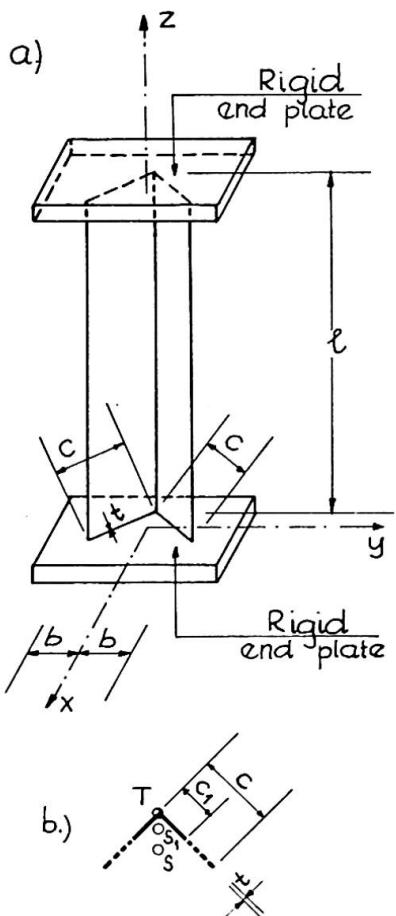
Fig 2.

Let us illustrate this on the pure
torsional buckling of a straight
bar with the cross section of an
angle /Fig. 2a/. When the critical
load is exceeded, the angle begins
to buckle with the rotation of the
cross sections around their shear
centre T /Fig. 2b/. We can assume,
as an approximation, that the free
ends of the cross sections cease to
bear any load. Thus, instead of the
original flange width c of the
angle only a part of it, of width
c_1, will be effective. This part,
however, can carry more load than
the original whole structure. This
can be seen in the formula for the
critical load of torsional buckling
for an angle with built-in ends 5 :

$$P_{cr} = 2 \frac{G\,t^3}{c} .$$

Since P_{cr} is inversely proportional
to flange width c, the smaller c, the greater the critical load
will be. Condition a/ is thus fulfilled.

In this case the redistribution of stresses means that the
point of action of the load must shift from the original centroid
S to the centroid S_1 of the smaller cross section. If the end con-
ditions make this possible /e.g. in case of rigid end plates/,
then condition b/ is also fulfilled, thus we obtain an increasing
postbuckling load-bearing capacity.

Essentially the same considerations can be made in relation
to the torsional buckling of shell-arches 1 , 3 , plate buckling
 5 etc., i.e. in all cases where the critical load is inversely
proportional to some dimension of the structure, and even in some
other cases. Sometimes it is also possible to establish a simple
upper bound for the maximum value of the postbuckling load the

Fig. 3.
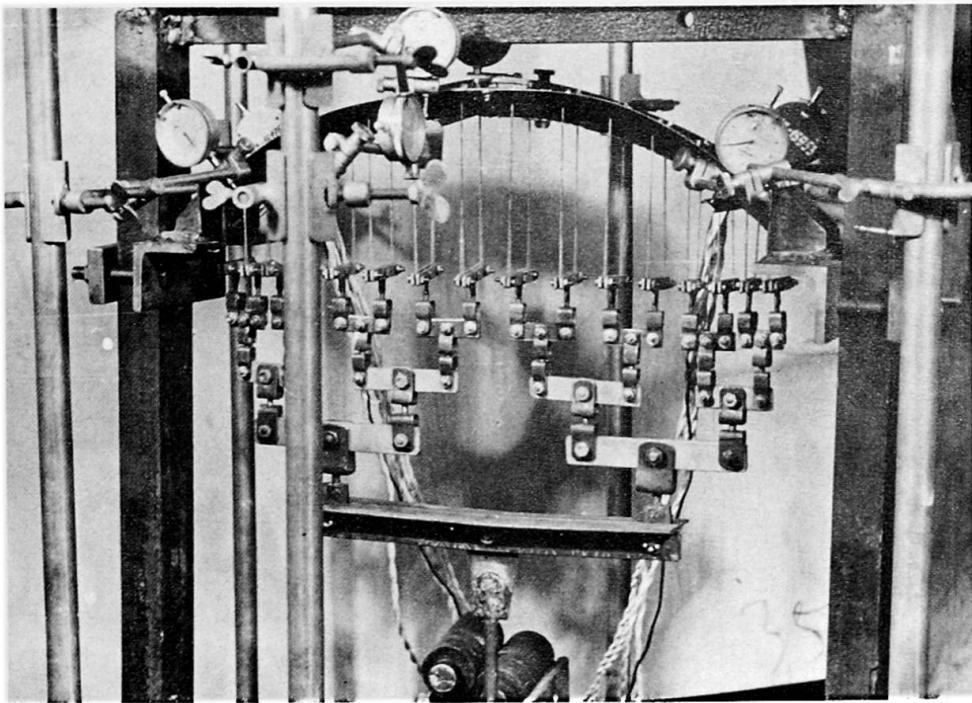
structure can carry [2]. For illustration, Fig. 3 shows a steel model of a shell-arch with built-in ends under centrical compression. The rotation of the middle cross section, as characteristic for the torsional buckling, is plotted in Fig. 4. After exceeding the linear critical load P_{cr}^{lin} = 512 kp, the load-deflection curve has a markedly ascending character, represented in Fig. 1a.

Fig. 4.

In cases, however, when these theoretical considerations cannot be applied, there is another possibility to predict postbuckling behaviour from non-destructive model tests.

$$P_{cr}^{lin} = \frac{b}{a}$$
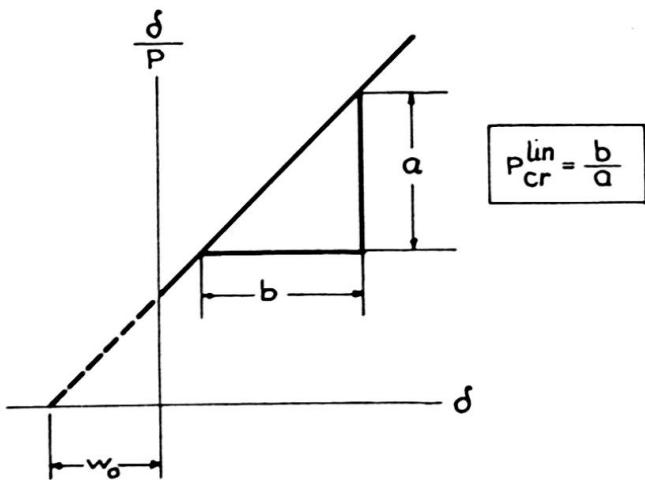
Fig. 5.

It is well known [5] that for structures corresponding to Fig. 1b, the asymptotic curves for the imperfect cases can be made straight by plotting the ratio δ/P against the buckling deformation $\delta = = w - w_o$, measured from the initial /imperfect/ state w_o /Fig. 5/. The inverse slope of this line gives the critical load. This procedure, called Southwell's plot, greatly facilitates the determination of this latter since it would be much more uncertain to determine the asymptotic value of the curves in Fig. 1b by extrapolation.

It can be easily shown [2], [4] that in case of increasing or decreasing
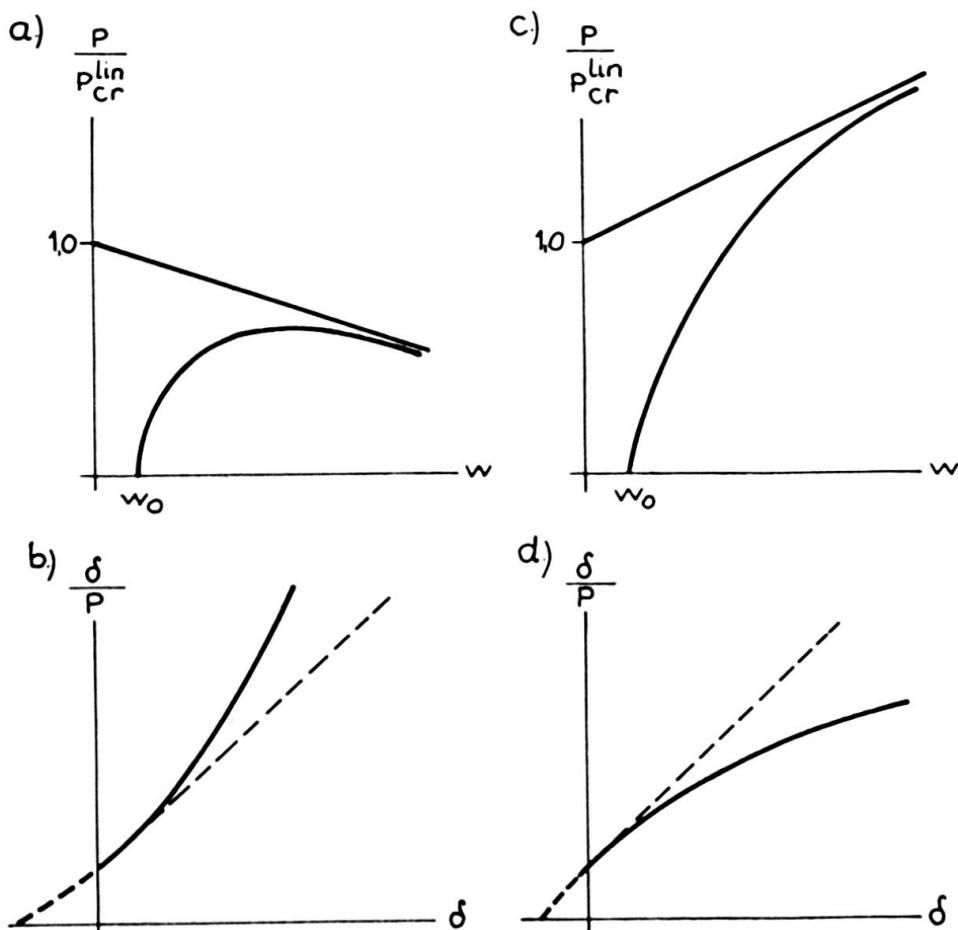
Fig. 6.
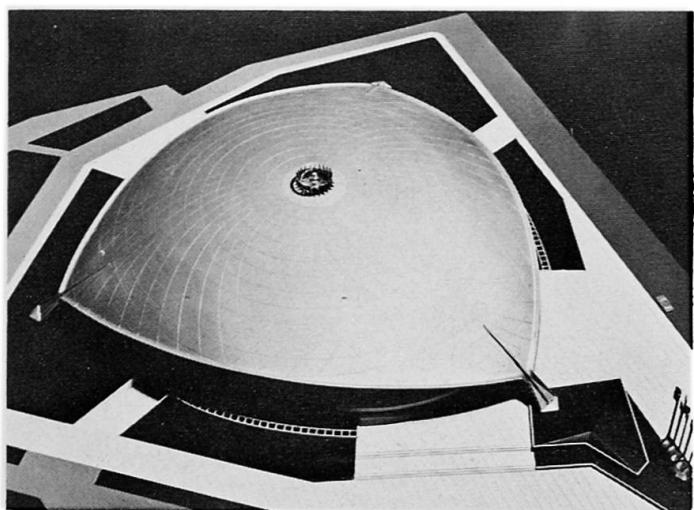
Fig. 7.
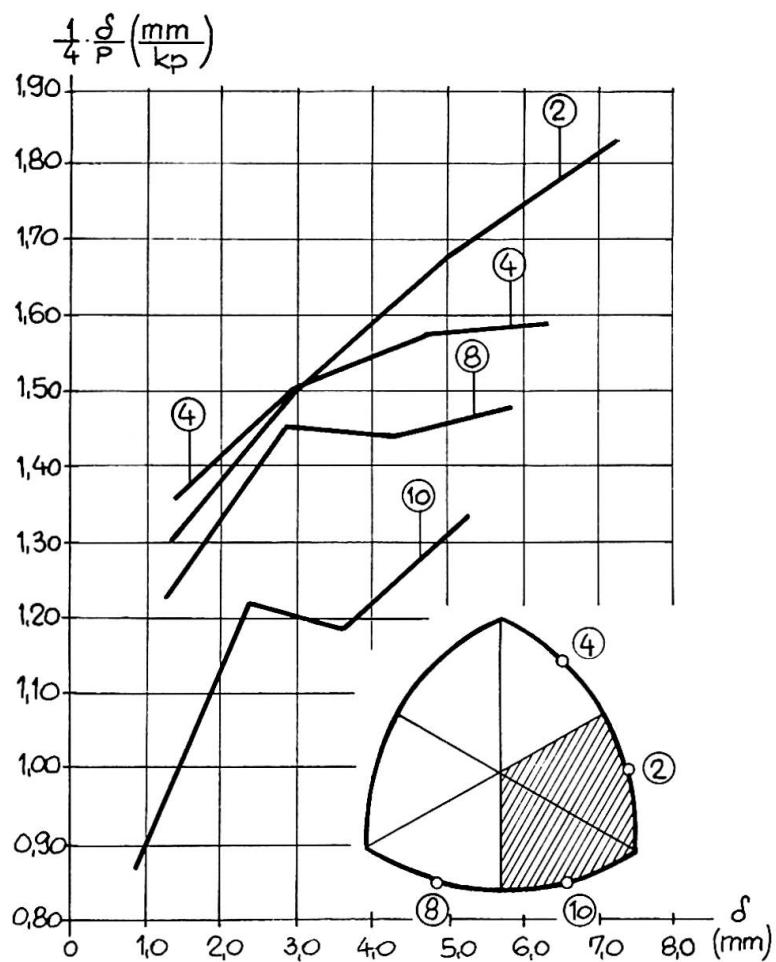
Fig. 8.

postbuckling load-bearing capacities, the Southwell diagram becomes curved downwards or upwards, respectively /Fig. 6/. Thus, measuring the buckling deformations of the model and plotting δ/P against them, we can decide at once and without destructing the model whether it has a constant /Fig. 1b/, an increasing /Fig. 1a/ or a decreasing /Fig. 1c/ postbuckling load-bearing capacity.

For illustration we show some results of the model test of the new Budapest Sports Hall, designed recently /Fig. 7/. Its structure is a reticulated steel shell without stiffening edge arches, supported by three points at a distance of 112,80 m.

For the stability of the structure only rough estimates could be

made in the course of design. Thus we had to resort to a model
test. Since we intended to study its behaviour under several
loading cases, it was desirable to clear up postbuckling charac-
teristics by a non-destructive model test in order to avoid
costs of several models. Fig. 8 shows the Southwell diagrams of
four edge points for the loading indicated by hachure. All dia-
grams show a definite downward curvature. The ensuing increasing
postbuckling load-bearing capacity has been confirmed by the final
test when we loaded the model with total load up to failure.

I hope these viewpoints might be of some use for designers.

References

[1] Kollár, L.: On Postbuckling Behaviour of Shell-arches.
             Bulletin of the International Association for
             Shell Structures, N. 30, June 1967, 21-32.
[2] Kollár, L.: On the Behaviour of Shells in the Post-Buckling
             Range
             Bulletin of the International Association for
             Shell Structures, N. 39, Sept. 1969, 41-51.
[3] Kollár, L.: Statik und Stabilität von Schalenbogen und
             Schalenbalken.
             W. Ernst und Sohn, Berlin - Akadémiai Kiadó,
             Budapest, 1971.
[4] Roorda, J.: Some thougths on the Southwell plot.
             Journ. Eng. Mech. Div. /Proc. ASCE/ 93 EM 6,
             37-48 /Dec. 1967/
[5] Timoshenko, S. - Gere, J.: Theory of Elastic Stability.
             McGraw-Hill, New York, 1971

Summary

After description of the three main types of postbuckling
behaviour of structures two conditions, necessary for the in-
creasing postbuckling load-bearing capacity, will be established.
For determination of postbuckling behaviour from non-destructive
model tests, the generalized Southwell plot will be presented.

Leere Seite

Blank page

Page vide

Überkritisches Verhalten der Stabkonstruktionen

Post-Critical Behaviour of Structures

Comportement post-critique des structures

J. SZABÓ   Zs. GÁSPÁR
Prof.   Wissenschaftlicher Mitarbeiter
Technische Universität
Budapest, Ungarn

1. Einleitung

Die auch für grosse Verschiebungen gültige Zustandsänderungs-Differentialgleichung der aus endlichen Stabelementen bestehenden Stabkonstruktionen besitzt die folgende Form /s. [1] /

$$
\begin{bmatrix} \underline{\underline{D}}(\underline{u},\underline{s}) & \underline{\underline{G}}^{*}(\underline{u}) \\ \underline{\underline{G}}(\underline{u}) & \underline{\underline{F}}(\underline{u},\underline{s}) \end{bmatrix} \cdot \begin{bmatrix} d\underline{u} \\ d\underline{s} \end{bmatrix} + \begin{bmatrix} d\underline{q} \\ d\underline{t} \end{bmatrix} = \underline{0} \tag{1}
$$

Dabei bedeuten

$$
D_{jk} = \frac{\partial G_{ij}}{\partial u_k} s_i \quad,
$$

$\underline{\underline{G}}$ die geometrische Matrix der Stabkonstruktion,

$\underline{\underline{G}}^{*}$ die Transponierte von $\underline{\underline{G}}$,

$\underline{\underline{F}}$ die Nachgiebigkeits-Matrix der Stabkonstruktion,

$\underline{u}$ der Vektor der unabhängigen Verschiebungskomponenten der Knotenpunkte,

$\underline{s}$ der Vektor der inneren Kräfte und Momente,

$\underline{q}$ der Vektor der auf die Knotenpunkte wirkenden äusseren Kräfte und Momente

$\underline{t}$ der Vektor der vorgeschriebenen Relativverschiebungen der Stäbe.

Diese Gleichung auf eine einparametrige Last angewandt, lässt sich die die indifferente Last bestimmende Differentialgleichung ableiten, die im allgemeinen Falle nach einem auf die Lösung eines

Eigenwertproblems beruhenden Iterationsverfahren ausgerechnet
wird. Der postkritische Zustand lässt sich nach einer modifizier-
ten Variante des für grosse Verschiebungen ausgearbeiteten Verfah-
rens errechnen. Die für die einzelnen Fälle ausgearbeiteten Aufga-
ben wurden derart gewählt, dass die analytische Lösung bekannt
sei, so konnte das allgemeine Verfahren kontrolliert werden. Es
wurden ebene Aufgaben gelöst und damit nicht die numerischen
Schwierigkeiten vorherrschen, wurde die Anzahl der Stabelemente
nicht hoch gewählt.

2. Das Modell der Stabkonstruktion

Die Stabkonstruktion kann aus elastischen Elementen oder aus
starren Elementen mit elastischen Gelenken aufgebaut werden. Die
geometrische Matrix $\underline{\underline{G}}$ der Stabkonstruktion aus elastischen Ele-
menten erhält man aus der Matrix

$$\underline{\underline{G}}_o = \left[\underline{\underline{G}}_{ij}\right] \quad , \tag{2}$$

indem die bei der Kopplung der Stabelemente zu den gleichen Ver-
schiebungskomponenten gehörenden Spalten summiert, sodann die zu
den vorgeschriebenen Verschiebungskomponenten gehörenden Spalten
getrennt werden. Übrigens

$$\underline{\underline{G}}_{ij} = \begin{cases} - \underline{\underline{T}}_{jv} & \text{wenn der Anfangspunkt des } j\text{-ten Stabelements} \\ & \text{der } i\text{-te Knotenpunkt ist,} \\ \underline{\underline{T}}_{jv} \underline{\underline{T}}_{jk}^{*} \underline{\underline{B}}_{j} \underline{\underline{T}}_{jk} & \text{wenn der Endpunkt des } j\text{-ten Stabelements} \\ & \text{der } i\text{-te Knotenpunkt ist,} \\ \underline{0} & \text{wenn die obigen Bedingungen nicht erfüllt sind.} \end{cases}$$

In Matrix (2) gilt

$$\underline{\underline{T}}_{jk} = \begin{bmatrix} \underline{\underline{T}}_{jok} & \underline{0} \\ \underline{0} & \underline{\underline{T}}_{jok} \end{bmatrix}, \qquad \underline{\underline{T}}_{jv} = \begin{bmatrix} \underline{\underline{T}}_{jov} & \underline{0} \\ \underline{0} & \underline{\underline{T}}_{jov} \end{bmatrix},$$

$$\underline{\underline{B}}_{j} = \begin{bmatrix} 1 & & & & \zeta_{j} & -\eta_{j} \\ & 1 & & -\zeta_{j} & & \xi_{j} \\ & & 1 & \eta_{j} & -\xi_{j} & \\ & & & 1 & & \\ & & & & 1 & \\ & & & & & 1 \end{bmatrix} \tag{3}$$

wo durch die Orthogonalmatrizen $\underline{\underline{T}}_{jok}$ bzw. $\underline{\underline{T}}_{jov}$ der im Koordinaten-
system x, y, z angegebene Vektor in das zum Anfangs- bzw. zum End-
punkt gehörende lokale Koordinatensystem ξ, η, ζ gedreht wird.

Die Bedeutung der Grössen in der Übertragungsmatrix $\underline{\underline{B}}_j$ ist in Abb.1. zu sehen.
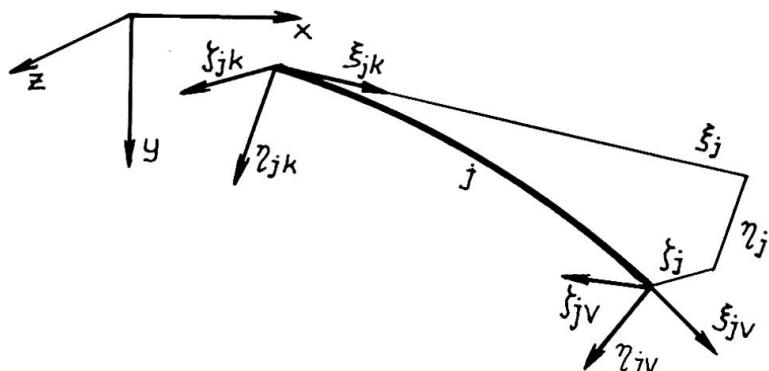
Abb. 1.

Die Nachgiebigkeitsmatrix $\underline{\underline{F}}$ ist quasi-diagonal, die einzelnen Blöcke haben die Form

$$\underline{\underline{F}}_i = \underline{\underline{T}}_{iv}\, \underline{\underline{T}}_{ik}^{*}\, \underline{\underline{\hat{F}}}_i\, \underline{\underline{T}}_{ik}\, \underline{\underline{T}}_{iv}^{*} \tag{4}$$

mit

$$\underline{\underline{\hat{F}}}_i = \begin{bmatrix} \dfrac{\ell}{EA} & & & & & \\ & \dfrac{\ell^3}{3EJ_\zeta} & & & & \dfrac{\ell^2}{2EJ_\zeta} \\ & & \dfrac{\ell^3}{3EJ_\eta} & & -\dfrac{\ell^2}{2EJ_\eta} & \\ & & & \dfrac{\ell}{GJ_\xi} & & \\ & & -\dfrac{\ell^2}{2EJ_\eta} & & \dfrac{\ell}{EJ_\eta} & \\ & \dfrac{\ell^2}{2EJ_\zeta} & & & & \dfrac{\ell}{EJ_\zeta} \end{bmatrix}_i \tag{5}$$

Wird das Modell der Stabkonstruktion durch die Kopplung von starren Elementen mit elastischen Gelenken zusammengestellt, so sind die entsprechenden Achsen der zum Anfangs- bzw. zum Endpunkt gehörenden Koordinatensysteme zueinander parallel, daher erübrigt es sich, die dazugehörige Drehmatrix zu unterscheiden /d.h. $\underline{\underline{T}}_{iv}=\underline{\underline{T}}_{ik}=\underline{\underline{T}}_i$/. Wegen der Orthogonalität der Matrix $\underline{\underline{T}}_i$

$$\underline{\underline{T}}_i\, \underline{\underline{T}}_i^{*} = \underline{\underline{E}} \tag{6}$$

vereinfachen sich die Beziehungen (2) und (4), und in Matrix (3) ist $\xi_j=\ell_j$, $\eta_j=\zeta_j=0$. Sind die elastischen Gelenke gewissen Beanspruchungen gegenüber starr, so ist die Matrix $\underline{\underline{F}}$ singulär, daher müssen die in der Arbeit [2] angegebenen Transformationen durchgeführt werden.

Nach dem Iterationsverfahren in [1] können die Verschiebungen und Beanspruchungen des Modells ermittelt werden. Um das Modell und den Algorithmus zu überprüfen, wurde das Problem in Abb. 2. mit Hilfe beider Modelle gelöst. Die Angaben wurden so angesetzt, dass in der genauen Lösung, der Kragträger Viertelkreisform habe. Der spezifische Wert des Endpunkt verschiebungsfehlers ist in Abb.3. über der Elementenanzahl dargestellt /in der Abbildung bedeuten ε den Endpunktverschiebungsfehler und r den Kreisbogenhalbmesser./
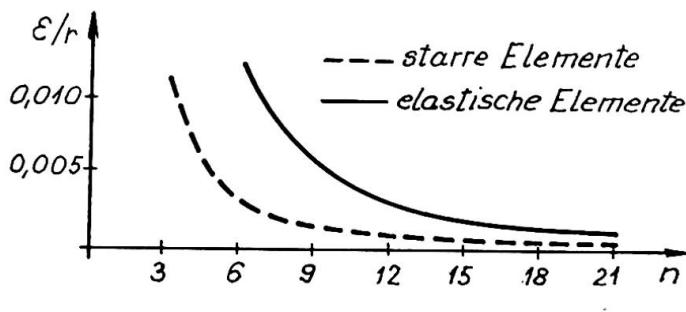
Abb. 2.

Abb. 3.

3. Stabilitätsnachweis

Der kritische Parameter einer einparametrigen Last der Stabkonstruktion wurde nach der Arbeit [3] ermittelt. Wird als Last keine relative Verschiebung vorgeschrieben, so lautet bei einer Einparameterlast die Zustandsänderungs-Differentialgleichung (1)

$$\begin{bmatrix} \underline{\underline{D}}(\underline{u},\underline{s}) & \underline{\underline{G}}^{*}(\underline{u}) \\ \underline{\underline{G}}(\underline{u}) & \underline{\underline{F}}(\underline{u},\underline{s}) \end{bmatrix} \begin{bmatrix} d\underline{u} \\ d\underline{s} \end{bmatrix} + dR \begin{bmatrix} \underline{\underline{f}} \\ \underline{0} \end{bmatrix} = \underline{0} \tag{7}$$

wo

$$D_{jk} = \frac{\partial G_{ij}}{\partial u_k} s_i + R \frac{\partial f_j}{\partial u_k}$$

und

$$\underline{\underline{f}} = \underline{\underline{f}}(\underline{u})$$

$$\left\| \underline{\underline{f}} \right\| = \text{const}$$

eine eindeutige Funktion ist.

Beim Angriff der kritischen Last hat der homogene Teil der Differentialgleichung (7) auch eine von der trivialen verschiedene Lösung, die zum Eigenwertproblem

$$\left(\left[\frac{\partial \underline{\underline{G}}^{*}}{\partial \underline{\underline{u}}} \underline{\underline{s}} \right] + R \frac{\partial \underline{\underline{f}}}{\partial \underline{\underline{u}}} - \underline{\underline{G}}^{*} \underline{\underline{F}}^{-1} \underline{\underline{G}} \right) d\underline{u} = \underline{0} \tag{8}$$

führt.

Da sowohl die Matrix $\underline{\underline{G}}$ als auch die Vektoren $\underline{f}$ und $\underline{s}$ Funktionen von R sind, lässt sich das Eigenwertproblem nicht direkt bestimmen. Ist der zum Parameter R_i gehörende Zustandsvektor bekannt, werden die veränderlichen Grössen des Eigenwertproblems (8) nach dem Verschiebungsvektor in eine Taylorsche Reihe entwickelt und nur deren erste zwei Glieder berücksichtigt, so erhält man das verallgemeinerte Eigenwertproblem

$$\left(\underline{\underline{A}} + R\underline{\underline{B}}\right) d\underline{u} = \underline{0} \tag{9}$$

das bereits direkt gelöst werden kann, wo

$$\underline{\underline{A}} = \underline{\underline{D}}_1 + \underline{\underline{D}}_3 - R_i\left(\underline{\underline{D}}_2 + \underline{\underline{D}}_2^* + \underline{\underline{D}}_4\right)$$

$$\underline{\underline{B}} = \underline{\underline{D}}_2 + \underline{\underline{D}}_2^* + \underline{\underline{D}}_4 + \underline{\underline{D}}_5$$

$$\underline{\underline{D}}_1 = -\underline{\underline{G}}_i^* \; \underline{\underline{F}}^{-1} \; \underline{\underline{G}}_i$$

$$\underline{\underline{D}}_2 = -\left(\frac{\partial \underline{\underline{G}}^*}{\partial \underline{\underline{u}}}\bigg|_{\underline{u}=\underline{u}_i} \left(\underline{\underline{H}}^{-1}\underline{f}_i\right)\right) \underline{\underline{F}}^{-1} \; \underline{\underline{G}}_i$$

$$\underline{\underline{D}}_3 = \left[\frac{\partial \underline{\underline{G}}^*}{\partial \underline{\underline{u}}}\bigg|_{\underline{u}=\underline{u}_i} \underline{s}_i\right]$$

$$\underline{\underline{D}}_4 = -\left[\frac{\partial \underline{\underline{G}}^*}{\partial \underline{\underline{u}}}\bigg|_{\underline{u}=\underline{u}_i} \left(\underline{\underline{F}}^{-1}\underline{\underline{G}}_i\underline{\underline{H}}^{-1}\underline{f}_i\right)\right]$$

$$\underline{\underline{D}}_5 = \frac{\partial \underline{f}}{\partial \underline{\underline{u}}}\bigg|_{\underline{u}=\underline{u}_i}$$

$$\underline{\underline{H}} = -\underline{\underline{D}}_1 - \underline{\underline{D}}_3 - R_i\underline{\underline{D}}_5$$

Ist der Wert $|R - R_i|$ höher als ein vorgeschriebener Wert, so wird der Zustandsvektor für einen Parameterwert R_i bestimmt, der dem kritischen Parameterwert näher liegt und das Verfahren wird wiederholt.

Wenn beim Angriff der kritischen Last nur eine geringe oder gar keine Formänderung entsteht, so ist das Eigenwertproblem (9) nur einmal zu lösen und auch die Koeffizientenmatrizen werden aus weniger Gliedern bestehen.

Zur Überprüfung des Algorithmus wurde der Stabilitätsnachweis des Bogenträgers der Form einer Parabel zweiten Grades in Abb. 4 mit Hilfe eines Modells aus starren Elementen durchgeführt. Der Parameter der kritischen Last änderte sich in Abhängigkeit von der Teilungszahl nach Abb.5.
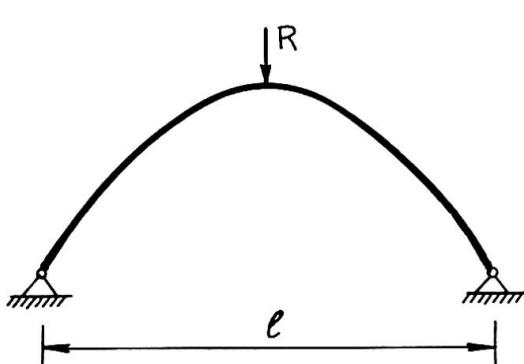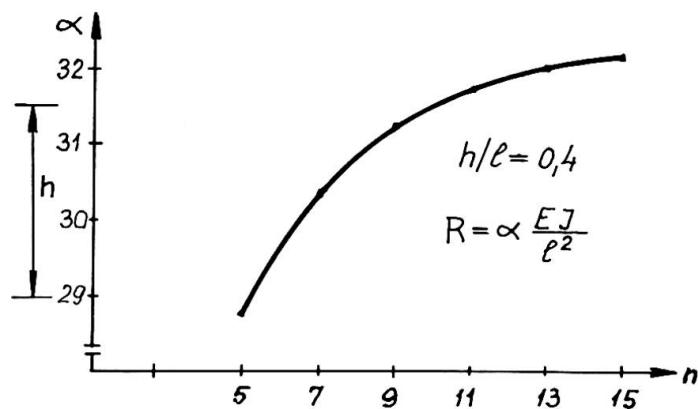
Abb.4.   Abb.5.

4. Postkritischer Zustand bei Stabilitätsverlust ohne Verzweigungspunkt

Die Zustandsänderungskurve des Problems in Abb.6. lässt sich auch in Umgebung des Durchschlagpunktes ohne Schwierigkeit auch auf analytischem Wege ermitteln /z.B. [4] und [5] /, wenn die Biegesteifigkeit der Stäbe im Vergleich zur Normalsteifigkeit genügend gross ist und der Durchschlag ohne Stabknickung erfolgt. Das Trägermodell wird aus 6 elastischen Stabelementen gleicher Länge aufgebaut. Jeder beliebige Punkt im Abschnitt AB der Zustandsänderungskurve in Abb.7. lässt sich mit Hilfe der obenerwähnten iterativen Lösung der Differentialgleichung (7) für grosse Verschiebungen ermitteln.
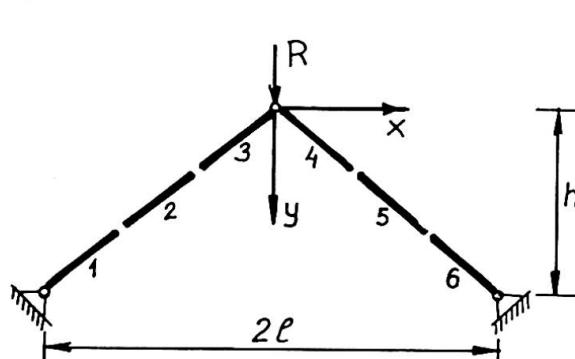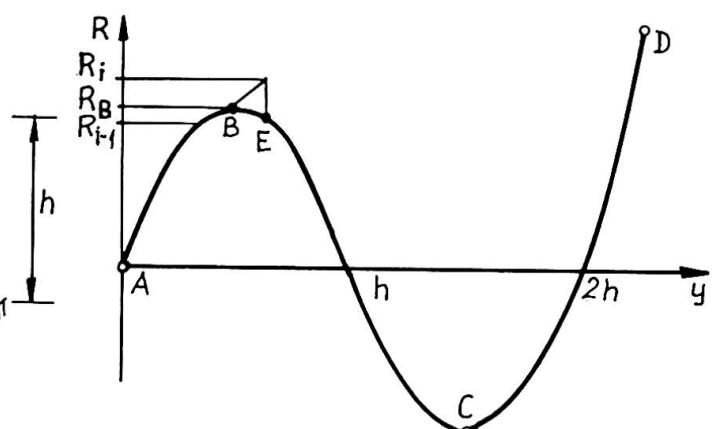
Abb.6.   Abb.7.

Da der Wert R_B unbekannt ist und die Last stufenweise auf den Träger aufgebracht wird, kann es vorkommen, dass ein, zum Parameterwert $R_i > R_B$ gehörender Zustandsvektor gesucht wird, der lediglich mit einer ganz anderen Geometrie des Trägers ausgeglichen werden kann, daher wird beim Iterationsverfahren die Fehlervektornorm die Laststufennorm wesentlich übersteigen und die Iteration nicht konvergieren. Dafür wird durch das folgende Verfahren Ab-

hilfe geschafft, das sich um die Konvergenz zu beschleunigen auch
dann verwenden lässt, wenn einige − jedoch nicht genau bestimmte −
Punkte der zum Parameter R gehörenden Zustandsänderungskurve er-
mittelt werden sollen.

Wird die Differentialgleichung (7) als Differenzgleichung
auf die Laststufe angewandt, so kann in Kenntnis der erhaltenen
geometrischen Lage und der inneren Kräfte, der Vektor der äusseren
Kräfte, die ausgeglichen werden können, in der Form

$$\underline{q}^{(1)} = - \underline{\underline{G}}^* \underline{\underline{s}}$$

errechnet werden. Der Parameter R wird derart gewählt, dass
$\| \underline{q}^{(1)*} - R\underline{\underline{f}} \|$ minimal sei. Dies wird durch den Parameter

$$R = \frac{\underline{q}^{(1)*}\underline{\underline{f}}}{\underline{\underline{f}}^* \underline{\underline{f}}} \tag{1o}$$

erfüllt. Wird der Parameter R jeweils so bestimmt, so erhält
man den Punkt E in Abb.7. Soll der Parameter wieder vergrössert
werden, so geht man auf der Zustandsänderungskurve nach Punkt B
aus, der Parameter muss also auf dem labilen Abschnitt vermindert
werden. Ob der so bestimmte Punkt auf dem labilen oder auf dem sta-
bilen Zweig liegt, wird nach dem Energieprinzip festgestellt. Die
Verschiebung unter Einwirkung des Lastzuwachses $\Delta R\underline{\underline{f}}$ /$\Delta R > 0$/ er-
gibt sich mit der Genauigkeit der Theorie zweiter Ordnung zu

$$\Delta\underline{u} = \Delta R \; \underline{\underline{H}}^{-1}\underline{\underline{f}}$$

die Arbeit der Last $R\underline{\underline{f}}$ beträgt bei dieser Verschiebung

$$L = R\underline{\underline{f}}^* \Delta\underline{u} \; .$$

Ist $L > 0$, so ist das Vorzeichen für ΔR gleich dem Vor-
zeichen von R zu wählen; ist $L < 0$, so wird für ΔR das ent-
gegengesetzte Vorzeichen wie das von R genommen. Kurz, gilt
$\underline{\underline{f}}^*\underline{\underline{H}}^{-1}\underline{\underline{f}} > 0$, so liegt der Punkt im stabilen, gilt $\underline{\underline{f}}^*\underline{\underline{H}}^{-1}\underline{\underline{f}} < 0$, so
liegt der Punkt im labilen Kurvenzweig. Im indifferenten Zustand
ist die Matrix $\underline{\underline{H}}$ singulär.

Der Konvergenzradius des Iterationsverfahrens ist dem Krüm-
mungsradius der Zustandsänderungskurve proportional, so kann die
Berechnung in jedem Schritt mit einer grossen Laststufe begonnen
werden, nimmt jedoch die Fehlervektornorm innerhalb einiger
Schritte nicht wesentlich ab, so muss die Schrittgrösse vermindert

werden. In Abb.7. wurde für h=0,375 ℓ der Kurvenabschnitt AD
– bei in 40 Stufen aufgetragener Last – bestimmt.

## 5. Postkritischer Zustand nach dem Verzweigungspunkt

Wird das Modell des Trägers in Abb.6. nur aus durch biegungs-
elastische Gelenke verbundenen Stabelementen aufgebaut, so kann
der Durchschlag lediglich mit Knickung erfolgen.

Bei einer Last unter der kritischen, tritt keine Formänderung
ein, so hat das Eigenwertproblem (9) die Form

$$\left(\underline{\underline{D}}_1 + R\underline{\underline{D}}_5\right)d\underline{\underline{u}} = \underline{\underline{0}}$$

Der kleinste Eigenwert gibt die erste kritische Last, durch
den dazugehörenden Eigenvektor wird die Knickform von einem freien
Parameter abgesehen bestimmt. Um die Punkte der zur Knickform ge-
hörenden Zustandsänderungskurve nach dem Verzweigungspunkt zu be-
stimmen, muss auf dem Träger das Skalarfache der durch den Eigen-
vektor bestimmten Form erzeugt werden. Die richtige Annahme des
Skalarparameters ist von grosser Wichtigkeit, da bei einem zu
niedrigen Parameterwert, die Matrix $\underline{H}$ schlecht konditioniert
/ill-conditioned/ ist, und das für die Elimination des Fehlervek-
tors, zufolge der eingeschalteten endlichen Verschiebung, erfor-
derliche Iterationsverfahren nicht konvergiert. Wird der Skalar
zu hoch gewählt, so ist die Fehlervektornorm grösser als der Kon-
vergenzradius.

Mit richtigen Werten gerechnet und durch die in Punkt 4 be-
schriebene Minimalisierung des Fehlervektors erhält man einen
Punkt der Zustandsänderungskurve. Das Vorzeichen von ΔR, wieder
dementsprechend angenommen, ob der Punkt auf dem stabilen oder
auf dem labilen Abschnitt liegt, können die Punkte der Zustands-
änderungskurve nach dem für die grossen Verschiebungen gültigen
Verfahren, mit beliebiger Dichte ermittelt werden.

Abb.9.
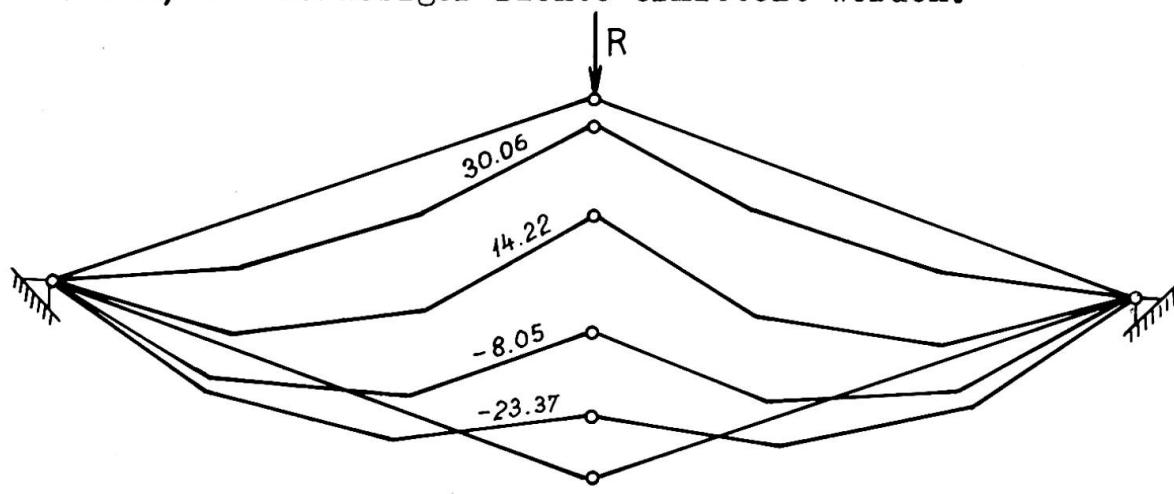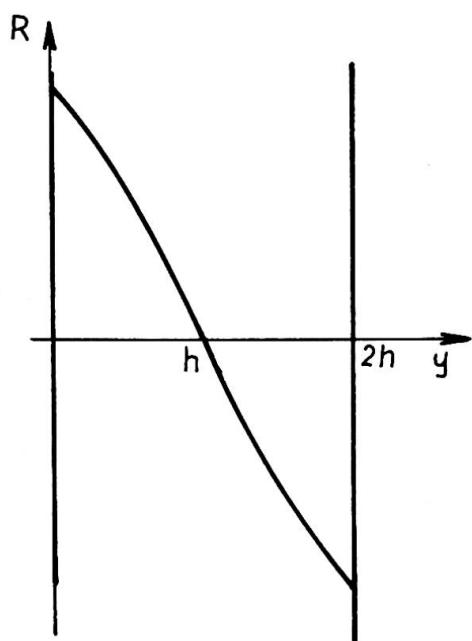
Abb.8. zeigt den Träger im ursprünglichen und im Endzustand, der nach einer, mit einem Eigenvektor der Norm 0,2 begonnenen Iteration berechnet wurde, weiterhin einige Zwischenzustände des Durchschlags, wobei die jeweiligen Grössen der Ausgleichkraft angegeben sind.In Abb.9. ist die Grösse der Ausgleichkraft in Abhängigkeit von der Verschiebung des Gelenks C dargestellt.

Literatur

[1] Szabó,J.-Rózsa,P.: Grosse Verschiebungen von Stabkonstruktionen. /Acta Technica Acad.Sc.Hungaricae, im Druck/.

[2] Szabó,J.-Rózsa,P.: Die Matrizengleichung von Stabkonstruktionen. /Acta Technica Acad.Sc.Hungaricae, Tomus 71, Fasc.1-2. 1971. Budapest/.

[3] Gáspár,Zs.: Stabilitätsprüfung von Stabkonstruktionen. /Acta Technica Acad.Sc.Hungaricae, im Druck/.

[4] Falk, S.: Technische Mechanik, Dritter Band. /Springer-Verlag 1969. Berlin-Heidelberg-New York/.

[5] Kollbrunner,C.F.-Meister,M.: Knicken, Biegedrillknicken, Kippen. /Springer-Verlag p.322 1961.Berlin-Göttingen-Heidelberg/.

Zusammenfassung

Durch die Lösung eines Eigenwertproblems, das aus der Zustandsänderungs-Differentialgleichung einer mit starren oder elastischen Stabelementen modellierten, durch einparametrige Belastung belasteten Stabkonstruktion folgt, lassen sich der Parameter der kritischen Last und das Affinbild der Knickform bestimmen. Die Punkte der Zustandsänderungskurve werden numerisch mit Hilfe eines konvergenten Iterationsverfahrens bestimmt.

Leere Seite

Blank page

Page vide

Post-Critical Behaviour of Inelastic Structures

Comportement post-critique de structures non-élastiques

Überkritisches Verhalten unelastischer Träger

GIULIANO AUGUSTI
Assoc. Professor of Structural Engineering
Università di Firenze
Florence, Italy

As illustrated by Professor Bieniek's Report, it is now increasingly recognized that in structural engineering the knowledge of the post-critical behaviour is almost as essential as that of the critical load itself: in fact, the unavoidable imperfections that make actual structures different from the "ideally perfect" models of applied mechanics, affect their strength in a way that depends largely on the post-critical behaviour of their "ideally perfect" models.

This contribution presents an elementary (but hopefully stimulating) discussion of the joint effects of imperfections and inelastic deformations on the behaviour of structures that, if perfect, would exhibit a point of bifurcation of equilibrium. As in Ref. (A.1) (°), buckling will be used as a synonym for bifurcation of equilibrium, while collapse load will indicate a (local) maximum on an actual load-deformation path. Dynamical and time-rate effects will not be considered.

The most rational approach to the study of the effect of imperfections on structural strength is through statistics and probability theory, as indicated by Bieniek (p.38) and proved by an increasing number of research papers. From this point of view, an actual structure is seen as a sample structure taken out of a population of nominally identical structures, different from each other because of random variations of the design parameters (yield stress, geometric dimensions, etc.). The ideal structure, corresponding exactly to the design, is the average structure of this population. With some qualifications (°°), it can be stated that the average (expected) strength of the actual structure is approximately equal to the strength of the average structure in absence of phenomena of geometrical instability, and is lower if these phenomena are present. In the latter case, the introduction of probabilistic methods becomes of utmost importance in order to obtain economical and reliable designs. This point is illustrated, in the following Section 1, by the summary of a probabilistic investigation

---

(°) See list of References at the end of this contribution.

(°°) The following statement is too general to be more than an approximation. For instance, it has already been proved (A.2) that the average plastic collapse load of a ductile structure is smaller than the collapse load of the average structure, but in the first numerical examples their difference is rather small.

of slender imperfect columns, fully published elsewhere (A.3). A basic differ-
ence between this study and previous works by other Authors is the introduction
of other random quantities (namely, the yield stress and the free buckling
length) besides the geometrical imperfections.

In Ref. (A.3), collapse occurs because <u>inelastic deformations</u> develop:
this appears to be the most frequent cause of collapse of actual structures, and
it is rather surprising that the interaction of inelasticity and instability is
still a comparatively little-explored field, perhaps avoided by most researchers
because of its great analytical difficulties.

Section 2 below presents two examples of <u>asymmetric behaviour</u> (i.e.,
of load-deformation paths that depend on the sign of the deformation) of struc-
tures that, if perfect, would buckle elastically. In the first example, the
asymmetry occurs in the <u>inelastic</u> range of deformations and is due to an asym-
metry in the <u>strength</u> of structural cross-section. The second example illus-
trates <u>asymmetric elastic buckling</u>, a phenomenon now well known, after the great
amount of research spurred by Koiter's fundamental works (Bieniek's Refs. 47 and
71), and apparently the only practically significant case in which collapse may
be completely independent of the onset of inelastic deformations.

Finally, the last Section of this paper discusses and compares differ-
ent cases of <u>buckling</u> in the <u>inelastic</u> range. Again, it will be shown that
either a strength asymmetry or a geometry effect may cause <u>asymmetry</u> of the
post-buckling load-deformation paths of the "perfect" structure: consequently,
in such cases the collapse load of the actual structure depends on the <u>sign</u> of
the imperfection.

1) ELASTIC BUCKLING AND PLASTIC COLLAPSE: A PROBABILISTIC ANALYSIS

Consider a simple compressed strut, for instance pin-ended as in Fig.
1.1, and made of an elastic-perfectly plastic material with yield stress σ_y.
If the strut is initially perfectly straight, it is well known that it remains
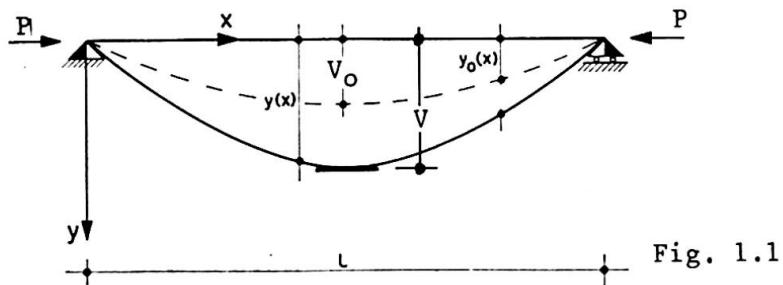
Fig. 1.1

straight and stable as long as the compressive load P is smaller than both the
elastic buckling load

$$P_E = \pi^2 EI/l^2 = \pi^2 EA/\lambda^2 = \sigma_E A \quad \text{and the squash load } P_y = \sigma_y A$$

If $P_E < P_y$, the load remains constant at $P = P_E$ (within the first-
order, small-displacements theory) in the early stages of buckling, and begins
decreasing as soon as the first plastic deformations take place; the axial load
vs. mid-span displacement (P-V) path remains below, and tends asymptotically
to, the P-V curve corresponding to full yielding of the cross-section $V = M_p/P$
(Fig. 1.2a): both curves have a horizontal asymptote at $P = 0$.
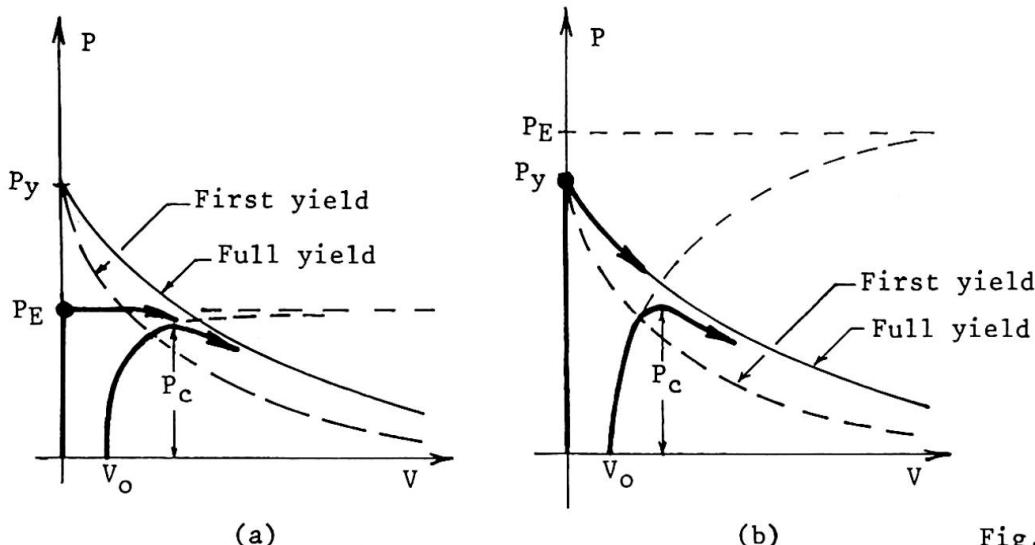
(a)   (b)   Fig. 1.2

If $P_y \leq P_E$, the strut buckles at $P = P_y$; the load P starts decreasing quite rapidly at the very onset of the deformations following the full-yield curve, and again tends asymptotically to zero when $V \to \infty$ (Fig. 1.2b).

If the material has a constant, non-zero tangent modulus E_T in the inelastic range, the horizontal asymptotes are at the load $P = P_K$ (defined in Section 3) rather than at $P = 0$ (A.4).

If the strut is affected by an initial geometrical imperfection, for instance in the form of a half sine-wave

$$Y_o = Y_o(x) = V_o \sin \pi x/l \qquad (1.1)$$

(Fig. 1.1), the P-V path in the elastic range is given, with very good approximation, by (Fig. 1.2)

$$V = V_o / (1 - P/P_E) \qquad (1.2)$$

The actual elastic-plastic path remains below the full-yield curve: collapse occurs when sufficient plastic deformations have developed. The relation between imperfection magnitude and collapse load P_c of the type (A.3)

$$\gamma = \frac{V_o}{r} = 3 \left[\frac{P_y}{P_c} - 1 \right] \left[1 - \sqrt[3]{\frac{P_c}{P_E}} \right] \qquad (1.3)$$

where r is the relevant core radius of the section.

If the relationship between P_c and γ is known and γ is a random variable, it is conceptually easy to obtain the probability distribution of the dependent random variable P_c or $\sigma_c = P_c/A$. In Ref.(A.3), eq.(1.3) was assumed to hold throughout the relevant range; and, since the geometrical imperfection is essentially due to errors of fabrication with respect to the straight strut one aims at, it appeared logical to take γ to be normally distributed with zero mean, although only its absolute value, γ , appears in eq.(1.3). Fig.1.3 shows typical probability density curves of the collapse stress σ_c, calculated under the

Fig. 1.3

above assumptions for the yield stress $\sigma_y = 2800$ kg/cm^2, two slenderness ratios λ, and several values of the standard variation, s, of the imperfection coefficient γ. All these curves show a sharp cut-off at the collapse stress of the imperfect strut

$$\sigma_{co} = P_{co}/A = \min(\sigma_y, \sigma_E): \quad \sigma_{co} = \sigma_y$$

when $\lambda = 60$, $\sigma_{co} = \sigma_E = P_E/A$ when

$\lambda = 100$.

For a more realistic treatment, one must remember that the yield stress of a given material is also a random quantity : some earlier investigations seem to suggest that, at least in a first approximation, it can be considered to be normally distributed with a standard deviation, t, equal to about 10% of its mean value $\bar{\sigma}_y$. In the already quoted Ref. (A.3), it seemed appropriate to introduce also a random variability of the slenderness ratio λ, because this quantity may be different from the design value because of defective restraints and/or approximations introduced in the calculations; also λ has been assumed to be normally distributed, and its standard deviation, k, has been taken equal to 10% of the average value $\bar{\lambda}$. With these assumptions, the probability density curves of the collapse stress σ_c take the form shown in Fig. 1.4 : the upper cut-off disappears,


Fig. 1.4

because large values of σ_{co} are now possible, albeit with little probability. However, the average collapse stress $\bar{\sigma}_c$ remains much smaller than the collapse stress of the average, straight strut, $\sigma_{co} = \min(\bar{\sigma}_y, \bar{\sigma}_E)$.

In order to have indications for actual design practice, the relationship has also been investigated between the nominal safety factor ψ introduced in the calculations (ratio of nominal collapse stress σ_{co} to design admissible stress σ_{cam}) and the probability of collapse

$$P^* = \text{Prob}(\sigma_c \le \sigma_{cam}) \qquad (1.4)$$

A typical set of curves, plotted in semi-logarithmic scale in the relevant range of (very small) values of P^*, is shown in Fig. 1.5 : they can be well approximated by a set of parallel straight lines. It is also worth noting that very small variations of the nominal safety factor ψ can easily induce ten- or hundred-fold variations of actual safety; this clearly calls for a "rationalization" of design practice through the probabilistic approach. A qualitative and quantitative comparison between the results of the probabilistic treatment just summarized and the Italian Steel Building Code has also been presented in Ref. (A.3).
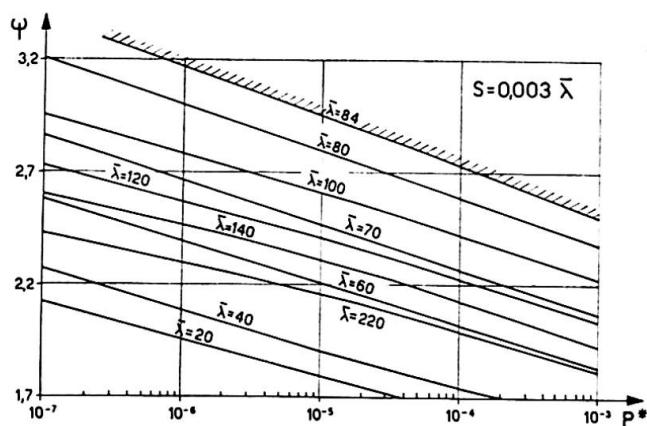
Fig. 1.5

2) ELASTIC BUCKLING: ASYMMETRIC BEHAVIOUR

The behaviour described in Section 1 is, within the elastic range, perfectly symmetrical with respect to the sign of the displacement and/or the imperfection, regardless of a possible asymmetry of the strut cross-section with respect to the axis of bending : in fact, the geometry of the section affects the behaviour of strut only through its moment of inertia. This type of behaviour (symmetric elastic buckling) is not limited exclusively to the pin-ended strut, but is common to many of the elastic structures that are liable to instability : indeed, before the development of Koiter's theory (Bieniek's Refs. 47 and 71), it was thought to be common to them all.
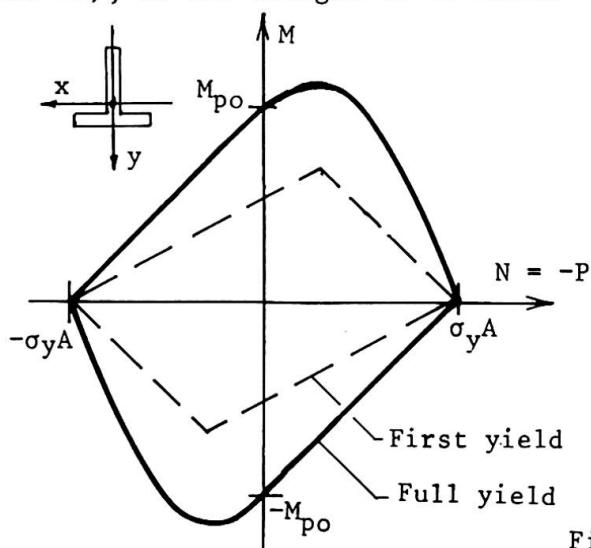
However, the symmetry of behaviour does not extend beyond the elastic range of deformation, unless the strength of the cross-section is symmetric (as it has implicitly been assumed throughout Section 1). For instance, if the strut of Fig. 1.1 has a T-section, the first- and full-yield interaction curves in the moment-axial load (M-N) plane are qualitatively indicated in Fig. 2.1. (For a detailed derivation, cf. Ref. (A.5).)

Fig. 2.1

Transformed into P-v coordinates, the interaction curves appear like in Fig. 2.2, and the P-v equilibrium paths become, on the whole, _asymmetric_ for both
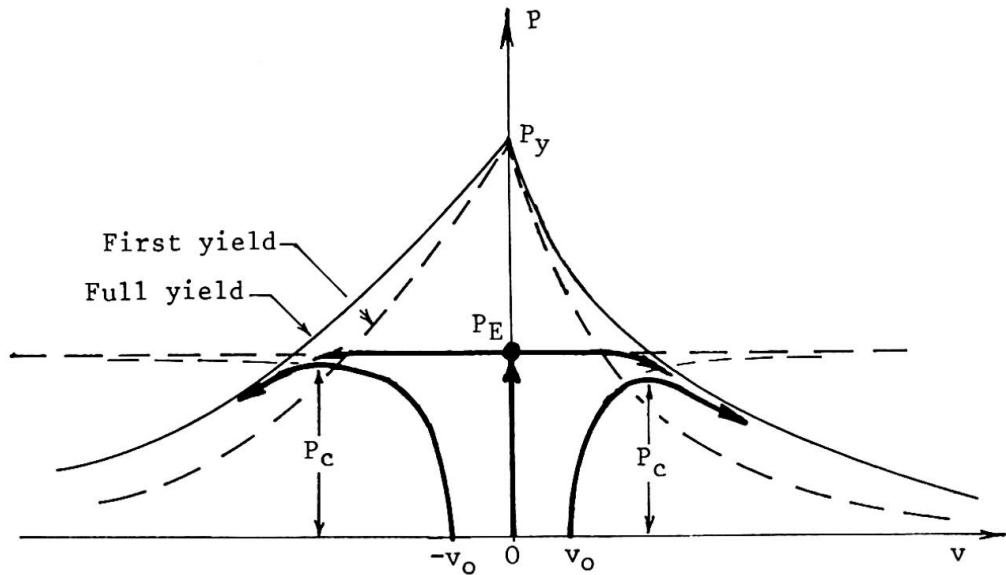

Fig. 2.2

the _perfect_ and the _imperfect_ strut, in both cases $P_E < P_y$ (illustrated by Fig. 2.2) and $P_y \leq P_E$ In particular, the collapse load does depend on the sign of the imperfection

$$P_c (V_o) \neq P_c (-V_o) \qquad (2.1)$$
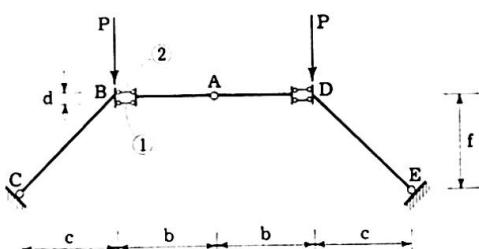
The preceding discussion has illustrated the case of _symmetric elastic buckling_, followed by _asymmetric plastic collapse_ due to an asymmetry of the cross-section : an asymmetry of yield stress (different yield points in tension and compression) would have the same qualitative effect.
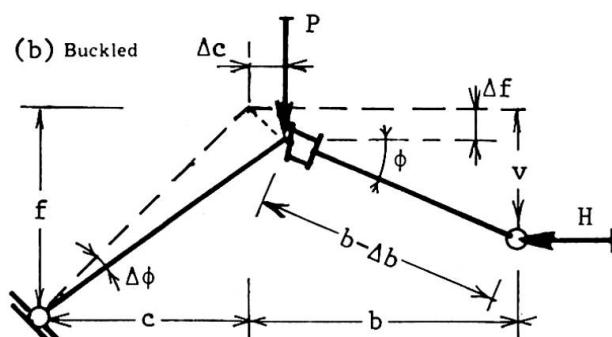
Another important case of asymmetric behaviour is that of _asymmetric elastic buckling_, analytically described in the already quoted works by Koiter and here illustrated by the simple model of a three-hinged arch shown in Fig. 2.3a: AB, BC, etc. are _rigid_ links; A, C, E are momentless hinges; the two deformable cells B and D consist of two parallel _elastic rods_ (1 and 2) and a soft _core_ that does not allow a shear deformation of the cell. Assume that Fig.2.3a represents the configuration at the point of buckling·with a load $P = P_E$ and a horizontal thrust

$$H_E = P_E c/f \qquad (2.2)$$

(a) Unbuckled

(b) Buckled

(c)
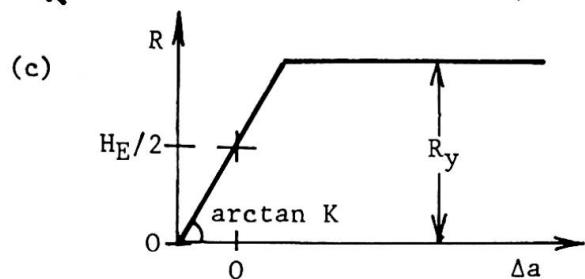
Fig. 2.3

The following treatment is limited to geometrically symmetrical <u>buckled</u> configurations, such as in Fig. 2.3b; equilibrium yields

$$P \ (c + \Delta c) \ = \ H \ (f - v)$$

$$H \ (v - \Delta f) \ = \ (R_1 - R_2) \ \frac{d}{2} \qquad\qquad (2.3)$$

$$H \ = \ R_1 + R_2$$

where R_1 and R_2 are the (compressive) reactions in the elastic rods, related to their variation of length by (Fig. 2.3c)

$$K \ \Delta a_i \ = \ R_i - H_E/2 \qquad (i = 1,2) \qquad\qquad (2.4)$$

Δa_i is measured with respect to the point of buckling, and is taken positive when a shortening.

In deriving the post-buckling P-v relationship, introduce firstly the (wrong) assumption that the deformable cells do not change length during the deformation. Then geometry yields, up to second-order infinitesimals

$$(\phi - \Delta\phi) \ d \ = \ \Delta a_1 - \Delta a_2 \qquad\qquad (2.5)$$

$$\Delta c \ = \ b \ (1 - \cos \phi) \ = \ \frac{b \ \phi^2}{2} \quad ; \quad \Delta f \ = \ \frac{c}{f} \ \Delta c \ = \ \frac{bc}{f} \ \frac{\phi^2}{2} \qquad (2.6)$$

$$\phi \ = \ \frac{v - \Delta f}{b} \ = \ \frac{v}{b} - \frac{c}{f} \frac{\phi^2}{2} \quad ; \quad \Delta\phi \ = \ \frac{\Delta f}{c} \ = \ \frac{\Delta c}{f} \ = \ \frac{b}{f} \ \frac{\phi^2}{2} \qquad (2.7)$$

Introducing into eqs. (2.3), taking account of (2.4) and letting

$$P_E \ = \ H_E \ \frac{f}{c} \ = \ K \ \frac{d^2}{2b} \ \frac{f}{c} \qquad\qquad (2.8)$$

some algebra leads to the following expression

$$P \ = \ P_E \ (1 - \frac{3}{2} \ \frac{v}{f} + \dots) \qquad\qquad (2.9)$$

Note that neglecting the second-order quantities $\Delta\phi$, Δc and Δf in the initial equations (2.3), the final equation would be

$$P \ = \ P_E \ (1 - \frac{v}{f}) \qquad\qquad (2.10)$$

i.e. would present an error of the same order of v : the possibility of such an error was pointed out by Koiter with reference to a simple fully elastic frame (A.6).

Actually, during buckling, the length of the elastic cells decreases of the quantity

$$\Delta b \ = \ (\Delta a_1 + \Delta a_2) \ / \ 2 \qquad\qquad (2.11)$$

Eqs. (2.6a) and (2.7b) become respectively

$$\Delta c \ = \ (b - \Delta b) \ (1 - \cos \phi) \ = \ b(\frac{\phi^2}{2} + \frac{\Delta b}{b}) \qquad\qquad (2.12)$$

$$\Delta\phi \ = \ \frac{\Delta c}{f} \ = \ \frac{b}{f} \ (\ \frac{\phi^2}{2} + \frac{\Delta b}{b})$$

Introducing these new expressions into (2.3) and (2.4) and rearranging, one obtains

$$2 \phi \frac{\Delta b}{b} = - \frac{d^2}{2f} (\frac{\phi^2}{2} + \frac{\Delta b}{b}) \qquad (2.13)$$

so that, up to second-order terms,

$$\frac{\Delta b}{b} = - \frac{\phi^2}{2} \quad ; \quad \Delta c = \Delta f = \Delta \phi = 0 \qquad (2.14)$$

and eq. (2.10) holds, at least in the vicinity of the P-axis: this equation has been accepted in an earlier presentation of this arch model (A.7).

The limit condition of the arch corresponds to the most stressed rod reaching its yield value R_y (Fig.2.3c): the first- and full-yield M-N interaction profiles of the cells coincide into a diamond (Fig.2.4). Neglecting, in accord with eq. (2.14), all second-order displacements, it is easy to transform this diamond into the following P-v curves:
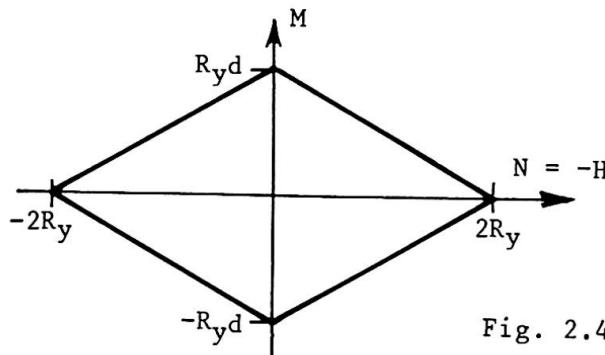
$$v > 0; \quad R_1 = R_y; \quad P = P_y \frac{1-v/f}{1+2\ v./d} \qquad (2.15)$$

Fig. 2.4
$$v < 0; \quad R_2 = R_y; \quad P = P_y \frac{1-v/f}{1-2\ v/d} \qquad (2.16)$$

where

$$P_y = 2\ R_y\ f/c \qquad (2.17)$$

Eqs. (2.15) and (2.16), qualitatively sketched in Fig. 2.5, have the horizontal asymptote

$$P = \mp P_y\ d/2f \qquad (2.18)$$

respectively; eq. (2.15) intersects the v-axis at $v = f$, with a slope

$$\left[\frac{dP}{dv}\right] P = 0 \quad = - \frac{P_y}{f} \quad \frac{1}{1+2\ f/d} \qquad (2.19)$$

so that, provided $P_y > P_E > P_y/(1+2\ f/d)$, eq.(2.10) intersects both eqs. (2.15) and (2.16) (Fig. 2.5). In words, <u>elastic buckling</u> of the perfect elastic arch just described is followed by compression yielding in the deformable cell.
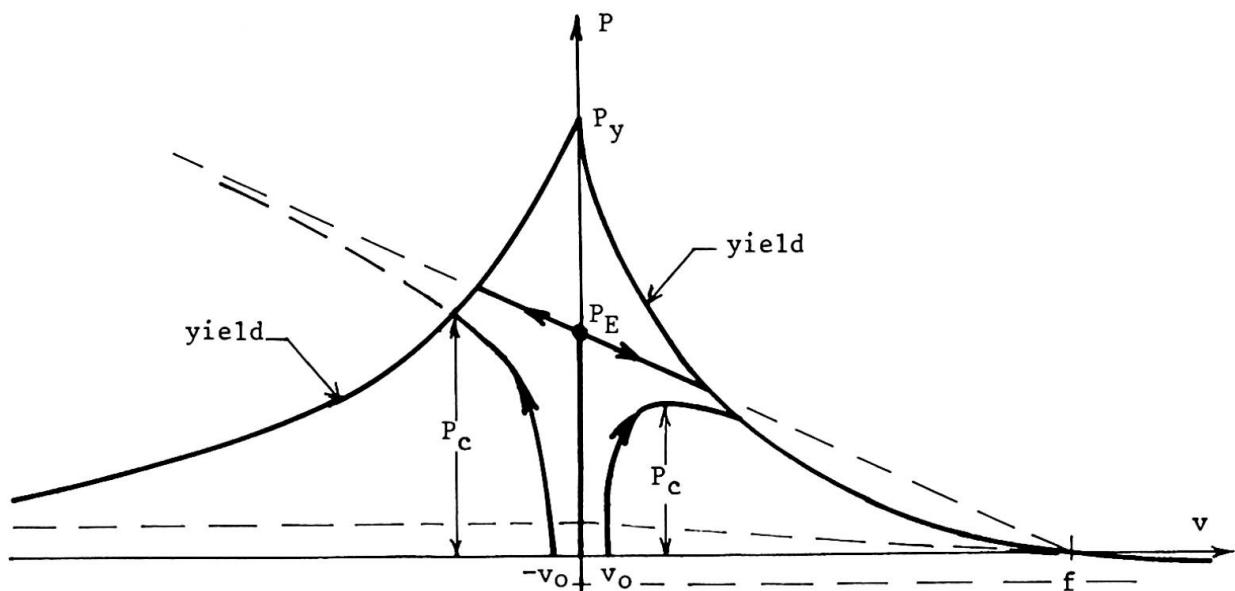
Fig. 2.5

If an initial imperfection, v_o, is present, the elastic P–v paths tend asymptotically to the straight line, eq. (2.10). Therefore, as shown in Fig. 2.5, when $v_o > 0$ the collapse load P_c is most probably reached within the elastic range of behaviour, while if $v_o < 0$ collapse occurs at the yield limit curve. It is thus shown that, in a structure liable to asymmetric elastic buckling, (a) the sign of the imperfection may affect the value of the collapse load as well as the qualitative type of collapse; and (b) the possibility of yielding may have no influence on collapse, if the imperfection weakens the structure.

3) STRUCTURES THAT BUCKLE IN THE INELASTIC RANGE

If the structural material is elastic-perfectly plastic, inelastic buckling occurs, under a rapidly decreasing load, when $P_y < P_E$, as in Fig.1.2b: the corresponding modifications of Figs. 2.2 and 2.5 are immediate. If the material has a non-zero inelastic modulus E_T, the simplest case of buckling beyond the elastic range is well illustrated by the well known Shanley's strut model (A.8). Assuming a constant modulus E_T and elastic unloading (Fig. 3.1),
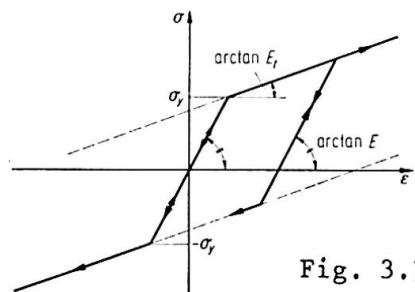

Fig. 3.1
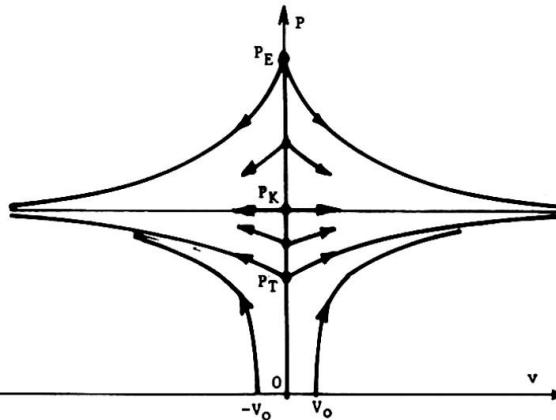
Fig. 3.2
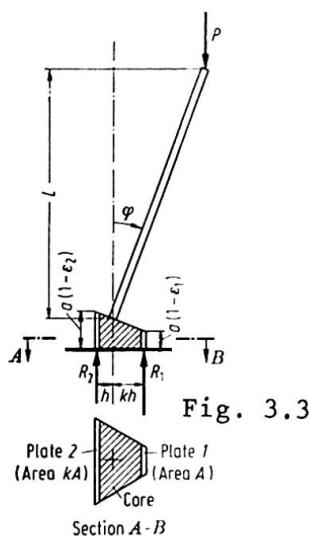
Fig. 3.3
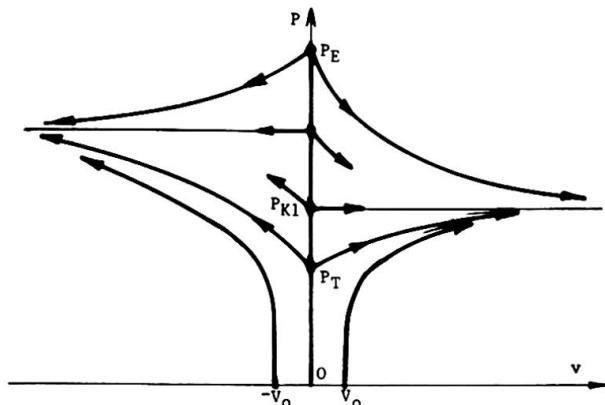
Fig. 3.4

the inelastic perfect strut may buckle at any load comprised between P_T and P_E; all P–v paths have a horizontal asymptote at a load $P = P_K \in (P_T, P_E)$, so that the load increases with $|v|$ (and the strut is stable,(A.1)) if buckling starts between P_T and P_K, decreases if buckling starts between P_K and $P_E(°)$. The

(°) The validity of these statements is limited to comparatively small values of v. Otherwise, not only the small-displacements approximation loses validity, but the material may yield in tension in the "unloading" zone, or E_T may vary in the "loading" zone. Note that the latter probably occurs before the former in a real material, at least in the more significant range $P \leq P_K$, where the average stress $\sigma = P/A$ increases with the deformation.

loads P_T and P_K are obtained from the formula for the elastic buckling load P_E, substituting the elastic (Young's) modulus E, respectively with the tangent modulus E_T and with the so-called reduced modulus E_K, that depends on E, E_T and the shape of the section.

If the strut is not initially straight, the P–v path lies on either side of the P–axis according to the sign of the initial imperfection V_o, and below the lowest path of the perfect strut (which starts from $P = P_T$, Fig.3.2), to which path it tends when $V_o \to 0$. But some degree of imperfection is unavoidable in an actual structure; therefore, of the infinite theoretically possible buckling paths, only the lowest ones seem to be significant from an engineering point of view. Collapse of the inelastic strut, be it perfect or not, occurs with one of the phenomena mentioned in the footnote on the previous page; for detailed examples see e.g. Refs.(A.4) and (A.9) dealing respectively with Shanley's model and with the practically important case of mild steel columns with residual stresses.

In Shanley's treatment and in the above description, the strut cross-section is assumed to be symmetric with respect to the axis of bending: the whole picture in Fig.3.2 is also symmetric with respect to the P–axis. But if the cross-section is not symmetric (as in the example of Fig.3.3, Ref.(A.1))the buckling interval of the perfect strut (P_T, P_E) remains unique, but each P–v path is different for v > 0 and v < 0, including the initial slope $[dP/dv]_{v=0}$ and the horizontal asymptote (Fig.3.4). In case of inelastic buckling, therefore, an asymmetry of strength implies asymmetric behaviour from the first stages of deformation. Again, the P–v path of any imperfect strut "is below the relevant lowest branch of the perfect strut ... and tends to such branch when the imperfection tends to zero" (A.1); the effects of an imperfection clearly depend on its sign.

The previous examples illustrate the inelastic behaviour of structures that, in the elastic range, exhibit symmetric buckling. The model arch of Fig.(2.3) was used in Ref.(A.7) to exemplify the inelastic behaviour of a structure liable to asymmetric elastic buckling; the effects of imperfections on this model have been investigated in detail by Batterman (A.10). Another simple model and a more realistic example have been presented by Hutchinson (A.11), with qualitatively similar results.

Referring to (A.9) and (A.10) for the analytical treatment (°), the behaviour of the perfect arch is summarized by Fig.3.5, and that of the imperfect arch by Fig.3.6 (reproduced from (A.10)).
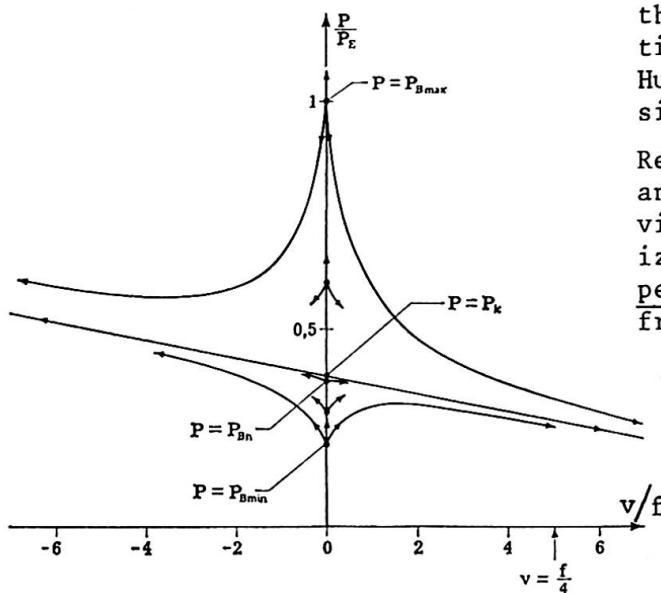

Fig. 3.5

(°) The second-order quantities Δc, Δf, etc., were neglected in the analysis (cf. eqs.(2.3) seqq.). This can be approximately justified, for small v, by the result of the complete elastic analysis, eqs.(2.14) and (2.10).
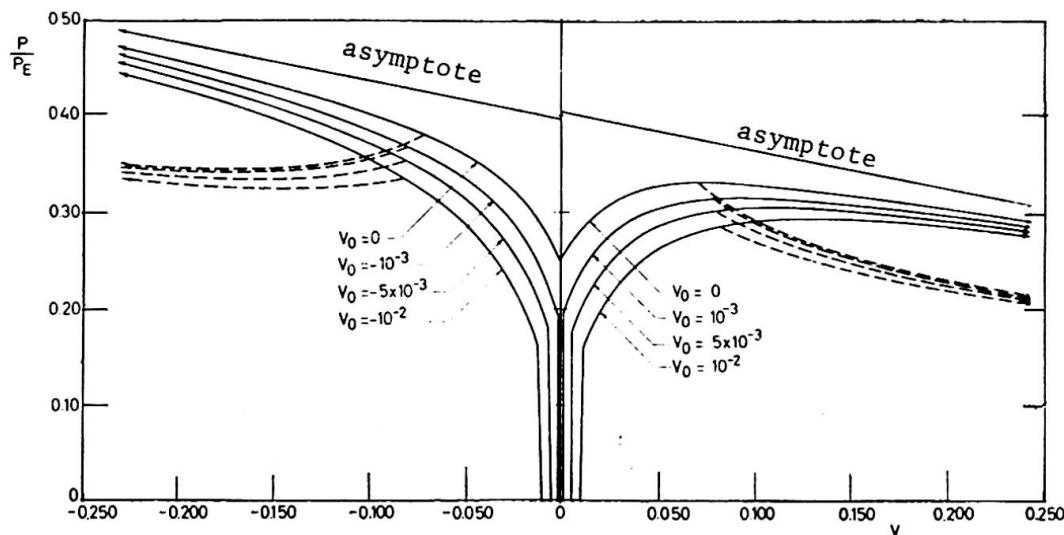
Fig. 3.6

Inspection of these Figures shows that the behaviour of the arch is markedly asymmetric, in the sense that it depends strongly on the sign of the displacement (and the initial imperfection). As in the previous examples, all paths of the imperfect structure ($v_0 \neq 0$) lie below the lowest paths of the perfect one ($v_0 = 0$) and tend to either of these when $v_0 \to 0$ (Fig. 3.6); the straight asymptotes have a finite slope and, as noted by Batterman, are different on either side of the P-axis. The perfect arch is stable, for zero displacement, up to a load indicated by P_{Bn} in Fig. 3.5; but, when buckling with positive v, it always reaches a collapse point and becomes unstable. The imperfect arch collapses only (and always) when $v_0 > 0$, unless account is taken of the possibility of tension yielding (which leads to the dashed lines of Fig.3.6) or of a decrease in E_T.

The behaviour illustrated by Figs. 3.5 and 3.6 is the inelastic analogue of Koiter's asymmetric elastic buckling.

REFERENCES

(A.1) G. Augusti, Instability of Continuous Systems (IUTAM Symposium Herrenalb 1969, edited by H. Leipholz), pp.175-182; Springer, Berlin 1971.
(A.2) G. Augusti and A. Baratta, Journ.Structural Mechanics, 1, No.1, 1972.
(A.3) G. Augusti and A. Baratta, Costruzioni Metalliche, 23, No.1, 1971 (in Italian) and Construction Metallique, 8, No.2, 1971 (in French).
(A.4) G. Augusti, Ingegneria Civile, No.11, 1964.
(A.5) J. Baker and J. Heyman, Plastic Design of Frames, Vol.I, pp.25-28; Cambridge Univ. Press 1969.
(A.6) W.T. Koiter, Recent Progress in Applied Mechanics (The Folke Odqvist Volume); pp.337-354; Almqvist & Wiksell, Stockholm 1967.
(A.7) G. Augusti, Meccanica (AIMETA), 3, No.2, 1968.
(A.8) F.R. Shanley, J.Aero.Sci., 14, No.5, 1947.
(A.9) G. Augusti, Journ.Engrg.Mech.Div., ASCE, 91, No.EM4, 1965.
(A.10) S.C. Batterman, Israel J. Technology, 9, No.5, 1971.
(A.11) J.W. Hutchinson, Conference on Computer-Oriented Analysis of Shell Structures, Palo Alto, California, 1970.

SUMMARY

The influence of random imperfections and inelastic deformations on the buckling and post-buckling behaviour of structures has been examined in several cases.

Leere Seite

Blank page

Page vide

Interaction of Postcritical Plate Buckling with Overall Column Buckling
of Thin-Walled Members

Interaction du voilement post-critique de plaques et du flambement de
colonnes aux parois minces

Wechselwirkung von überkritischem Plattenbeulen und Knicken des ganzen
dünnwandigen Stabes

JOHN   DeWOLF   TEOMAN   PEKOZ   GEORGE   WINTER
Cornell University, Ithaca, New York, USA

I.   Introduction

The interaction of postcritical plate buckling with overall
column buckling in thin-walled members is a complex phenomenon which
is very important in many situations. Thin-walled steel construc-
tion in buildings has increased greatly in the past two to three
decades; thin-walled members have always been used extensively in
aircraft construction.

In thin-walled members plate buckling is of major importance
and constitutes one of the chief design criteria. The classical
critical plate buckling stress for the component plates, which is
the stress at which local bifurcation buckling occurs, is often re-
garded as the chief design criterion. However, this is by no means
the maximum load which the component plate can carry. The plate
will usually continue to take increasing load, often more than twice
the critical local buckling load. This postcritical plate buckling
strength can be used to achieve substantial economies.

This paper concerns itself with postcritical plate buckling and
its effect on the overall buckling of columns. For most thin-walled
columns of low and medium slenderness, critical plate buckling of
one or more of the component plates occurs first, and is then fol-
lowed by overall column buckling at some point in the postcritical
plate buckling range. The prior plate buckling lowers the overall
capacity of the column, but the load at which local bifurcation
buckling occurs is less than the actual carrying capacity of the
member and may not be used as a reasonable indication of the over-
all capacity.

The investigation reported herein has been sponsored at Cornell
University by the American Iron and Steel Institute. It is aimed at
developing information on this interaction between postcritical
plate buckling and overall column buckling. Thirty-three tests have
been conducted on columns in which both the postcritical plate buck-
ling strength and the overall column buckling strength were varied
systematically. The results of these tests illustrate clearly the
interaction effects between postcritical plate buckling and overall

column buckling.

II. Survey of Previous Work

Many researchers have investigated plate buckling and a number have done work in the postcritical plate buckling range; also, overall column buckling has been extensively investigated. However, little has been done in the area of the interaction of postcritical plate buckling with overall column buckling. In fact, postcritical plate buckling by itself needs further clarification. This refers particularly to the later stages, where relatively large plate deflections interact with nonlinear materials' behavior.

One researcher, T.R.G. Smith in England[1], has made a very important contribution in the field which considers both of the above nonlinearities in the postcritical plate buckling range as they interact with overall column buckling. Unfortunately his analysis is limited to tubes and cannot be applied to other shapes without repeating his lengthy derivations for each type of section.

Some work has been done toward a simpler method of treating different types of common sections such as by Uribe [2] and Wang [3] at Cornell University, though their work was primarily involved with things other than interaction effects and was not very extensive. Others [4-7] have made contributions to the field of interaction, but their work has not involved both types of nonlinearities as has T.R.G. Smith. There appears to be no thorough set of tests utilizing different column shapes upon which a general method of design of thin-walled columns subject to the interaction of postcritical plate buckling with overall column buckling can be based.

III. Testing

Since thin-walled members are made of essentially two types of elements, elements with one edge stiffened by a web, flange or stiffener and elements with both edges stiffened, two types of sections were chosen in order to test each type of element separately. One section was composed entirely of stiffened elements; it was made of two channels connected together at the flanges to form a rectangular tube (see Fig. 1a). The other was composed primarily of unstiffened elements (the stiffened element was designed so that local buckling would not occur); it was made of two channels connected back to back along the webs to form an "H" type section (see Fig. 1b).

Four sections of each type were fabricated. The dimensions of the sections were chosen so that the critical and postcritical plate buckling strength were varied by varying the element width-thickness ratios over a wide range. The dimensions are given in Table 1.

For each section, the overall column buckling strength was varied by varying the slenderness ratio L/r. In addition to a stub column test (no column buckling), three different column lengths were chosen to cover the region in which local buckling had an effect on the ultimate load a column will support.
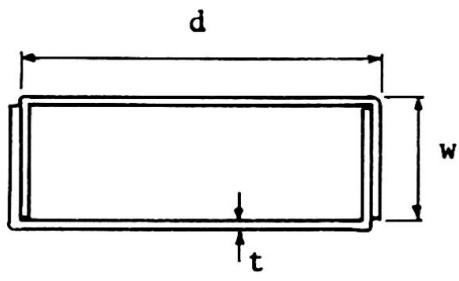
(a) Section S
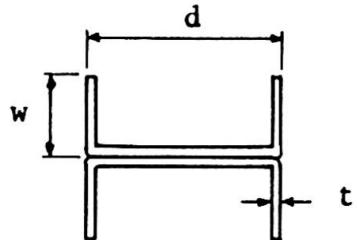
(b) Section U
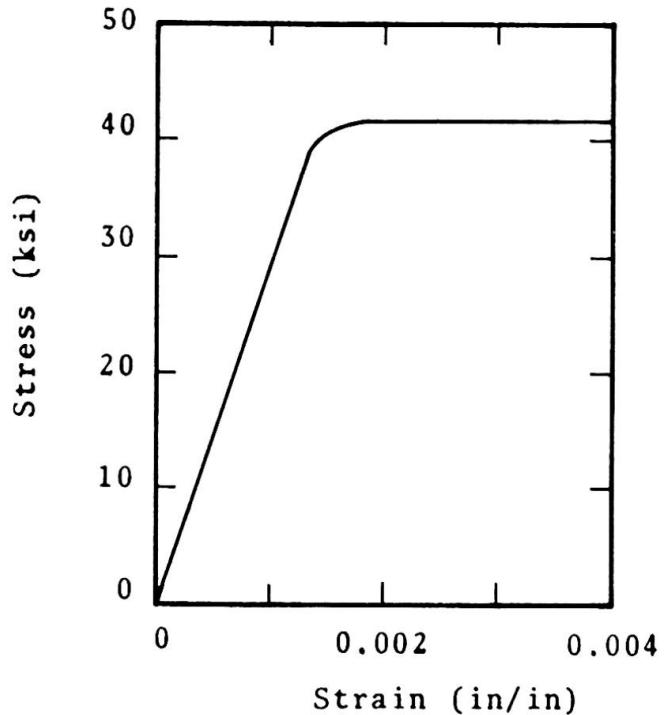
Fig. 1 Column Cross-Sections

Fig. 2 Material Stress-
Strain Curve

The testing arrangement was such that concentric loads were
achieved. This was done by loading to approximately twenty percent
of the expected failure load and then unloading and making adjust-
ments in the centering as necessary. Dial gages were used to mea-
sure the lateral deflections and strain gages to obtain the strain
distributions, as well as to determine approximately when local
buckling occurred in the plate elements. It is easily verified from
the strain gage results that nearly concentric loads were achieved
in all of the columns, except for three tests which were eccentric
and whose results are ignored.

Measurements of the out-of-plane deflections were taken for all
of the unstiffened plate elements. It was found that these deflec-
tions were minimal until failure, being no more than a few thou-
sandths of an inch.

The initial portion of the stress-strain curve for the material
used, a carbon steel of a structural quality, is shown in Fig. 2.
The average yield stress was 41.9 ksi., and the average ultimate
stress was 53.8 ksi. Strain hardening occurred at an average strain
of 0.014. The average percentage of elongation of a two-inch gage
length at rupture was 37 percent.

IV. Results

(a) General

The results of these tests illustrate clearly the interaction
between postcritical plate buckling behavior and overall column

Table 1

DIMENSIONS OF SECTIONS

(a) Sections S

Specimen	w (in)	d (in)	t (in)	Width/Thickness Single Thickness Element (d/t)	Width/Thickness Double Thickness Element (w/2t)
S-1	2.0	3.5	0.058	57.2	16.7
S-2	2.0	5.0	0.058	83.0	16.7
S-3	2.0	7.0	0.058	117.4	16.7
S-4	2.0	9.0	0.058	151.8	16.7

(b) Sections U

Specimen	w (in)	d (in)	t (in)	Width/Thickness Single Thickness Element (w/t)	Width/Thickness Double Thickness Element (d/2t)
U-1	1.0	3.0	0.058	16.2	24.8
U-2	1.25	3.0	0.058	20.5	24.8
U-3	1.5	3.0	0.058	24.8	24.8
U-4	1.75	3.0	0.058	29.1	24.8

buckling. The ultimate carrying capacities for the columns are given graphically in Figs. 3 and 4. The figures compare the experimental carrying capacity with the expected strength (1) when local instability is entirely neglected; (2) when the effect of local instability is based on the critical bifurcation stress, neglecting postcritical strength; (3) when postcritical buckling is included approximately by means of an effective width concept. These will now be discussed separately.

(b) Local Instability Neglected

A concentric, perfect column which is elastic will fail at the critical Euler stress or at the yield stress, provided that local instability and residual or cold-forming effects are nonexistent. For this type of column behavior, column curves, i.e. slenderness ratio vs. critical stress, are given as curves (1) in Figs. 3 and 4 for each of the different sections.

As mentioned, this neglects the effects of local instability, which were present in the test specimens. Additionally, the specimens were cold-worked so that cold-forming effects were present. However, since cold-forming effects are related to the area of the corners as a fraction of the total area (8), and since the ratio of the corners to the total area was less than one percent for all of the sections, the cold-forming effects were negligible. The columns

(a) Column S-1

(b) Column S-2

(c) Column S-3

(d) Column S-4

○   Test

———   (1) Local instability neglected

- - -   (2) Theoretical critical stress

-·-   (3) Effective width approach
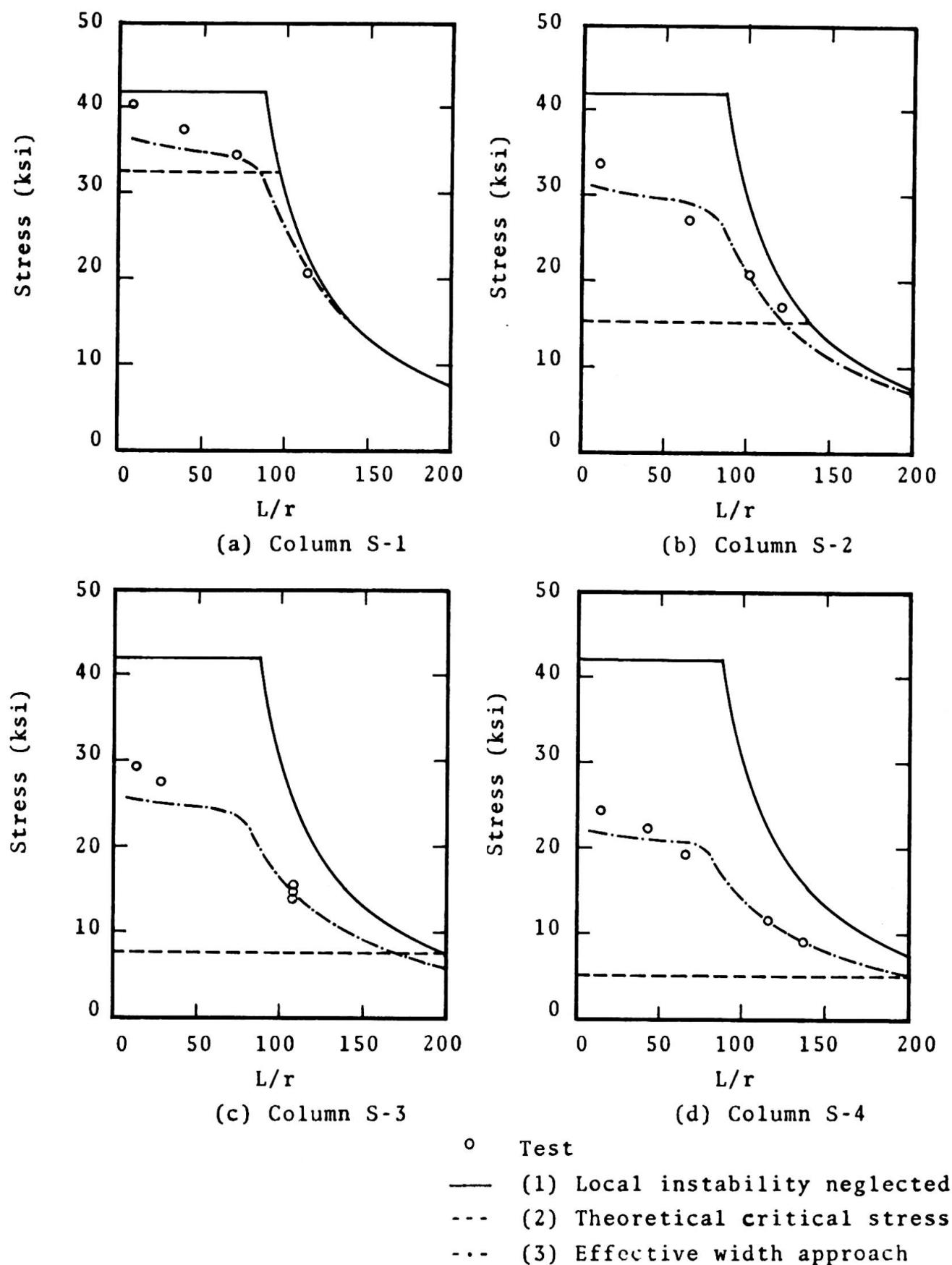
Fig. 3   Comparison of Test Results and Column Curves
   For Column Specimens S
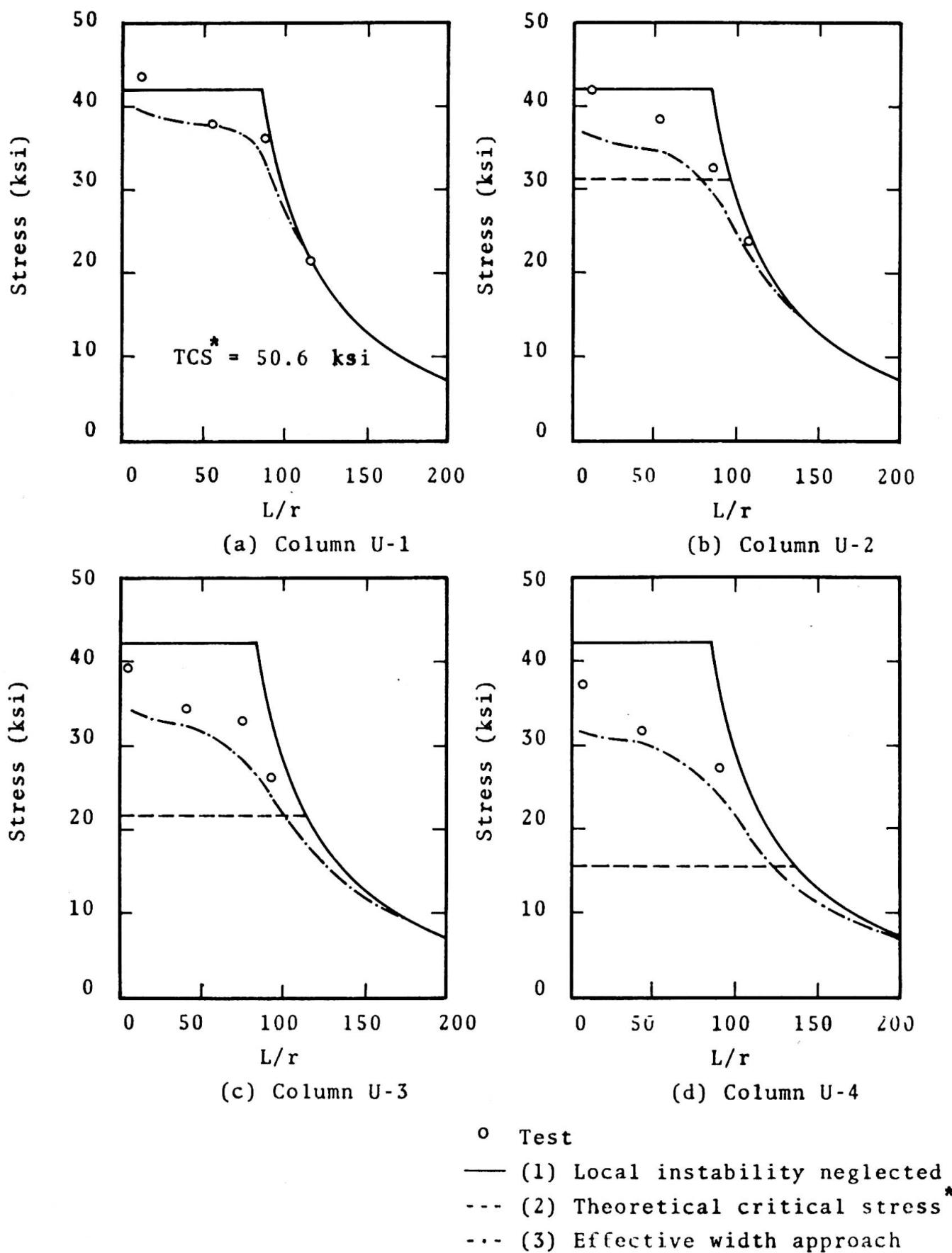
Fig. 4   Comparison of Test Results and Column Curves
         For Column Specimens U

were thus assumed to have a uniform stress-strain curve which is approximated by the material stress-strain curve in Fig. 2.

It is seen that almost all test points fall significantly below curves (1) which indicates that local instability had a great effect on strength. This effect became greater as the width/thickness ratios of the elements were increased.

(c) Theoretical Critical Stress

The theoretical critical bifurcation stress is that stress at which a perfect plate begins to buckle. Here it refers to the widest elements for the closed tubular sections and to the unstiffened flanges for the "H" sections. The theoretical critical stress by definition is the stress at which postcritical strength begins.

The classical critical stress for a plate element that buckles elastically is calculated from:

$$\sigma_{cr} = k \; \frac{\pi^2 E}{12(1 - \mu^2)(\frac{w}{t})^2} \qquad\qquad 1$$

where E is the modulus of elasticity, μ Poisson's ratio, w the plate width, t the plate thickness, and k depends on the edge conditions, chiefly along the longitudinal edges parallel to the compression stress. Values of k which are often used in practice, and which in some cases will be conservative, are 0.5 for elements with one edge supported by a web and the other edge unsupported, and 4.0 for elements with both edges supported by a web.

For the purpose of comparing the test results to a theoretical stress, these two values of k were used for the sections under study. The results are given in curve (2) in Figs. 3 and 4. With the exception of Fig. 4a the theoretical critical stress was below the highest load at failure, indicating that postbuckling strength existed. For Fig. 4a, the theoretical elastic critical stress was above the yield stress, though the section showed local waving prior to failure during the tests. It is seen that, except for Fig. 4a, almost all test points fall significantly above curve (2) indicating that postcritical strength does add considerably to the carrying capacity. This effect increases with increasing width/thickness ratios.

(d) Effective Width Approach

In order to consider the postbuckling strength, an effective width approach is now under development. At present, this approach is only an approximate method for considering postbuckling strength, and in its present form is not always satisfactorily accurate. The concepts of the method are these:

The bifurcation stress of a column is well accepted to be given by the Engesser-Shanley tangent-modulus equation:

$$\sigma_t = \frac{\pi^2 E_t}{(\frac{KL}{r})^2} \qquad\qquad 2$$

where E_t is the tangent modulus for the material, L is the column length, r is the radius of gyration, and K is the effective length factor. Dividing the cross-section into j elements, one can define:

$$E_t r^2 = \frac{\sum\limits_{i=1}^{j} E_{ti} I_i}{A} \qquad\qquad 3$$

Then, for K = 1.0, by substitution, Eq. 2 becomes:

$$L^2 = \frac{\pi^2 \sum\limits_{i=1}^{j} E_{ti} I_i}{\sigma A} \qquad\qquad 4$$

where, for any selected strain, E_{ti} is the tangent modulus of the ith element, I_i is the moment of inertia of the ith element about the weak principal axis, A is the full area of the cross-section, and σ_{cr} is given by:

$$\sigma = \frac{\sum (A_{eff})_i \sigma_i}{A} \qquad\qquad 5$$

where $(A_{eff})_i$ is the effective area of the ith sub-element at the stress σ_i corresponding to the assumed strain ε, and A is the full area of the section. Essentially, Eq. 5 considers the effects of local buckling and postbuckling strength by reducing the area to an effective area, using the effective widths of the elements.

The general equation for the effective width on which American specifications are now based is:

$$\frac{b}{w} = \sqrt{\frac{\sigma_{cr}}{\sigma_{max}}} \left(1 - 0.22 \sqrt{\frac{\sigma_{cr}}{\sigma_{max}}}\right) \qquad\qquad 6$$

which constitutes a slight revision of the equation first given by Winter [9]. Here b is the effective width, w is the real width of the particular plate element, σ_{cr} is the classical plate bifurcation buckling stress for the given edge conditions, and σ_{max} the edge stress in the postbuckling range. This equation can be transformed into the more convenient form:

$$b = C_1 t \sqrt{\frac{E}{\sigma_{max}}} \left(1.0 - C_2 \frac{t}{w} \sqrt{\frac{E}{\sigma_{max}}}\right) \qquad\qquad 7$$

where t is the plate element thickness, E the modulus of elasticity, and C_1 and C_2 are constants which depend on the edge conditions. For elements with one side supported by a web and the other side unsupported, approximately $C_1 = 0.672$ and $C_2 = 0.148$. For elements with both edges supported, approximately $C_1 = 1.9$ and $C_2 = 0.415$.

The ultimate loads predicted using this effective width approach

are given in curves (3) in Figs. 3 and 4. It is seen that the test results agree best with the last of the three methods (curve 3), which includes the effect of postcritical plate buckling strength on column capacity. At the same time, it is also seen that the accuracy of this approach is inadequate. Further development of this method is needed, and is under way at the present time.

V.   Conclusions

On the basis of extensive test results and theoretical comparisons, it is shown that:

(1) The strength of thin-walled columns can be considerably reduced by local plate buckling.

(2) Column capacities calculated on the basis of the classical critical plate buckling stress considerably underestimate the actual column strength.

(3) The effect of the postcritical strength of the component plates increases the column strength significantly over that determined by the critical plate buckling stress.

(4) A tentative method, based on the postcritical effective width of plates, is now under development and promises to furnish a satisfactory tool for calculating the strength of thin-walled columns.

References

1.   Smith, T.R.G., "The Ultimate Strength of Locally Buckled Columns of Arbitrary Length," Ph.D. Thesis, Cambridge University, 1966.

2.   Uribe, J., "Aspects of the Effects of Cold-Forming on the Properties and Performance of Light-Gage Structural Members," Department of Structural Engineering, Report No. 333, Cornell University, May 1969.

3.   Wang, S.T., "Cold-Rolled Austenitic Stainless Steel: Materials Properties and Structural Performance," Department of Structural Engineering, Report No. 334, Cornell University, July 1969.

4.   Bijlaard, P.P., and Fisher, G.P., "Interaction of Column and Local Buckling in Compression Members," NACA T.N. 2640, 1952.

5.   Bijlaard, P.P. and Fisher, G.P., "Column Strength of H-Sections and Square Tubes in the Post-Buckling Range of the Component Plates," NACA T.N. 2994, 1953.

6.   Klöppel, K., and Schubert, J., "Die Berechnung der Traglast mittig und aussermittig gedrückter, dünnwandiger Stützen mit kastenförmigem Querschnitt in überkritischen Bereich," Veröffentlichung des Institutes für Statik und Stahlbau der Technischen Hochschule Darmstadt, Darmstadt, 1971.

7.   Skaloud, M., and Zörnerová, M., "Experimental Investigation into the Interaction of the Buckling of Compressed Thin-Walled Columns with Buckling of their Plate Elements," ACTA Technica CSAV, No. 4, 1970, pp. 389-424.

8.   Karren, K.W., "Effects of Cold-Forming on Light-Gage Steel Members," Department of Structural Engineering, Report No. 318, Cornell University, June 1965.

9.   Winter, G., "Light-Gage (Thin-Walled) Steel Structures for Buildings in the United States of America," Int. Assoc. Bridge and Structural Engineering, Fourth Congress, Prel. Publ., 1952, pp. 523-538.

Summary

Experimental data are given which illustrate clearly the interaction of postcritical plate buckling with overall column buckling in thin-walled members. The experimental carrying capacity is compared with the expected strength when (1) local instability is entirely neglected; (2) the effect of local instability is based on the critical bifurcation stress, neglecting postcritical strength; (3) postcritical buckling is included approximately by means of an effective width concept.

Post-Buckled Behaviour and Incremental Collapse of
Webs Subjected to Concentrated Loads

Comportement post-critique de voilement et ruine des
âmes soumises à des charges concentrées

Überkritisches Beulverhalten und zusätzlicher Kollaps
von Stahlblechen infolge konzentrierter Lasten

MIROSLAV ŠKALOUD
Docent, Ing., Dr.Sc.
Senior Research Fellow
at the Institute of Theoretical
and Applied Mechanics of the
Czechoslovak Academy of Sciences
in Prague, CSSR

PAVEL NOVÁK
Docent, Ing., CSc.
Research Fellow
at the Structural Institute
in Prague, CSSR

1. Introductory Remarks

After the completion of the investigation into the post-buckled behaviour of webs in shear, which was conducted partially by K.C.Rockey and the first of the authors in Swansea and Cardiff /1/ and partly, after the return of the author to Czechoslovakia, at the Institute of Theoretical and Applied Mechanics in Prague /2/, a new research project was started. This deals with the influence of flange stiffness upon the ultimate load behaviour and incremental collapse of thin webs subjected to a concentrated (or, more accurately, to a narrow partial edge) load. The investigation is carried out by a research team that consists of the first of the authors, Ing.Drdácký, Ing.Kratěna, Ing.Zörnerová (all of them from the Institute of Theoretical and Applied Mechanics in Prague), the other author and Ing.Bohdanecký (both from the Structural Institute in Prague). The objective is to obtain (together with other investigators /3/, /4/, /5/) enough information about the ultimate load behaviour of plate girders the webs of which are subjected to a patch load, such as are crane run-way girders, certain types of bridge girders and similar structures.

2. Test Girders

Two series of test girders were tested. The general details of the test girders of the first series are given in Fig. 1a, the corresponding dimensions (in mm) in Table 1a. The details of the second series girders are shown in Fig. 1b, and the dimensions in Table 1b.

An inspection of the figures shows that the test girders of the second series had two web panels. Each of them was tested individually, the supports being positioned under the boundary vertical stiffeners of the panel. Web panel W 2 was tested first, the girder being subjected to a static load.

Table 1a

Girder	Loading	Web Depth b [mm]	Web Thickness t [mm]	b/t	Flange Width bf [mm] Upper	Flange Width bf [mm] Lower	Flange Thickness tf [mm] Upper	Flange Thickness tf [mm] Lower	If/a³t [Units of 10⁻⁶] Upper	If/a³t [Units of 10⁻⁶] Lower	RB Pcr [T]	Pult [T]
PTG1	static						5.95	5.95	3.48	3.48	2.78	3.6
PTG2	static				50	50	5.97	5.93	3.50	3.43	2.2	4.0
PTG3	cyclic						5.09	5.03	2.77	2.09	2.38	5.0
PTG4	cyclic						5.08	5.06	2.16	2.13	2.19	4.6
PTG5	static						16.21	16.14	63.89	63.07	2.53	5.5
PTG6	cyclic	500	2	250	45	45	16.24	16.74	64.25	63.04	2.53	5.5
PTG7	cyclic						16.17	16.07	63.48	62.31	2.52	5.6
PTG8	static						16.25	16.11	64.36	62.72	2.53	5.5
PTG9	cyclic						24.25	24.78	237.68	253.60	2.83	7.2
PTG10	cyclic				50	50	24.64	24.24	249.33	237.38	2.83	7.0
PTG11	static						24.80	24.84	254.22	255.45	2.84	7.5
PTG12	static						24.40	25.00	242.11	260.42	2.85	8.0

Table 1b

| Girder	Web	Loading	Web Depth b [mm]	Web Thickness t [mm]	b/t	Flange Width bf [mm] Upper	Flange Width bf [mm] Lower	Flange Thickness tf [mm] Upper	Flange Thickness tf [mm] Lower	If/a³t [Units of 10⁻⁶] Upper	If/a³t [Units of 10⁻⁶] Lower	RB Pcr [T]	Pult [T]
TG1	W1	cyclic				160	160	5.50	5.18	0.887	0.741	2.2	6.5
	W2	static											5.0
TG1'	W1	cyclic						5.42	5.56	0.849	0.917		
	W2	static											
TG2	W1	cyclic						10.09	10.08	8.85	6.83	2.24	7.0
	W2	static											6.5
TG3	W1	cyclic	7000	2.5	400	200	200	16.24	16.15	28.55	28.08	2.36	9.2
	W2	static											7.0
TG4	W1	cyclic						20.17	20.12	54.70	54.30	2.48	9.8
	W2	static											9.0
TG5	W1	cyclic						30.88	30.44	245.39	235.05	2.78	18.0
	W2	static				250	250						18.0
TG5'	W1	cyclic						30.50	30.48	238.44	236.00		
	W2	static											

Fig. 1a

Fig. 1b



Fig. 2

Then this web panel was cut off, and web panel W 1 was subjected to a cyclic load.

All web panels in both aforesaid series had aspect ratio α of 1. Test girders with other α -ratios will be tested in 1972. In each series the depth-to-thickness ratio λ = b/t of the web was constant, but the flange dimensions varied from girder to girder, so that the effect of the flexural rigidity of flanges upon the ultimate load behaviour of webs could be studied.

The research on steel girders was accompanied by a photoelasticity investigation conducted by the first of the authors and J.Kratěna on reduced-scale epoxy-resin models.

In all tests the web panels were subjected to a narrow partial edge load, applied on to the upper flange at the mid-distance of the vertical stiffeners. The width of the load c = a/10 (in one case c = a/5), a denoting the width of the web panel (Fig.2).

3. Apparatus

A description of the experimental apparatus and of the programme of measurements was the objective of the paper /6/ presented by the authors at the Congress of RILEM in Buenos Aires. For this reason only a brief information about the apparatus will be given in this publication, the aim of which is to discuss main test results.

The buckled pattern of the web was measured by means of a stereophotogrammetric method /7/. The application of this method was advantageous in the aforesaid tests, since it enabled the authors to take all readings in a very short time moment (0,001 sec.). This was desirable in the static load tests (because a study of the final, plastic, stage — in which the web and flanges were already yielding — was one of the main objectives of the investigation) and indispensable in the cyclic load tests (in which the web and flanges were "breathing").

A special device, designed by P.Pašník, enabled the authors to take deflection readings at a given moment of loading cycles; for example, when, in a "breathing" cycle, the web deflection attained its maximum (amplitude) value. Moreover, the stereophotogrammetric method made it possible to measure not only the deflection perpendicular to the web, but also the in-plane distortion of the mesh that was marked on the web, and the deformation of the boundary frame of the web panel.

A set of strain gauges was attached to both sides of the
web and of the upper flange in order the stress pattern in the
girder could be studied. Several of the strain gauges, as well
as two deflection pick-ups, were linked to an automatic recorder
"Ultralette". Thus it was possible to study, as a function of
time, the progression of the plastification of the girder in
the static load tests and the deflection (and strain) stability
in the cyclic load ones.
      The post-failure plastic residue in the web and flanges of
each test girder was also carefully measured.

4. Static Load Tests

The first part of the investigation was concerned with the
post-buckled behaviour of webs subjected to a static patch load.
The influence of the flexural rigidity of flanges upon the
buckled pattern and stress state in the web and flanges, and
upon the ultimate load of the whole girder was studied.
      The post-failure plastic residues w_{pl} in web panels W 2
of test girders TG 1 (flexible flanges) and TG 5 (rigid flanges)
are plotted in Figs. 3a and b. The plastic residues in the
upper (i.e. loaded) flange of girders TG 1, TG 3 and TG 5 are
given in Fig. 3c. A photo of the collapsed girder TG 4 is shown
in Fig. 3d.
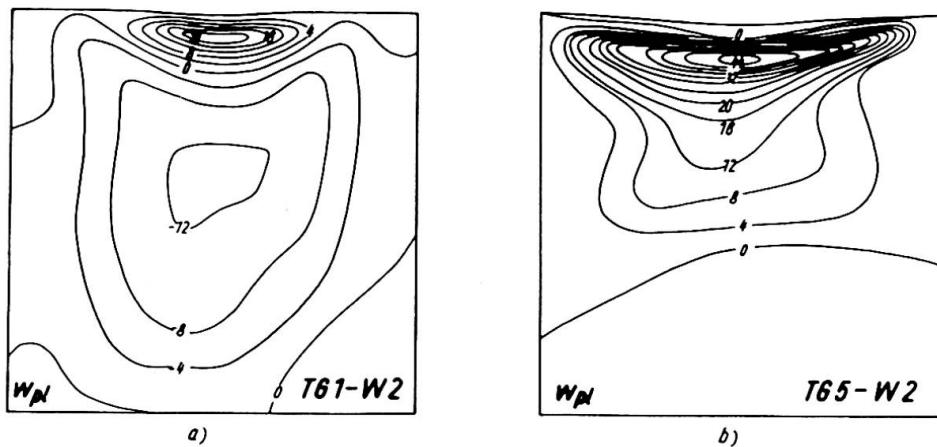
Fig.3

An inspection of the aforesaid figures shows the pronounced
influence that flange stiffness has on the deformation of the
test girder. While, in the case of flexible flanges, the
buckling of the web and the deflection of the flanges are
localized in the neighbourhood of the partial edge load, for
heavy flanges the buckled pattern of the web and the flexure
of the flange are distributed almost over the whole width of
the web panel. The performance of the web panel is then more
homogeneous; this affecting – as it will be demonstrated
below – very beneficially the ultimate load behaviour of the
girder.
      The pattern of ε_{my} (ε_{my} denoting the vertical – i.e.
parallel to the load – membrane strain) in web W 2 of girder
TG 1 (flexible flanges) is given in Fig. 4. Fig. 4a shows the
values of ε_{my} along two horizontal lines (the first of them
being situated 30 mm and the other 300 mm from the top flange),
and Fig. 4b gives the strains ε_{my} along the vertical axis of
the web. The bending strains ε_{bx} in the upper (i.e. loaded)
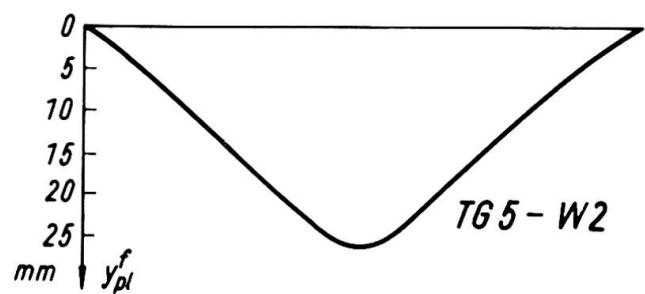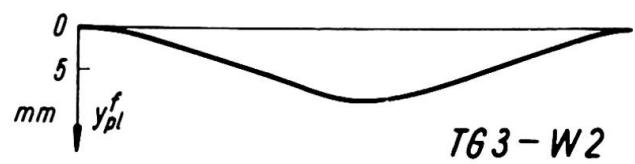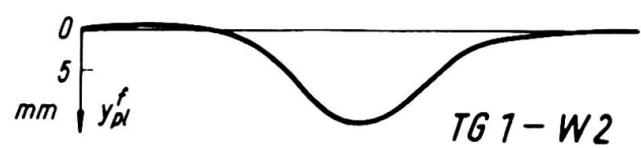
Fig. 3c
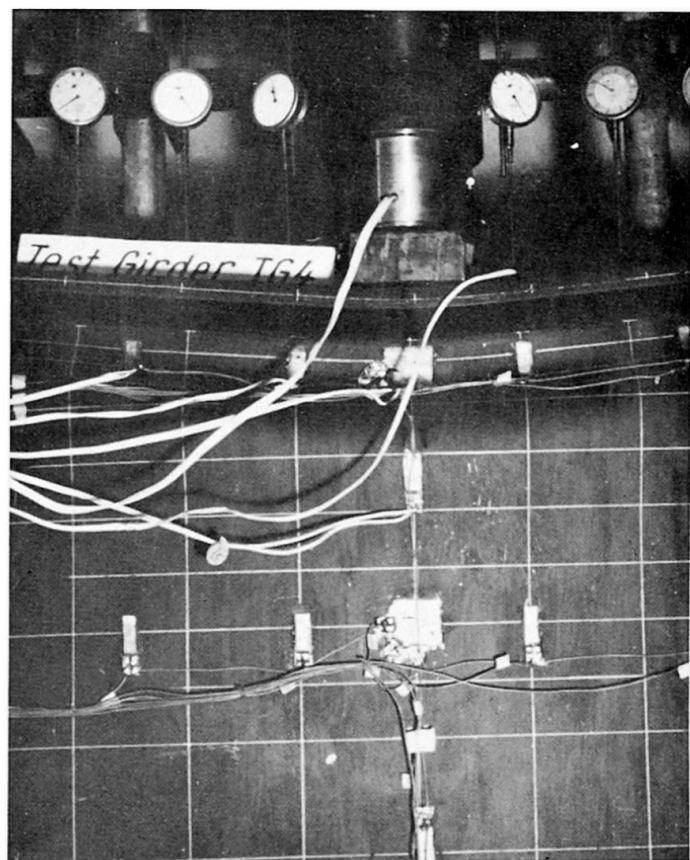
Fig. 3d

Fig. 4

Fig. 5

Fig. 6

Fig. 7

flange of the same girder are plotted in Fig. 5.

The membrane strain distribution in web W 2 of girder TG 5 (heavy flanges) is shown in Fig. 6, the bending strains in the flange of the same girder are given in Fig. 7.

A comparison of the membrane strain patterns plotted in Figs. 4 and 6 again shows the considerable influence of flange inertia upon the post-buckled performance of the web. In the case of a girder with flexible flanges, the membrane stress pattern, like the buckled surface of the web discussed above, is localized in the neighbourhood of the partial edge load. Moreover, in this case are the strains still small for a load amounting to 90 % of the experimental load-carrying capacity. This indicates that the upper flange and the adjacent part of the web buckled inwardly (and the girder failed) before, or shortly after, the onset of yielding in the web. On the other hand, for a girder with rigid flanges, the stress pattern is wider (more distributed over the width of the web panel); and, even after the web has plastified in a considerable portion, the girder can sustain further load - thanks to the rigidity of the boundary framework consisting of the flanges and vertical stiffeners. Besides that, in this case the collapse of the girder is a slower process (and, therefore, not so dangerous a type of failure) than that which occurs with a girder having flexible flanges.

The ultimate loads P_{ult} of the test girders are given in Tables 1a, b, and the ratios P_{ult}/P_{cr}^{RB} (P_{cr}^{RB} denoting the critical load evoluated by Rockey's theory /5/, which takes account of flange dimensions) are plotted, in terms of the flange stiffness parameter $I_f/a^3 t$ and of the depth-to-thickness ratio $\lambda = b/t$ of the web, in Fig. 8. An analysis of the tables and figure indicates that thin webs subjected to a concentrated load, applied on to the upper flange between the vertical stiffeners of the web, manifest (like thin webs subjected to shear, bending and the like) a considerable post-critical reserve of strength, which ought to be taken into account in an optimum design of steel plate girders. This post-buckled strength grows with the depth-to-thickness ratio of the web and with the moment of inertia of the flange.

The effect of flange stiffness is very significant. For example, for girder TG 1, which had flexible flanges with

Fig. 8

$I_f /a^3 t = 0,89$, the load-carrying capacity was 5 tons. On the other hand, for girder TG 5, having rigid flanges with $I_f /a^3 t = 254.4$, the ultimate load attained 18 tons; which is 260% higher than the abovementioned collapse load of TG 1.

5. Cyclic Load Tests

The other part of the investigation dealt with "breathing" of the web, with stability of plastic post-critical web deflection and with incremental collapse.

The position of the concentrated load was the same as in the case of static tests; but the load cycled between 0.5 T and P_i , P_i denoting various loading steps. For each loading step, 1000 loading cycles were applied.

Three questions then needed replying:

(i) When a girder, subjected to a load cycling between 0.5T and an amplitude value P, operates in the plastic range, does an increase in web deflection occur during a certain number of loading cycles?

(ii) If it is so, do these deflection increments cease after a limited number of cycles of load applications?

(iii) Does the aforesaid deflection increase lead to a premature failure of the girder and to a reduction in its ultimate load, if compared to the value resulting from a static test?

Thanks to deflections and strains being measured carefully on an automatic recorder Ultralette, it was possible to give answers to the abovementioned questions.

An increase in web deflection (and strain) under a cyclic load was observed frequently in the plastic stage of the tests (see, for example, Fig. 9). This phenomenon "shook down", however, after a few (usually 3-5) cycles, the deflection
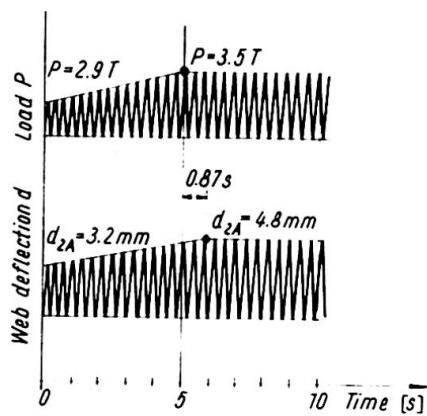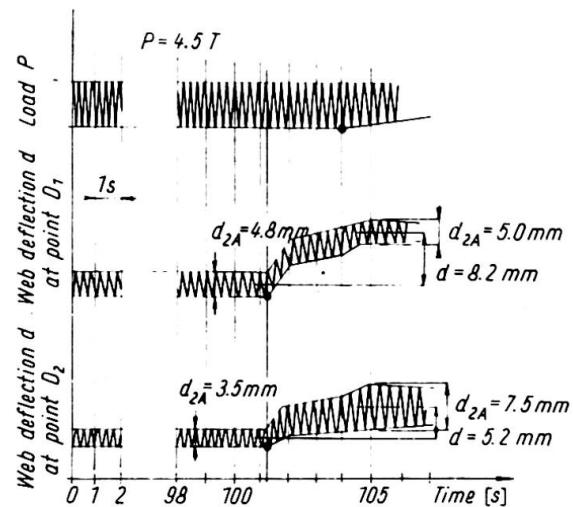
Fig. 9   Fig. 10

stabilized, and the girder was able to sustain a higher load
(Fig. 9). This happened for several successive loading steps;
and only then the girder failed by deflection instability and
incremental collapse (Fig. 10).

The failure loads P_{ult} resulting from the cyclic load tests
are listed in Tables 1a, b and plotted, in terms of the flange
stiffness $I_f/a^3 t$ and the depth-to-thickness ratio λ , in Fig.11.

In almost all tests, the cyclic ultimate loads were not
lower than the load-carrying capacities resulting from the
corresponding static experiments; and, in several cases, they
were even higher. The cyclic loading and the incremental collapse
did not, therefore, lead to any reduction in ultimate strength.

An inspection of Tables 1a, b and Fig. 11 also shows that
the load-carrying capacities P_{ult} grew substantially with the
flange stiffness, thereby demonstrating again the beneficial
effect of flanges of great inertia.
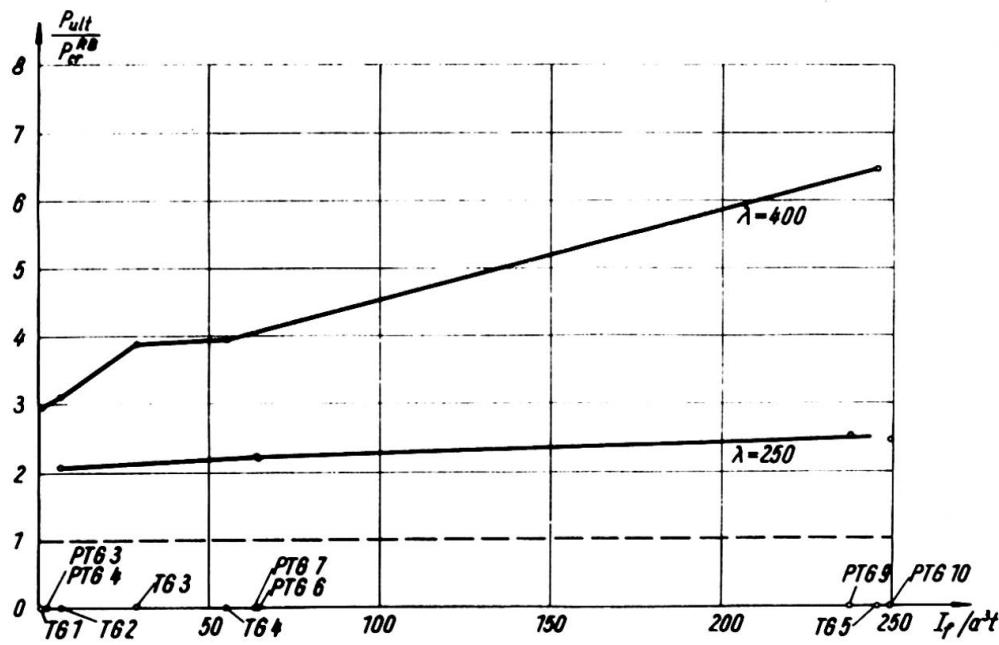
Fig. 11

Bibliography

/1/ Rockey, K.C., Škaloud, M.: The ultimate load behaviour of plate girders loaded in shear. Contribution presented at the IABSE Colloquium "Design of Plate and Box Girders for Ultimate Strength", London, March, 1971.

/2/ Škaloud, M.: Ultimate load and failure mechanism of thin webs in shear. dtto.

/3/ Bergfelt, A.: Studies and tests on slender plate girders without stiffeners. dtto.

/4/ Bossert, T.W., Ostapenko,A.:Fritz Eng. Lab. Report No. 319.1, June, 1967.

/5/ Rockey, K.C., El-gaaly, M., Bagchi, D.: Buckling and ultimate strength of thin walled members when subjected to patch loading. University College Cardiff, 1971.

/6/ Novák, P., Škaloud M.: Experimental investigation into the post-buckled behaviour and incremental collapse of thin webs. Congress of RILEM, Buenos Aires, 1971.

/7/ Novák, P.: Méthode photostéréométrique dynamique des modèles. Colloque International de RILEM, Bucuresti, Septembre, 1969.

Summary

The paper deals with the ultimate load behaviour of thin webs subjected to a) static b) cyclic narrow partial edge load. An analysis of the experimental results shows that such webs (like those in shear, bending, etc.) posses a considerable post-buckled reserve of strength. It was also demonstrated that the post-critical behaviour and the ultimate load of the girder were very significantly affected by the flexural rigidity of flanges.